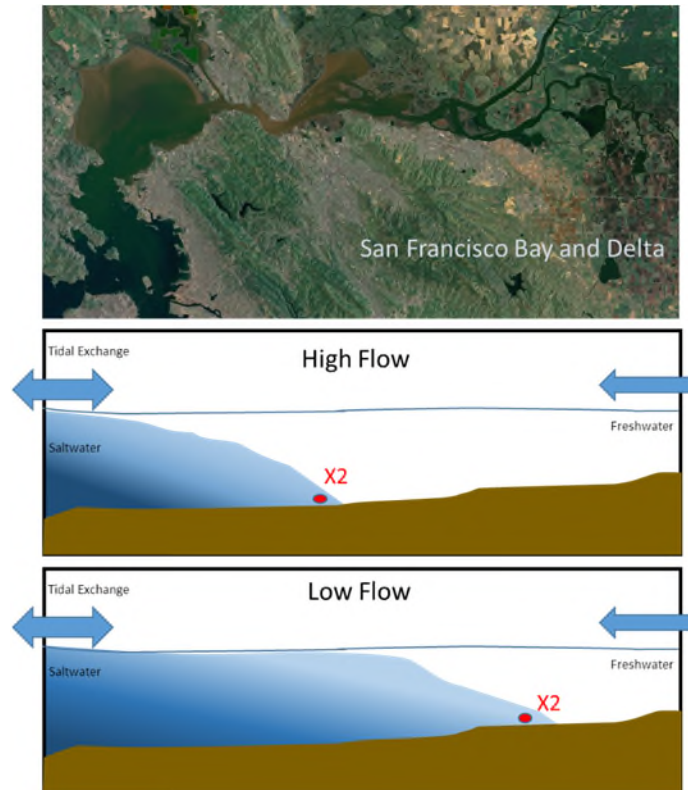


# MODELING SALINITY IN SUISUN BAY AND THE WESTERN DELTA USING ARTIFICIAL NEURAL NETWORKS

Addendum to Reports Dated April 12, 2013 & April 18, 2014  
Final Report



*Prepared for:*

**Paul Hutton, Ph.D., P.E.**  
**Metropolitan Water District of Southern California**  
**1121 L Street, Suite 900**  
**Sacramento CA 95814-3974**

*Prepared by:*

**Limin Chen, John S. Rath and Sujoy B. Roy**  
**Tetra Tech Inc.**  
**3746 Mt. Diablo Blvd, Suite 300**  
**Lafayette, CA 94549**

**August 26, 2015**



This page intentionally left blank.





---

4.7	DSG residual-based ANN models .....	4-52
4.7.1	Model 3A (Sacramento River) .....	4-52
4.7.2	Model 3B (San Joaquin River) .....	4-66
4.8	Evaluation of ANN Model Performance With Respect to X2.....	4-78
4.9	Comparison to Daily DSG Model.....	4-78
4.10	Comparison to Daily K-M Model.....	4-78
4.11	Comparison to MacWilliams et al. (2015) Model.....	4-78
<b>5.</b>	<b>Summary and Recommendations.....</b>	<b>5-1</b>
<b>6.</b>	<b>References.....</b>	<b>6-1</b>

# LIST OF FIGURES

---

Figure 3-1	Overview of ANNs developed as part of this analysis.....	3-6
Figure 3-2	Overview of analysis performed on ANNs focused on the salinity gradient. ....	3-7
Figure 3-3	Relationship between Jersey Point (JER) EC values and Qwest and G-flow (both in thousand cfs, tcfs). Plots (a), (c), and (e) show the expanded range of flow values on the x-axis; plots (b), (d), and (f) show the same data with a limited x-axis to show the behavior at low flows. ....	3-2
Figure 4-1	Performance of trained Sacramento River Model using Qrio, Qwest, MSL and tidal range as inputs (n=1, d=60). Results are shown for multiple trained ANNs, each initialized with randomized weights and biases. ....	4-2
Figure 4-2	Sensitivity of trained Sacramento River Model (n=1, d=60) at EMM to changes in Qwest flow of 2000 cfs (+2000 cfs to Qwest flow, and -2000 cfs to Qrio flow). Results are shown for multiple trained ANNs, each initialized with randomized weights and biases. ....	4-3
Figure 4-3	Sensitivity of trained Sacramento River Model (n=1, d=60) at EMM to mean sea level rise of 0.5 ft. Results are shown for multiple trained ANNs, each initialized with randomized weights and biases. ....	4-4
Figure 4-4	Performance of trained ANN networks at Sacramento River with Qout as input (n=1, d=60). Results are shown for multiple trained ANNs, each initialized with randomized weights and biases. ....	4-6
Figure 4-5	Sensitivity of trained Sacramento River model to changes in Qout flow of 2000 cfs at Emmaton (n =1, d = 60). Results are shown for multiple trained ANNs, each initialized with randomized weights and biases. ....	4-7
Figure 4-6	Sensitivity of trained Sacramento River model to tide increase of 0.5 ft at Emmaton (n=1, d=60). Results are shown for multiple trained ANNs, each initialized with randomized weights and biases. ....	4-8
Figure 4-7	Performance of trained San Joaquin River model (n=1, d=60). Results are shown for multiple trained ANNs, each initialized with randomized weights and biases. ....	4-9
Figure 4-8	Sensitivity of trained San Joaquin River model to changes in Qwest flow of 2000 cfs at Jersey Point (n=1, d=60). Results are shown for multiple trained ANNs, each initialized with randomized weights and biases. ....	4-10
Figure 4-9	Sensitivity of trained San Joaquin River model to tide increase of 0.5 ft at Jersey Point (n=1, d=60). Results are shown for multiple trained ANNs, each initialized with randomized weights and biases. ....	4-11

Figure 4-10	Performance of trained San Joaquin River model with Qout as input (n = 1, d=60). Results are shown for multiple trained ANNs, each initialized with randomized weights and biases. ....	4-13
Figure 4-11	Sensitivity at Jersey Point for trained San Joaquin River model to changes in Qout flow of -2000 cfs (n=1, d=60). Results are shown for multiple trained ANNs, each initialized with randomized weights and biases. ....	4-14
Figure 4-12	Sensitivity at Jersey Point for trained San Joaquin River model to tide increase of 0.5 ft (n=1, d=60). Results are shown for multiple trained ANNs, each initialized with randomized weights and biases. ....	4-15
Figure 4-13	Performance of trained ANN networks at Emmaton (n=1, d=60). Results are shown for multiple trained ANNs, each initialized with randomized weights and biases. ....	4-16
Figure 4-14	Sensitivity of trained ANN networks at Emmaton to changes in Qwest flow of 2000 cfs (+2000 cfs to Qwest flow, and -2000 cfs to Qrio flow; n=1, d=60). Results are shown for multiple trained ANNs, each initialized with randomized weights and biases. ....	4-17
Figure 4-15	Sensitivity of trained ANN networks at Emmaton to mean sea level increase of 0.5 ft (n=1, d=60). Results are shown for multiple trained ANNs, each initialized with randomized weights and biases. ....	4-18
Figure 4-16	Performance of trained ANN networks at Jersey Point (JER; n=1, d=120). Results are shown for multiple trained ANNs, each initialized with randomized weights and biases. ....	4-21
Figure 4-17	Sensitivity of trained ANN networks at Jersey Point (JER) to changes in Qwest flow of 2000 cfs (+2000 cfs to Qwest flow, and -2000 cfs to Qrio flow; n=1, d=120). Results are shown for multiple trained ANNs, each initialized with randomized weights and biases. ....	4-22
Figure 4-18	Sensitivity of trained ANN networks at Jersey Point (JER) to changes in Qwest flow of 2000 cfs (+2000 cfs to Qwest flow, and -2000 cfs to Qrio flow; n=2, d=90). Results are shown for multiple trained ANNs, each initialized with randomized weights and biases. ....	4-23
Figure 4-19	Time series example of ANN response at Jersey Point (JER) to changes in Qwest flow of 2000 cfs (+2000 cfs to Qwest flow, and -2000 cfs to Qrio flow; n=2, d=90). ....	4-24
Figure 4-20	Sensitivity of trained ANN networks at Jersey Point (JER) to mean sea level increase of 0.5 ft (n=1, d=120). Results are shown for multiple trained ANNs, each initialized with randomized weights and biases. ....	4-25
Figure 4-21	DSG parameter ranges for the Sacramento River model fit (Model 2A-1). Black points are pre-Project conditions (1922-1967), and blue points are post-Project conditions (1968-2012). ....	4-28
Figure 4-22	DSG parameter ranges for the San Joaquin River model fit (Model 2B-1). Black points are pre-Project conditions (1922-1967), and blue points are post-Project conditions (1968-2012). ....	4-29

Figure 4-23	Sensitivity in EC ( $\mu\text{S}/\text{cm}$ ) of Sacramento River fitted DSG model to changes in delta outflow (-2000 cfs). Results are shown for multiple trained ANNs, each initialized with randomized weights and biases. ....	4-32
Figure 4-24	Sensitivity in EC ( $\mu\text{S}/\text{cm}$ ) of Sacramento River fitted DSG model to changes in mean sea level (0.5 ft). Results are shown for multiple trained ANNs, each initialized with randomized weights and biases. ....	4-33
Figure 4-25	Sensitivity in EC ( $\mu\text{S}/\text{cm}$ ) of San Joaquin River fitted DSG model to changes in Delta outflow (-2000 cfs). Results are shown for multiple trained ANNs, each initialized with randomized weights and biases. ....	4-34
Figure 4-26	Sensitivity in EC ( $\mu\text{S}/\text{cm}$ ) of San Joaquin River fitted DSG model to changes in mean sea level (0.5 ft). Results are shown for multiple trained ANNs, each initialized with randomized weights and biases. ....	4-35
Figure 4-27	X2 model fit for the Sacramento River ( $n = 2, 5, 10$ ) with time delay of 15, 30 and 60 days. ....	4-37
Figure 4-28	Sensitivity of fitted X2 model to Qwest flow change (Sacramento River model, $n=2, 5, 10$ ) with time delay of 15, 30 and 60 days. ....	4-38
Figure 4-29	Sensitivity of fitted X2 model to mean sea level increase of 0.5 ft (Sacramento River model, $n=2, 5, 10$ ) with time delay of 15, 30 and 60 days. ....	4-39
Figure 4-30	X2 model fit for the Sacramento River model ( $n =1, d = 120$ ). Results are shown for multiple trained ANNs, each initialized with randomized weights and biases. ....	4-41
Figure 4-31	X2 model fit for the Sacramento River model ( $n=2, d=120$ ). Results are shown for multiple trained ANNs, each initialized with randomized weights and biases. ....	4-42
Figure 4-32	Sensitivity of fitted X2 (km) model to delta outflow change (Sacramento River model, $n =1, d=120$ ). Results are shown for multiple trained ANNs, each initialized with randomized weights and biases. ....	4-43
Figure 4-33	Sensitivity of fitted X2 model to delta outflow change (Sacramento River model, $n=2, d=120$ ). Results are shown for multiple trained ANNs, each initialized with randomized weights and biases. ....	4-44
Figure 4-34	Sensitivity of fitted X2 model to mean sea level increase of 0.5 ft (Sacramento River model, $n=1, d=120$ ). Results are shown for multiple trained ANNs, each initialized with randomized weights and biases. ....	4-45
Figure 4-35	Sensitivity of fitted X2 model to mean sea level increase of 0.5 ft (Sacramento River model, $n=2, d=120$ ). Results are shown for multiple trained ANNs, each initialized with randomized weights and biases. ....	4-46
Figure 4-36	X2 model fit for the San Joaquin River ( $n = 1, 2, 5, 10$ ) with time delay of 2, 15 and 30 days. ....	4-48
Figure 4-37	Sensitivity of fitted X2 model to Qwest flow change (San Joaquin River model, $n=1, 2, 5, 10$ ) with time delay of 2, 15, and 30 days. ....	4-49
Figure 4-38	Sensitivity of fitted X2 model to sea level increase of 0.5 ft (San Joaquin River model, $n =1, 2, 5, 10$ ) with time delay of 2, 15 and 30 days. ....	4-50

Figure 4-39	X2 model fit for the San Joaquin River model ( $n = 1$ , $n = 2$ ) with a time delay of 14 days .....	4-51
Figure 4-40	Sensitivity of fitted X2 model to delta outflow (San Joaquin River model, $n = 1$ , $n = 2$ ) .....	4-52
Figure 4-41	Sensitivity of fitted X2 model to mean sea level of 0.5 ft (San Joaquin River model, $n = 1$ , $n = 2$ ) .....	4-52
Figure 4-42	Sacramento River X2 targets interpolated from observed EC data against ANN predictions for the subset of data used to train the model, separated by month. The black line is $y = x$ , and the blue line is a linear regression of the plotted points. Each panel's regression $r^2$ and standard error, $\sigma$ , are also shown.....	4-54
Figure 4-43	Sacramento River X2 targets interpolated from observed EC data against ANN predictions for the subset of data used to train the model, all months. The black line is $y = x$ , and the blue line is a linear regression of the plotted points. Each panel's regression $r^2$ and standard error, $\sigma$ , are also shown. ....	4-55
Figure 4-44	Sacramento River X2 targets interpolated from observed EC data against ANN predictions for all available data, separated by month. The black line is $y = x$ , and the blue line is a linear regression of the plotted points. Each panel's regression $r^2$ and standard error, $\sigma$ , are also shown. Plots are displayed as binned counts of points to prevent overplotting. ....	4-56
Figure 4-45	Sacramento River X2 targets interpolated from observed EC data against ANN predictions for all available data, all months combined. The black line is $y = x$ , and the blue line is a linear regression of the plotted points. Each panel's regression $r^2$ and standard error, $\sigma$ , are also shown. The plot is displayed as binned counts of points to prevent overplotting. ....	4-57
Figure 4-46	Distribution of residuals from the DSG model compared to the residuals from the ANN model for the Sacramento River. ....	4-58
Figure 4-47	Increase in Sacramento River X2 position due to uniform increase of 0.5 ft to mean sea level input for Approach 3 ANN model, conditioned on G-flow, for the subset of data used to train the model.....	4-59
Figure 4-48	Increase in Sacramento River X2 position due to uniform increase of 0.5 ft to mean sea level input for Approach 3 ANN model, conditioned on G-flow and predicted X2 position, for the subset of data used to train the model. ....	4-60
Figure 4-49	Increase in Sacramento River X2 position due to uniform increase of 0.5 ft to mean sea level input for Approach 3 ANN model, conditioned on G-flow, for all available data. The plot is displayed as binned counts of points to prevent overplotting. ....	4-61
Figure 4-50	Increase in Sacramento River X2 position due to uniform increase of 0.5 ft to mean sea level input for Approach 3 ANN model, conditioned on G-flow and predicted X2 position, for all available data. ....	4-62
Figure 4-51	DSG-ANN model (black) at each station (with channel distance in km) on the Sacramento River. Observed data are plotted as binned counts to prevent overplotting. ....	4-63

Figure 4-52	Sacramento River observed EC targets against EC predictions from DSG model using ANN X2. Points are displayed as binned counts to prevent overplotting. The black line is $y = x$ , and the blue line is a linear regression of the underlying points. ....	4-64
Figure 4-53	Observed EC targets against EC predictions from DSG model using ANN X2, at each station along the Sacramento River. Each black line is $y = x$ , and each blue line is a linear regression of the underlying points. Duplicated station names at different distances come from combining Bulletin 23 and CDEC datasets. ....	4-65
Figure 4-54	San Joaquin River X2 targets interpolated from observed EC data against ANN predictions for the subset of data used to train the model, separated by month. The black line is $y = x$ , and the blue line is a linear regression of the plotted points. Each panel's regression $r^2$ and standard error, $\sigma$ , are also shown. ....	4-67
Figure 4-55	San Joaquin River X2 targets interpolated from observed EC data against ANN predictions for the subset of data used to train the model, all months. The black line is $y = x$ , and the blue line is a linear regression of the plotted points. Each panel's regression $r^2$ and standard error, $\sigma$ , are also shown. ....	4-68
Figure 4-56	San Joaquin River X2 targets interpolated from observed EC data against ANN predictions for all available data, separated by month. The black line is $y = x$ , and the blue line is a linear regression of the plotted points. Each panel's regression $r^2$ and standard error, $\sigma$ , are also shown. Plots are displayed as binned counts of points to prevent overplotting. ....	4-69
Figure 4-57	San Joaquin River X2 targets interpolated from observed EC data against ANN predictions for all available data, all months combined. The black line is $y = x$ , and the blue line is a linear regression of the plotted points. Each panel's regression $r^2$ and standard error, $\sigma$ , are also shown. The plot is displayed as binned counts of points to prevent overplotting. ....	4-70
Figure 4-58	Increase in San Joaquin River X2 position due to uniform increase of 0.5 ft to mean sea level input for Approach 3 ANN model, conditioned on G-flow, for the subset of data used to train the model. ....	4-71
Figure 4-59	Increase in San Joaquin River X2 position due to uniform increase of 0.5 ft to mean sea level input for Approach 3 ANN model, conditioned on G-flow and predicted X2 position, for the subset of data used to train the model. ....	4-72
Figure 4-60	Increase in San Joaquin River X2 position due to uniform increase of 0.5 ft to mean sea level input for Approach 3 ANN model, conditioned on G-flow, for all available data. The plot is displayed as binned counts of points to prevent overplotting. ....	4-73
Figure 4-61	Increase in San Joaquin River X2 position due to uniform increase of 0.5 ft to mean sea level input for Approach 3 ANN model, conditioned on G-flow and predicted X2 position, for all available data. ....	4-74
Figure 4-62	DSG component (black) and non-parametric adjustment (blue) model at each station (with channel distance in km) on the San Joaquin River. Observed data are plotted as binned counts to prevent overplotting. ....	4-75

---

Figure 4-63	San Joaquin River observed EC targets against EC predictions from DSG model using ANN X2. Points are displayed as binned counts to prevent overplotting. The black line is $y = x$ , and the blue line is a linear regression of the underlying points. ....	4-76
Figure 4-64	Observed EC targets against EC predictions from DSG model using ANN X2, at each station along the San Joaquin River. Each black line is $y = x$ , and each blue line is a linear regression of the underlying points. Duplicated station names at different distances come from combining Bulletin 23 and CDEC datasets. ....	4-77
Figure 4-65	Interpolated X2 compared to X2 estimates from ANN model 3A, the daily DSG model and the MacWilliams (2015) model (Red line 1:1; blue line: linear regression). Dates with negative Delta outflows were not used in the MacWilliams et al. computation. ....	4-83

# LIST OF TABLES

---

Table 3-1 ANN Model Summary .....	3-2
Table 3-2 Available Data for ANN Model Training.....	3-9
Table 3-2 (continued) Available Data for ANN Model Training.....	3-10
Table 4-1 Model fit of trained ANN models at Sacramento River (in terms of r) for different network size and time delay.....	4-5
Table 4-2 Sensitivity range of trained ANN models at Sacramento River (in $\mu\text{S/cm}$ ) to mean sea level increase of 0.5 ft.....	4-5
Table 4-3 Model fit of trained ANN models at San Joaquin River (in terms of r) for different network size and time delay.....	4-12
Table 4-4 Sensitivity range of trained ANN models at San Joaquin River (in $\mu\text{S/cm}$ ) to mean sea level increase of 0.5 ft.....	4-12
Table 4-5 Model fit of trained ANN models at EMM (in terms of r) for different network size and time delay .....	4-19
Table 4-6 Sensitivity of trained ANN models at EMM (in $\mu\text{S/cm}$ ) to mean sea level increase of 0.5 ft.....	4-19
Table 4-7 Model fit of trained ANN models at JER (in terms of r) for different network size and time delay .....	4-26
Table 4-8 Sensitivity of trained ANN models at JER (in $\mu\text{S/cm}$ ) to mean sea level increase of 0.5 ft (maximum change in EC from base case with no sea level change).....	4-26
Table 4-9 Performance of Trained Salinity ANN Model (Model 2A-1) ANN Salinity ( $\mu\text{S/cm}$ ) = $C1 + C2 \cdot \text{Observed Salinity } (\mu\text{S/cm})$ .....	4-30
Table 4-9 (continued) Performance of Trained Salinity ANN Model (Model 2A-2) ANN Salinity ( $\mu\text{S/cm}$ ) = $C1 + C2 \cdot \text{Observed Salinity } (\mu\text{S/cm})$ .....	4-31
Table 4-10 Model fit of trained ANN models at Sacramento River (in terms of r) for different network size and time delay.....	4-39
Table 4-11 Sensitivity of trained ANN models at Sacramento to mean sea level increase of 0.5 ft River (change X2 from base case, in km).....	4-40
Table 4-12 Model fit of trained ANN models at San Joaquin River (in terms of r) for different network size and time delay.....	4-51
Table 4-13 Sensitivity of trained ANN models at San Joaquin River to mean sea level increase of 0.5 ft (change in X2 from base case, in km) .....	4-51
Table 4-14 Scatterplot Statistics of ANN Model (Models 2A-1 and 2B-1), Grouped by River and Month ANN X2 (km) = $C1 + C2 \cdot \text{Observed X2 (km)}$ .....	4-79

---

Table 4-15 Scatterplot Statistics of ANN Model (Model 3A and 3B), Grouped by River  
and Month ANN Monthly X2 (km) = C1 + C2\*Observed Monthly X2 (km) ..... 4-80

Table 4-16 Scatterplot Statistics of Daily DSG Model, Grouped by River and Month.  
DSG Daily X2 (km) = C1 + C2\*Observed Daily X2 (km) ..... 4-81

Table 4-17 Scatterplot Statistics of Daily K-M Model, Grouped by River and Month. KM  
Daily X2 (km) = C1 + C2\*Observed Daily X2 (km) ..... 4-82

# ACRONYMS

---

ANN	Artificial Neural Network
DSM2	Delta Simulation Model II
CDEC	California Data Exchange Center
CDFG	California Department of Fish and Game
DWR	Department of Water Resources
IEP	Interagency Ecological Program
MLP	Multi-layer Perceptron
MSL	Mean Sea Level
SE	Standard Error
USGS	United States Geological Survey



# EXECUTIVE SUMMARY

---

The goal of this work was to develop a suite of Artificial Neural Network (ANN) models to predict daily average salinity in Suisun Bay and the western Delta. The models were designed to accept various inputs representing net flow conditions as well as tidal condition. Net flow inputs include: flow past Rio Vista on the Sacramento River (Qrio), flow past Jersey Point on the San Joaquin River (Qwest), and Delta outflow. Tidal inputs include mean sea level and the daily difference between the maximum and minimum water level, termed as the tidal range. This work was built upon prior analyses where we explored the use of a wide range of input variables for predicting salinity in western Delta stations along a gradient and at specific locations (Chen and Roy, 2013). The inputs identified above were selected based this prior work. In addition, we previously tested the potential for different modeling approaches for salinity, such as using the data alone for training, or utilizing a modeling framework in conjunction with the salinity data (Chen et al., 2014). The present approach utilizes these concepts to identify ANNs that fit observed data and also provide physically plausible responses to changes in selected input variables.

Salinity data utilized in this work were assembled through a parallel data compilation and cleaning effort and cover water years 1922–2012 (Roy et al. 2014, Hutton et al. 2015). Data from the earlier part of the record represent grab sample measurements, while data from the latter part of the record represent continuous measurements. A daily record of salinity at multiple stations was created from these data sources, albeit with some gaps in the early part of the record.

Three broad gradient approaches, as described below, were used for the ANN training:

- **Data-Driven Approach:** In this approach, ANN models were trained with station-level salinity data for the period where daily continuous records (using on-line conductivity sensors as opposed to grab samples) were available with minimal data gaps (i.e. October 1974 to June 2012). Different ANN models were developed for the Sacramento and San Joaquin River branches, and in each case different combinations of inputs, network sizes and time delays were explored to identify networks that fit the salinity data and also provided physically plausible responses to changes in flow and tidal conditions.
- **DSG-Based Approach:** In this approach, ANN models were trained with best-fit parameters associated with the Delta Salinity Gradient (DSG) model (Hutton 2014; Hutton et al., 2015). This approach has two major advantages. First, it explicitly incorporates a basic conceptual model of salinity transport in the estuary, with a strong downstream to upstream gradient; thus, the ANN training does not require a search over any general relationship, but over a more narrowly

defined one. Second, it allows for use of salinity data from the entire period of record, where gaps in data can be represented using the DSG model. As above, separate ANN models were developed for the Sacramento and San Joaquin River branches.

- **DSG Residual-Based Approach:** In this approach, ANN models were focused even more narrowly, with training being performed on the error residuals associated with DSG model X2 predictions and interpolated X2 obtained from the data. The DSG model was run to compute the X2, and errors with respect to the interpolated X2 were fit using an ANN that used the same set of inputs as above. Thus, the goal here was to relate the error in the DSG model to a broader set of inputs. Separate ANNs were developed for the Sacramento and San Joaquin River branches.

In addition to the three gradient approaches described above, two stations near the upstream end of the estuary, Emmaton on the Sacramento River and Jersey Point on the San Joaquin River, were the focus of targeted ANN model development. In prior work, we showed that these stations were less represented using a gradient model, and that a focused ANN provided better fits (Chen and Roy, 2013). Salinity prediction at these stations is important independent of the overall salinity gradient, and related to specific standards to maintain agricultural beneficial uses in the Delta. Given this importance, site-specific ANNs were developed for these stations.

This work identified suitable ANN models based on (1) the quality of fit to observed data and (2) sensitivity to changes in specific inputs such as freshwater flow, flow distribution between the Sacramento and San Joaquin Rivers, and tidal conditions. Specific ANNs (representing different combinations of time delays in flows and network size) are presented in this report, and for each input set, a specific structure is proposed for future use. Validation results presented here may be used to select a subset of ANN models that can be used in parallel to either represent salinity at a specific location or to calculate the X2 isohaline.

Overall, the ANN models developed in this work provide X2 estimates that are superior to those provided by currently available statistical methods such as the K-M and DSG models. Because the ANN models were trained on a large amount of data spanning a variety of conditions and account for variables in addition to Delta outflow, they are considered a credible alternative to the existing statistical models. Future application may allow examination of the relative significance of these secondary variables on salinity under specific conditions where improved predictive capability is needed. To a limited extent, the ANN models developed here may also be used to explore scenarios such as those related to future sea level rise. However, such analyses must be cognizant of the limited ability of ANNs to extrapolate beyond their training data sets. To evaluate scenarios with significant departures from training conditions, other modeling tools should be considered.

# 1. INTRODUCTION

---

The abundance of several biological populations in the upstream reaches of San Francisco Estuary has been correlated with the location of the low salinity zone, which depends strongly, but not solely, on freshwater outflows from the Delta (Jassby et al., 1995). The position of the 2 parts per thousand (ppt) bottom salinity isohaline, termed X2, is a regulated measure of the low salinity zone location in the estuary (State Water Resources Control Board, 2006). Depending on the water year type and season, flow requirements are based on numeric Delta outflow levels or the position of X2. Under current regulations, X2 is interpolated as an equivalent surface salinity from fixed monitoring stations and reported as a distance from Golden Gate Bridge. Besides regulations on X2 position, which are largely driven by fish and wildlife beneficial use considerations, there are also salinity regulations at compliance points in the estuary for municipal and agricultural beneficial uses. Salinity behavior in an environment such as the San Francisco Bay Delta estuary is known to be dynamic and dependent primarily on current and antecedent freshwater flows (Denton, 1993), with tidal effects playing also playing a role (Monismith et al., 2002).

Exports (and to a lesser degree upstream reservoir releases) are regulated to maintain target salinity levels, and there is great interest in accurately predicting salinity levels for efficient water operations. Robust quantitative relationships between salinity and related physical drivers are needed to better understand the historical response of salinity to different hydrologic conditions, anthropogenic modifications to rivers and upstream watersheds, and changing regulations. Over the past two decades, various modeling frameworks have been applied to predict X2 position and salinity patterns in the Delta and San Francisco Bay, ranging from simple statistical models to complex three-dimensional hydrodynamic models, as reviewed briefly in the following chapter.

The focus of this work is on artificial neural network (ANN)-based modeling for salinity. The ANN approach, containing some of the black-box aspects of all statistical models, has been demonstrated to approximate any general function (Bishop, 1995) and was considered in this work to evaluate the importance of different inputs. In the Delta and elsewhere, ANN-based prediction frameworks have demonstrated the ability to represent complex processes well, and may be considered an alternative to conventional statistical methods and mechanistic models. ANNs use simple elements (neurons) and connections between elements using a range of functional forms to represent complex real-world data. The ANN methodology has found broad application in the prediction and control of complex systems, specifically in the water resources domain (Maier et al., 2010; American Society of Civil Engineers, 2000). An ANN can be trained (in a manner similar to model calibration) to perform a particular function through adjusting values that form the connections between elements (weights and biases). The ANN approach has been used by the California Department of Water Resources (CDWR) for predicting Delta salinity response to changes in regulations, facility operations, and hydrologic changes such as sea level rise (Finch and

Sandhu, 1995; Sandhu et al., 1999; Seneviratne et al., 2008). The salinity ANNs currently being employed by CDWR are trained on hydrodynamic model (DSM2) simulation results.

The goal of this work is to develop a suite of ANN models considering a wider range of inputs than used in the most common statistical modeling frameworks for salinity in this region. For example, Kimmerer and Monismith (1992), Denton (1993), and Monismith et al. (2002) all assume Delta outflow as the main input term. This work builds on prior efforts to develop a set of salinity ANN models (Chen and Roy, 2013; Chen et al., 2014). Salinity data utilized in this work were assembled through a parallel data compilation and cleaning effort and cover water years 1922–2012 (Roy et al., 2014; Hutton et al., 2015). Data from the earlier part of the record represent grab sample measurements, while data from the latter part of the record represent continuous measurements. A daily record of salinity at multiple stations was created from these data sources, albeit with some gaps in the early part of the record.

The first phase of this work (Chen and Roy, 2013) utilized the latter part of the observed salinity record, from 1974–2012 with minimal data gaps and tested different input combinations to identify suitable models for predicting salinity as a function of distance from Golden Gate. The sole evaluation criterion was the quality of fit between observed and ANN-simulated data. Key inputs that were examined included the following net flow and tidal terms: Delta outflow, flows past Rio Vista on the Sacramento River and past Jersey Point on the San Joaquin River (identified as Qrio and Qwest, respectively, in DAYFLOW<sup>1</sup>), mean tide at Golden Gate, and tidal range at Golden Gate. For each combination of model inputs, separate ANN models were developed for the Sacramento and San Joaquin Rivers. Findings from this initial work suggested that using Qrio and Qwest flow inputs (rather than Delta outflow) slightly improved the training results. Models that used Qrio and Qwest (or Qrio and a residual between a Qrio-Qwest flow correlation) as flow inputs performed similarly, and either formulation was considered to be acceptable for future application. The comparison of ANN models trained with different tidal inputs suggested that relatively good agreement between observed and model predicted values could be achieved through use of one or two tidal terms either as tidal range, the astronomical tide, or the residual between actual and astronomical tide. Finally, although the ANNs adequately represented the salinity gradient, the furthest upstream stations were not as well represented. In particular, two of these stations (i.e. Emmaton and Jersey Point) are important water quality compliance locations and were better represented by single-station ANNs. All of these initial findings were used to guide a second phase of the ANN training.

The second phase (Chen et al., 2014) built on the initial work and employed two approaches for ANN training. One approach followed the first phase effort, i.e. ANNs were trained directly on the latter part of the data record (water year 1974–2012, containing daily data at multiple stations with minimal gaps) and the models were designed to predict salinity as a function of distance from Golden Gate. In another approach, a statistical salinity model was calibrated on the entire data record (water year 1922–2012) and the resulting best fit

---

<sup>1</sup> DAYFLOW is an accounting model used for determining Delta boundary hydrology; <http://www.water.ca.gov/dayflow/documentation/dayflowDoc.cfm>.

parameters were used for the ANN training. This latter approach has two major advantages: (1) it explicitly incorporates the basic conceptual model of salinity transport in the estuary with a strong downstream to upstream gradient, and (2) it allows for a more robust training through the use of a longer period of hydrologic and salinity record. The ability to use the longer data record is an important factor, given that ANNs (being data-driven constructs) extrapolate poorly and perform best within the training range.

In this third phase, we built upon the experience of the earlier phases and refined the ANN training methodology. The same underlying data were used for training; however, new evaluation criteria were defined that not only stressed fidelity to the training data but also stressed model sensitivity to specified changes in inputs. Both criteria were considered equally important in the selection of an appropriate model. Thus, an ANN is identified for use not only when it fits the data acceptably well, but also when the output for certain specified changes in inputs is consistent with what might be expected physically. For this application, these criteria imply that an increase in the sea level input should correspond to higher salinities, other conditions being constant. Note that we do not have a way of specifying the magnitude of the salinity change *a priori*, but we expect the sign of the salinity change to be positive when the sea level increase is positive. Similarly, these criteria imply that variation of Qrio and Qwest will have different effects on salinity in the Sacramento and San Joaquin River branches. This line of investigation is motivated by published literature on rainfall-runoff models which showed that ANN models are able to fit observed data but not always represent the sensitivity of inputs in a physically consistent manner (Kingston et al., 2005).

To more fully evaluate the benefits of the ANN modeling approach, we compared the results of this work with the DSG model (Hutton, 2014; Hutton et al., 2015) and the K-M model, with parameters as reported in the original analysis (Kimmerer and Monismith, 1992; Jassby et al., 1995), and more recent statistical models (MacWilliams et al., 2015). The remaining sections of this report describe previous work on salinity modeling in San Francisco Bay and the Delta (Chapter 2); the ANN modeling approach used (Chapter 3); results from the ANN models, comparison against existing tools and exploration of sensitivity of specific inputs such as flows and sea level (Chapter 4); and a summary of key findings and recommendations (Chapter 5).



## 2. PRIOR MODELING OF SAN FRANCISCO BAY AND DELTA SALINITY

---

Given the importance of salinity in the San Francisco Bay Delta estuary to municipal, agricultural and fish and wildlife beneficial uses, a variety of quantitative tools have been developed to describe salinity behavior in the region for different applications. This chapter presents a brief summary of the commonly used tools.

### 2.1 STATISTICAL MODELING

A widely used tool to predict salinity in the estuary is the autoregressive equation between Delta outflow and X2 position, termed the K-M model (Kimmerer and Monismith, 1992; Jassby et al., 1995). This equation was calibrated using salinity data in the estuary from October 1967 to November 1991, the most complete data set available at the time of publication. The monthly flow-X2 relationship (Kimmerer and Monismith, 1992) has been expressed as<sup>2</sup>:

$$X2(t) = 122.2 + 0.328X2(t-1) - 17.6 \log(Q_{out}(t)) \quad \text{Eq 2.1}$$

where  $Q_{out}$  is the mean monthly Delta outflow in terms of cubic feet per second (cfs) and  $X2(t-1)$  is the previous month isohaline position expressed as km from Golden Gate. As a general tool for estimating X2 under different flow conditions, the above equation is used widely. A similar formulation has been proposed (and calibrated with the same surface salinity dataset) using an exponential rather than a logarithmic  $Q_{out}$  term (Monismith et al., 2002). This was presented as:

$$X2(t) = 0.919X2(t-1) + 13.57Q_{out}(t)^{-0.141} \quad \text{Eq 2.2}$$

The constants above apply to X2 in units of km and  $Q_{out}$  in  $m^3/\text{second}$ . This formulation was also utilized by Gross et al. (2009) to fit modeled values of X2 from a three-dimensional hydrodynamic model (TRIM3D) resulting in slightly different fitted constants. The form of this equation was further extended by MacWilliams et al. (2015) who modified the Monismith et al. (2002) formulation with a weight applied to the autoregressive term and to the outflow term, and calibrated the equation parameters using modeled X2 values obtained from a three-dimensional hydrodynamic model (UnTRIM). Importantly, the X2 values used by Gross et al. (2009) and MacWilliams et al. (2015) were not derived from surface salinity--as used by Jassby et al., 1995; Monismith et al., 2002; and the present work--but based on near-bottom salinity obtained from their respective hydrodynamic models. X2, as described in Chapter 1, is defined in terms of bottom salinity, hence these three-dimensional model-based approaches, although using synthetic

---

<sup>2</sup> A slightly different intercept for this equation has also been reported for flow in  $m^3/\text{second}$ :  
 $X2(t) = 95 + 0.33X2(t-1) - 17.6 \log(Q_{out}(t))$  (Jassby et al., 1995)

data, are faithful to the original definition. Using data from 1994-1997, MacWilliams et al. (2015) reported that their statistical approach fitted the X2 data with greater accuracy than prior formulations.

Another tool to predict salinity in the estuary was developed by Denton (1993,1994) utilizing boundary salinity values representative of the downstream ocean and upstream riverine environments and a concept called antecedent outflow, representing flow time history in the Delta. The equation can be represented as:

$$S = (S_o - S_b) * \exp[-\alpha * G(t)] + S_b \quad \text{Eq. 2.3}$$

where  $S$  is the salinity at a given location,  $S_o$  and  $S_b$  are the ocean and river boundary salinities, and  $G(t)$  is the term representing the flow history, and  $\alpha$  is an empirically-determined constant, computed for selected Delta locations based on field data. The so-called G-model estimates salinity at individual locations, rather than the X2 position estimated using the K-M equation. This is important because some salinity standards are described in terms of electrical conductivity at individual stations in the current Water Quality Control Plan, e.g., Emmaton on the Sacramento River and Jersey Point on the San Joaquin River (State Water Resources Control Board, 2006). Specific EC target values at these stations are defined by the type of water year and the month.

A hybrid of the X2 models and the G-model was proposed by Hutton (2014; Hutton et al., 2015) and is called the Delta Salinity Gradient (DSG) model. In this model, by assuming the modified form of the X2 equation (Monismith et. al. 2002) and quasi-steady-state conditions, X2 is related to antecedent outflow as follows:

$$X2(t) = \Phi_1 * G(t)^{\Phi_2} \quad \text{Eq. 2.4}$$

where  $\Phi_1$  and  $\Phi_2$  are empirically determined coefficients. Salinity is then estimated at individual locations through the following relationship:

$$S = (S_o - S_b) * \exp[\tau * (X/X2)^{-1/\Phi_2}] + S_b \quad \text{Eq. 2.5}$$

where  $S$  is the salinity at a given location in mS/cm,  $S_o$  and  $S_b$  are representative downstream ocean and upstream riverine boundary salinities, and  $\tau = \ln[(2.64 - S_b)/(S_o - S_b)]$ . This equation can be used to determine salinity at any longitudinal distance from Golden Gate ( $X$ ) given X2 and  $\Phi_2$  and assuming reasonable values for  $S_o$  and  $S_b$ .

## 2.2 NUMERICAL MODELING

Numerical models of hydrodynamics and salinity, albeit more complex and demanding of computer time and user expertise, are often employed for different applications in the San Francisco Bay and Delta. The one-dimensional link-node model of Delta hydrodynamics and salinity, CDWR's Delta Simulation Model (DSM2), is used widely to represent salinity under different hydrologic, regulatory, and facility operations conditions. DSM2 runs can be used to represent multi-decade-long simulations over reasonable computational time frames, typically several hours.

Resource Management Associates (RMA) has developed a two-dimensional model for the Bay-Delta, the RMA-Bay Delta model. This model has recently been used to examine the effects of sea level rise as part of the Bay Delta Conservation Plan effort (Administrative Draft, March 2013, Appendix 29A).

Three-dimensional modeling for salinity and flow in the entire estuary and Delta has been performed to evaluate specific projects and to understand mechanistic processes of salinity intrusion under different flow and tidal conditions using the TRIM3D model (Gross et al., 2007, 2009) and the UnTRIM model (MacWilliams et al., 2015) and more recently using the SCHISM model (Semi-implicit Cross-scale Hydroscience Integrated System Model; Zhang, 2014)<sup>3</sup>. Although theoretically rigorous, the computational demands of three-dimensional models limit the length of the model runs. Recent published studies using the TRIM3D and UnTRIM models present runs that include calibration and application over two to three years (Gross et al., 2009; MacWilliams et al., 2015).

### 2.3 ANN-BASED MODELING

ANN models, the specific focus of this study, have also been used to represent flow and salinity in the Delta. Early work focused on the development of ANNs using observed data at selected locations (Finch and Sandhu, 1995); more recent work has employed ANNs trained on synthetic data generated from DSM2, including scenarios that are different from current/historical conditions and employ changes in sea level and tidal amplitude (Wilbur and Munevar, 2001; Mierzwa, 2002; Seneviratne et al., 2008). When used in this manner, ANNs emulate DSM2 behavior rather than serve as an independent model of salinity. Because ANNs run significantly faster than the mechanistic models they are trained on, the DSM-emulating ANNs can be employed within planning models used for water resources management, where there is a need to return results rapidly for a large number of flow scenarios. The approach presented in this work differs from the DSM2 based emulation approaches and is similar to the approach reported by Finch and Sandhu (1995), except for consideration of a much wider data set, inputs, and ANN structures.

---

<sup>3</sup> [http://baydeltaoffice.water.ca.gov/modeling/deltamodeling/models/bay\\_delta\\_schism/](http://baydeltaoffice.water.ca.gov/modeling/deltamodeling/models/bay_delta_schism/)



# 3. ARTIFICIAL NEURAL NETWORK MODELING APPROACH

---

This chapter provides an overview of the ANN modeling approaches and the data used. As described in Chapter 1, this work builds on previous ANN modeling efforts (Chen and Roy, 2013; Chen et al. 2014) in defining the model structure and inputs. The general naming convention used in the previous efforts was modified to provide a more intuitive nomenclature. The new approach developed in this work is termed the DSG Residual-Based approach. The following summarizes the previous and new approaches used:

- **Data-Driven Approach:** In this approach, ANN models were trained with station-level salinity data for the period where daily continuous records (using on-line conductivity sensors as opposed to grab samples) were available with minimal data gaps (i.e. October 1974 to June 2012). Different ANN models were developed for the Sacramento and San Joaquin River branches, and in each case different combinations of inputs, network sizes and time delays were explored to identify networks that fit the salinity data and also provided physically plausible responses to changes in flow and tidal conditions.
- **DSG-Based Approach:** In this approach, ANN models were trained with best-fit parameters associated with the Delta Salinity Gradient (DSG) model (Hutton 2014; Hutton et al., 2015). This approach has two major advantages. First, it explicitly incorporates a basic conceptual model of salinity transport in the estuary, with a strong downstream to upstream gradient; thus, the ANN training does not require a search over any general relationship, but over a more narrowly defined one. Second, it allows for use of salinity data from the entire period of record, where gaps in data can be represented using the DSG model. As above, separate ANN models were developed for the Sacramento and San Joaquin River branches.
- **DSG Residual-Based Approach:** In this approach, ANN models were trained on the error that remained on a DSG model of the data to interpolated X2. For each day, the DSG-based X2 was computed using Eq 2.4, and the error was trained with an ANN that used freshwater inflows, mean sea level, and tidal range as inputs. Separate ANNs were developed for the Sacramento and San Joaquin River branches.

In addition to the three gradient approaches described above, two stations near the upstream end of the estuary, Emmaton on the Sacramento River and Jersey Point on the San Joaquin River, were the focus of targeted ANN model development. In prior work, we showed that these stations were less represented using a gradient model, and that a focused ANN provided better fits (Chen and Roy, 2013). Salinity prediction at these stations is important independent of the overall salinity gradient, and related to specific standards to maintain

agricultural beneficial uses in the Delta. Given this importance, site-specific ANNs were developed for these stations.

Table 3-1 summarizes the ANN models that are described in the remainder of this chapter. The table assigns an alphanumeric code to each model for systematic reference; the table also summarizes the model type and relevant salinity output variable(s) and flow input variable(s) associated with each model.

**Table 3-1  
ANN Model Summary**

ANN Approach	Model Code	Model Type	Salinity Output	Flow Input Variable(s)
Data-Driven	1A-1	Gradient	Sacramento River EC	Qrio & Qwest
Data-Driven	1A-2	Gradient	Sacramento River EC	Delta Outflow
Data-Driven	1B-1	Gradient	San Joaquin River EC	Qrio & Qwest
Data-Driven	1B-2	Gradient	San Joaquin River EC	Delta Outflow
Data-Driven	1C-1	Station-Specific	Emmaton EC	Qrio & Qwest
Data-Driven	1D-1	Station-Specific	Jersey Point EC	Qrio & Qwest
DSG-Based	2A-1	Gradient	Sacramento River X2 and DSG parameters	Qrio & Qwest
DSG-Based	2A-2	Gradient	Sacramento River X2 and DSG parameters	Delta Outflow
DSG-Based	2B-1	Gradient	San Joaquin River X2 and DSG parameters	Qrio & Qwest
DSG-Based	2B-2	Gradient	San Joaquin River X2 and DSG parameters	Delta Outflow
DSG Residual-Based	3A	Gradient	Sacramento River DSG parameters	Qrio & Qwest to calculate X2; Antecedent Outflow to calculate salinity along gradient
DSG Residual-Based	3B	Gradient	San Joaquin River DSG parameters	Qrio & Qwest to calculate X2; Antecedent Outflow to calculate salinity along gradient

### 3.1 ARTIFICIAL NEURAL NETWORK (ANN) MODEL STRUCTURE

#### 3.1.1 Model Inputs

The inputs for the data-driven ANN models are:

- Station distance (in km) from Golden Gate

- Net Flow inputs (obtained from the DAYFLOW program) – Rio Vista flow on the Sacramento River (Qrio) and San Joaquin River flow downstream of Jersey Point (Qwest), or Delta outflow (Qout).
- Tidal inputs – mean sea level at Golden Gate and tidal range, defined as the difference between the maximum and minimum water levels on each day.

Model inputs for the DSG-based and DSG residual-based ANN models are similar to those used for the data-driven ANN models. However, as discussed in Chapter 1, the data-driven ANN models are trained on the more recent part of the data record (WY 1974-2012) while the other ANN models are trained on the entire period of record (WY 1922-2012). The DSG residual-based ANN models are unique in that they use antecedent outflow (see Eq 2.4) as a flow input.

### **3.1.2 Model Outputs**

Different ANN models were developed for the Sacramento River and San Joaquin River branches. The training was based on salinity at fixed stations on each river reach. Training stations for the Sacramento River ANN models were at a number of locations along the lower Sacramento River and several downstream stations. Training stations for the San Joaquin River ANN models were at a number of locations along the lower San Joaquin River and several downstream stations. Note that both sets of ANN models used the same downstream stations. The stations used for training are provided in Table 3-1 for the data-driven approach and Table 3-2 for the DSG-based and DSG residual-based approaches. Stations less than 50 kilometers from Golden Gate were excluded from training.

The data-driven ANN models predict salinity as a function of (1) distance along the Sacramento and San Joaquin Rivers, (2) flow inputs, (3) mean sea level and (4) tidal range. The remaining ANN models predict X2 position; this intermediate output is then used to predict salinity as a function of distance from Golden Gate.

Data-driven ANN models were also developed for two stations separately because of their importance in the existing salinity compliance regulations in the 2006 Water Quality Control Plan for the San Francisco Bay/Sacramento-San Joaquin Delta Estuary: Emmaton on the Sacramento River and Jersey Point on the San Joaquin River. In prior work we showed that the gradient ANN models performed relatively poorly at the upstream stations, and that the performance was improved by using site specific ANN models for these stations (Chen and Roy, 2013).

### **3.1.3 Network Structure**

The dynamic nature of flow and salinity in Suisun Bay and the western Delta requires a network structure that takes into account the time series of inputs. Although other network structures were used in different applications, the multi-layer perceptrons (MLPs) are by far the most popular network structures used in water resource applications to date, representing more than 90% of the peer-reviewed applications related to water resources generally (Maier et al. 2010), and two-thirds of recent publications specifically related to water quality (Wu et al. 2014). For this reason, the feedforward MLP network was selected for this application.

ANN models were generally developed by accounting for station distance (integrating all stations along a river). However, to remedy poorer performance of these gradient models at the more upstream locations (where salinity may be affected by land-side factors in addition to seawater intrusion), station-specific ANN models were developed for selected stations as described above.

### **3.1.4 Training Method**

#### **Data-Driven Approach**

ANN training was performed using the Neural Network Toolkit within the Matlab programming environment (Beale et al., 2011). ANN training approaches address the problem of over-fitting using two techniques for improved generalization: early stopping and regularization. Early stopping can be achieved through dividing the data into training, validation and testing. During training, the error using the validation data is monitored. When error using the training dataset decreases over continuing cycles of training, error from the validation dataset may increase beyond a point. This is a sign of over-fitting and the training is stopped. In this work, the data were divided in the following manner: 50%, 25%, and 25% for training, validation and testing, respectively, in order to prevent over-fitting. The training and validation data were used together in calculating the ANN model biases and weights, and the test data set were completely independent for additional evaluation of model performance. The dates for training, validation and testing were randomly selected from the entire dataset for each training cycle.

An alternative method for improving generalization during ANN training is termed regularization (Beale et al., 2011). This involves modifying the performance function that is used to track the error between the target and ANN-calculated data, by adding a term that consists of mean of the sum of squares of the network weights and biases. This leads the trained network to have smaller weights and biases, with smoother response, and reduced likelihood of over-fitting. Regularization was accomplished by using the Bayesian regularization training function (`trainbr`) in Matlab.

All data-driven ANN models utilized mean sea level and tidal range as tidal inputs. Models 1A-1, 1B-1, 1C-1 and 1D-1 utilized Qrio and Qwest as net flow inputs, while models 1A-2 and 1B-2 utilized Delta outflow (Qout) as the net flow input. Model performance was evaluated using two criteria: 1) overall fit of the model and 2) sensitivity analysis to input variables (flow and tide). The same values were used as input to using different model structures (with different number of neurons), and the training was performed multiple times (5 to 6 times) for each structure with a time delay of 120 days. This was done to examine the effect of multiple training instances on the results. In each instance, the weights and biases to be fitted were randomized at initiation and the training process resulted in ANN models that may have similar fits albeit different sensitivity. A sensitivity analysis to input variables (flow and tide) was performed. If the results for a certain network structure showed that the sensitivity responses to input variables were uniform across all trained models, that network structure was considered to be reasonable.

The sensitivity analysis was applied over the entire time period of the available data, with a specific input modified by a fixed amount. Thus, rather than evaluate steady state sensitivity, we evaluated sensitivity over a wide range of inputs. The sensitivity analysis

for flow components was done by adding 2000 cfs to Qwest flow and subtracting 2000 cfs from Qrio flow, i.e., the overall delta outflow remained unchanged. The sensitivity analysis for mean sea level consisted of imposing a 0.5 ft increase.

A broader range of network sizes (number of neurons in the hidden layer,  $n = 1$  to 5) and time delays (days,  $d = 15$  to 120 days) was also used in the training, and sensitivity analysis on the mean sea level term was performed. The model with the best performance (quality of fit) and a reasonable sensitivity may be considered for future use.

### **DSG-Based Approach**

The DSG-based approach is the same as the data-driven approach with respect to model inputs and outputs, but the structure of the calculations was different. In this case, an intermediate ANN model was developed to predict X2 position. This interpolated X2 from data (Hutton et al., 2015; Roy et al., 2014) was employed in Eq 2.5 to fit salinity data across the gradient for each day. The best fit parameters associated with Eq 2.5 ( $S_o$ ,  $S_b$ , and  $\Phi_2$ ) were then fitted with a second ANN model using the same inputs as the data-driven ANN models. During application, the first ANN model first computes the X2 and the second model uses the calculated X2 and other parameters in Eq. 2.5 to predict salinity along distance.

### **DSG Residual-Based Approach**

The hybrid structure of the DSG residual-based ANN models necessitated somewhat different fitting procedures. Rather than training an ANN model to provide an intermediate X2 prediction, the value is calculated as a function of antecedent outflow per Eq. 2.4 assuming the empirical DSG model best-fit parameters. The residual error between model prediction and observed X2 is then fit to an ANN model using the other inputs (Qwest, Qrio, tidal range and mean sea level). The parameters in the model are estimated in a Bayesian context with a Markov Chain Monte Carlo algorithm (Hoffman and Gelman 2014) that is an extension of an approach previously used for Bayesian neural network training (Neal 1995). We used a heavy-tailed likelihood distribution to decrease the sensitivity of the fitting process to outliers in the data.

Focusing the ANN model on the errors of the empirical DSG model (that already fits the X2 data quite well) allows for use of a small network structure (one layer, three hidden nodes). The prior distributions regularize the training towards the “null model” consisting of no ANN adjustment to the empirical DSG model estimate, helping prevent over-fitting. The effect of increasing mean sea level was restricted to be nonnegative via prior distributions on the associated weights and biases.

### **3.1.5 Summary of ANN modeling approaches**

The different ANNs are summarized graphically in Figure 3-1. The analysis approach used for each gradient-focused ANN is shown in Figure 3-2, where two different combinations of inputs were considered.

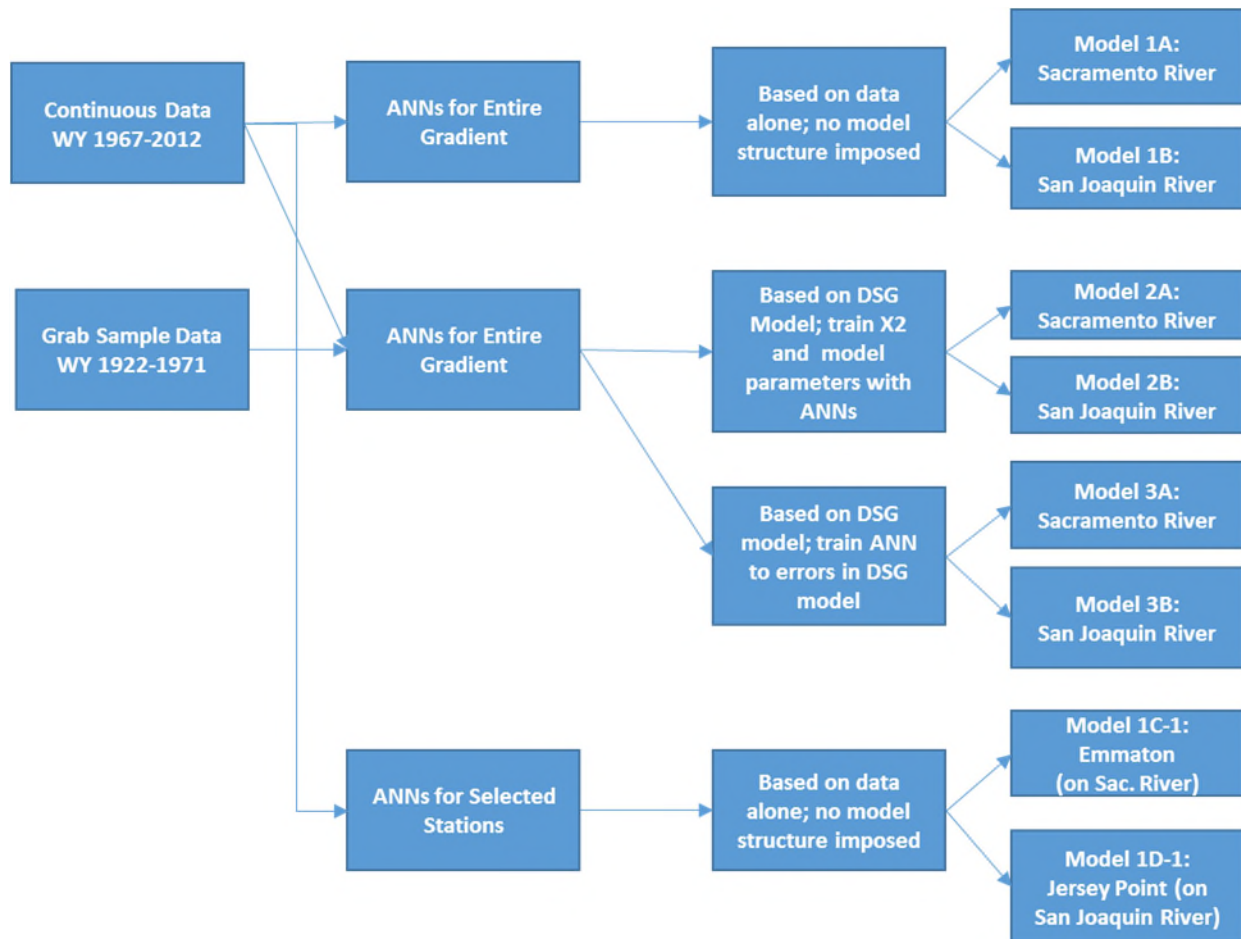


Figure 3-1 Overview of ANNs developed as part of this analysis.

## 3.2 DEVELOPMENT OF TRAINING DATA

### 3.2.1 Flow

Daily flow data used as input for the ANN models were obtained from the DAYFLOW program for WYs 1930-2012. Daily flow data for the period WYs 1922-1929, as developed for the DSG model (Hutton, 2014), were also utilized. The role of freshwater flow in regulating salinity in the Delta was evaluated by using Rio Vista and Qwest flow as two separate terms in the training.

### 3.2.2 Tide

Data for mean sea level and tidal range at Golden Gate used in the training were obtained from the National Oceanic and Atmospheric Administration (NOAA) (mean seal level, MSL at hourly time steps).

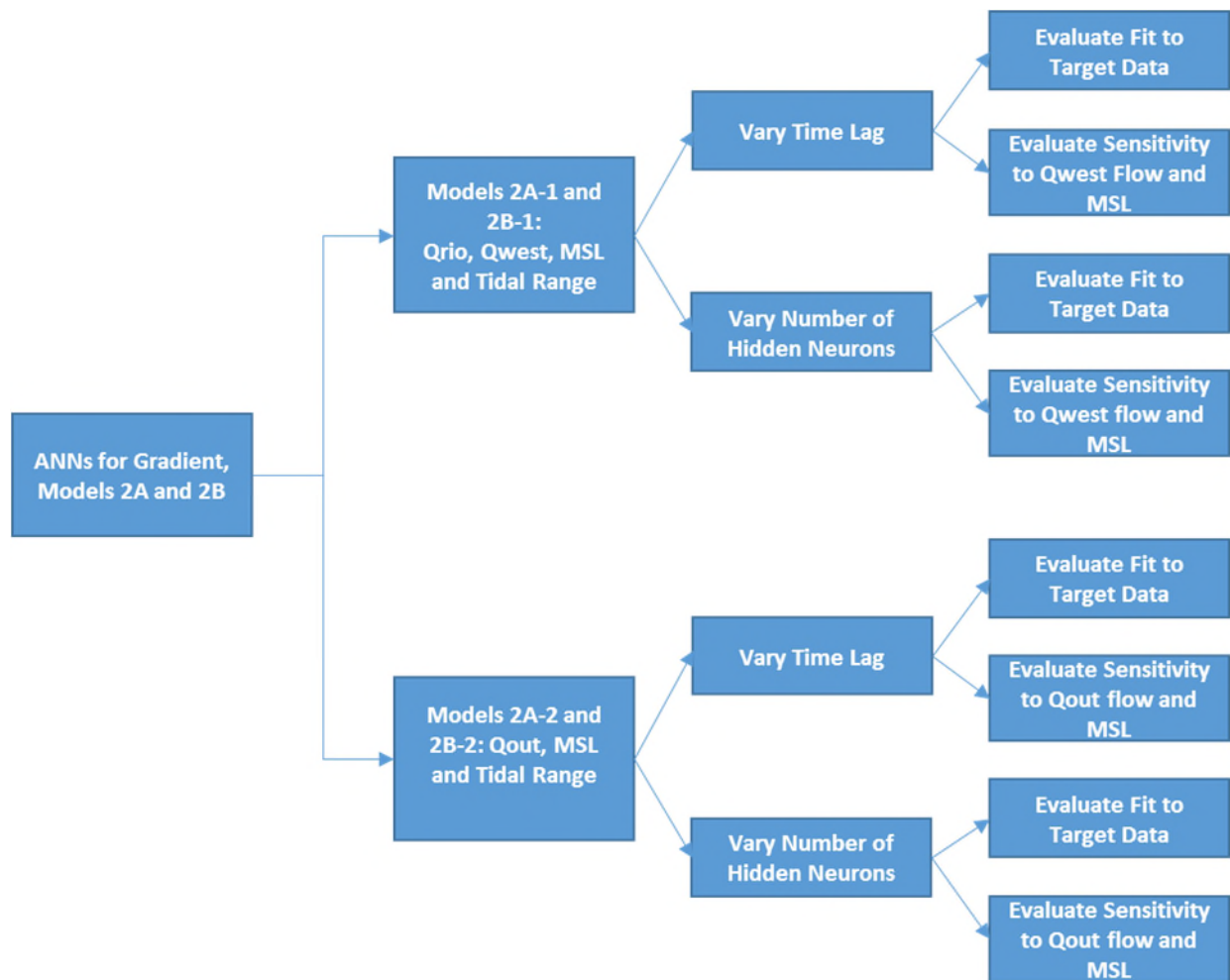


Figure 3-2 Overview of analysis performed on ANNs focused on the salinity gradient.

### 3.2.3 Salinity

The salinity data used for training were assembled from several sources as described below. The complete data set is summarized in Table 3-2.

#### 3.2.3.1 CDEC Data

The salinity data (in terms of electrical conductivity, EC, and reported in units of  $\mu\text{S}/\text{cm}$ ) used in the training were obtained from CDEC, IEP, and STORET for the period of 1964-2012. Data cleaning was accomplished using expected relationships between EC and flow at different locations and expected correlations between the adjacent stations. These expected functions were used to identify potential data errors in the dataset that were outside a certain range of the expected functions (e.g., two standard errors). The data cleaning procedures are described elsewhere (Roy et al. 2014; Hutton et al. 2015). Data filling was accomplished using linear interpolation for data gaps less than 8 days. For data gaps greater than 8 days, correlations with nearby stations were used to fill the gaps.

### 3.2.3.2 US Geological Survey (USGS) Data

The salinity data obtained from the USGS for stations in the Bay were reported in practical salinity units (psu). For consistency with other data sets, the USGS data were converted to EC using an approach outlined by Schemel (2001).

$$X_{25,S} = \left(\frac{S}{35}\right) \times (53087) + S(S - 35) \times [J_1 + (J_2 \times S^{\frac{1}{2}}) + (J_3 \times S) + (J_4 \times S^{\frac{3}{2}})]$$

Eq. 3.1

where:

$$X_{25,S} = \text{EC at } 25^{\circ}\text{C}, J_1 = -16.072, J_2 = 4.1495, J_3 = -0.5345, J_4 = 0.0261.$$

Similar to the CDEC data, correlations between adjacent stations were used to fill larger data gaps (> 8 days). The salinity data obtained from the USGS for stations in the Bay included Point San Pablo (PSP) at near-surface and Carquinez (CAR) at mid-depth. The CAR station did not have measurements at near-surface depths. Previous studies have shown that no single and straight-forward relationship exists between bottom and surface salinity across multiple Bay stations (List, 1994), therefore a conversion from mid-depth and surface salinity (at a different location) was not performed for CAR. The data obtained at mid-depth for CAR were used directly in the training. The non-availability of surface salinity data at this station may contribute to the uncertainty in X2 fits, especially during high flow periods when the X2 position is downstream, and when the salinity at CAR is used for interpolating X2 position. The filling procedure resulted in a continuous block of salinity data from 1964-2012 for the western Delta stations and from September 1990 to September 2008 for the Bay stations.

### 3.2.3.3 Bulletin 23 Data

Compilation of the 1921-1971 salinity data (referred to as Bulletin 23 data) is described in detail in Roy et al. (2014) and Hutton et al. 2015. The salinity data in these reports are grab samples collected at fixed locations typically every 4 days, one and one-half hours following higher high tide, which corresponds to the highest salinity for the day. There were exceptions in that on some dates data were not collected or not sampled at the higher high tide.

The development of the Bulletin 23 database included the following steps: converting observed data to a common salinity unit, accounting for tidal effects on grab samples, converting values to represent a daily average salinity, cleaning data, and filling data gaps. Once the Bulletin 23 data were converted to daily average EC, a more sophisticated cleaning exercise was performed by comparing daily average EC values at pairs of stations. The data filling was conducted based on the salinity data of nearby stations. The same regression relationships between pairs of stations that were used for data cleaning in the previous section were repeated on the cleaned dataset. After the “neighbor station filling” was completed, any remaining short gaps (up to 8 days, inclusive) in each station’s salinity record were linearly interpolated.

**Table 3-2  
Available Data for ANN Model Training**

Station Name	Code	Distance	Time Periods	Data Count
<b>Bay Stations</b>				
Point Orient	PTO	19.8	Bulletin 23	12,637
Point Davis	PTD	40.6	Bulletin 23	13,327
Crocket	CRK	44.6	Bulletin 23	12,521
Benicia	BEN	52.3	Bulletin 23	12,567
Martinez	MRZ	52.6	Bulletin 23	12,621
Bulls Head Point	BHP	54.7	Bulletin 23	7,680
West Suisun	WSN	59.5	Bulletin 23	12,032
Bay Point	BPT	64.2	Bulletin 23	9,100
Port Chicago	PCT	66	Bulletin 23	12,429
O. and A. Ferry	OAF	74.8	Bulletin 23	13,370

Station Name	Code	Distance	Time Periods	Data Count
<b>Sacramento River Stations</b>				
Collinsville	CLL	81.8	Bulletin 23	13,609
Emmaton	EMM	92.9	Bulletin 23	13,104
Threemile Slough Bridge	TSB	96.6	Bulletin 23	13,097
Rio Vista Bridge	RVB	102.2	Bulletin 23	13,229
Isleton Bridge	ITB	110.6	Bulletin 23	7,491
Point San Pablo	PSP	22	CDEC	16,839
Carquinez	CAR	45.5	CDEC	17,010
Martinez	MRZ	54	CDEC	6,033
Port Chicago	PCT	64	CDEC	17,389
Mallard	MAL	75	CDEC	17,505
Collinsville	CLL	81	CDEC	16,985
Emmaton	EMM	92	CDEC	17,420
Rio Vista Bridge	RVB	101	CDEC	17,420

**Table 3-2 (continued)**  
**Available Data for ANN Model Training**

Station Name	Code	Distance	Time Periods	Data Count
<b>San Joaquin River Stations</b>				
Antioch	ANH	88.4	Bulletin 23	13,315
Antioch Bridge	ANB	93.7	Bulletin 23	12,904
Jersey Point	JER	98.8	Bulletin 23	13,272
False River	FRV	101.2	Bulletin 23	12,171
Oulton Point	OPT	108.1	Bulletin 23	5,395
San Andreas Landing	SAL	113.1	Bulletin 23	5,395
Webb Pump	WBP	115.9	Bulletin 23	3,659
Point San Pablo	PSP	22	CDEC	16,839
Carquinez	CAR	45.5	CDEC	17,010
Martinez	MRZ	54	CDEC	6,033
Port Chicago	PCT	64	CDEC	17,389
Mallard Island	MAL	75	CDEC	17,505
Antioch	ANH	85.75	CDEC	17,561
Blind Point	BLP	92.85	CDEC	17,540
Jersey Point	JER	95.75	CDEC	17,388
Threemile Slough Bridge	TSL	100.4	CDEC	17,526
San Andreas Landing	SAL	109.2	CDEC	17,405

### 3.3 UNDERSTANDING THE ROLE OF QWEST

This work considered the use of Qrio and Qwest as inputs as an alternative to Qout. This was done to assess the impacts of the two flow components at different points along the salinity gradient. It is recognized that the mixing of the two flows will render the effects of the individual flow components indistinguishable after some travel distance along the estuary. However, it is thought that the Jersey Point location on the San Joaquin River may exhibit some characteristic responses to Qwest flows, particularly when the flows are low or negative. In the following chapter, we show the Jersey Point salinities from different ANNs corresponding to a fixed change in Qwest. Below, we show the observations over the entire data record being used (Figure 3-3). Jersey Point salinities may be higher during low Qwest flows, but not consistently so. Low and negative Qwest flows (disregarding antecedent flow) show a wide range of salinity outcomes. However, when antecedent flows are considered, it is more likely that Jersey Point salinities are high when these flows are very low. The lack of a clear response to Qwest alone highlights the limitations of the sensitivity test for this variable.

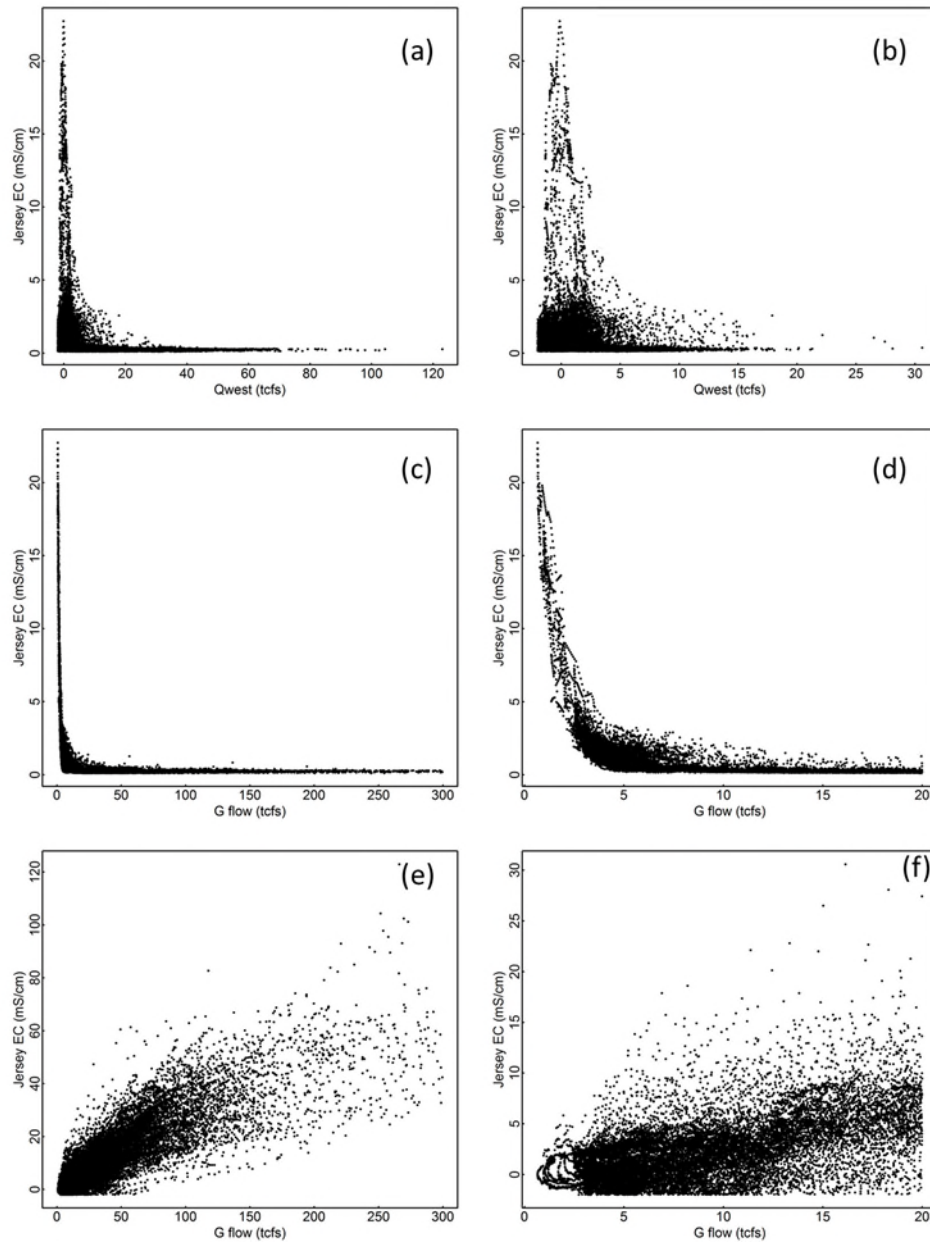


Figure 3-3 Relationship between Jersey Point (JER) EC values and Qwest and G-flow (both in thousand cfs, tcf). Plots (a), (c), and (e) show the expanded range of flow values on the x-axis; plots (b), (d), and (f) show the same data with a limited x-axis to show the behavior at low flows.

## 4. RESULTS

---

This chapter presents results of the ANN training for predicting salinity at stations in Suisun Bay and the western Delta. Trained models were evaluated using two criteria: (1) model fit and (2) performance of the sensitivity analysis to selected flow and tidal inputs. Refer to Table 3-1 for ANN model nomenclature.

### 4.1 DATA-DRIVEN SACRAMENTO RIVER ANN MODELS

#### 4.1.1 *Model 1A-1 (Using Qrio, Qwest, MSL and Tidal Range as Inputs)*

##### A. Training using time delay of 60 days

The overall model fit for five independently trained models (n=1 neuron in the hidden layer, d=60 days) was generally good, with correlation coefficient of 0.975 (Figure 4-1). Sensitivity to Qwest flow as tested for a station at Emmaton consistently ranged from 0 – 40  $\mu\text{S}/\text{cm}$  (Figure 4-2). Sensitivity of EC at Emmaton to a 0.5 ft increase of mean sea level was also consistent, and positive, from 0 – 400  $\mu\text{S}/\text{cm}$  (Figure 4-3). For a time delay of 60 days, sensitivity to mean sea level became less consistent when network size was greater than 1 hidden neuron (among trained models of n=1 to 3).

##### B. Training for different network sizes and time delay

The ANN models were also trained for a broader range of network sizes (1 to 3 neurons in the hidden layer) and time delay (30 to 120 days; Table 4-1). Each network was trained 2 to 3 times (in each instance the weights and biases are randomized). The sensitivity to mean sea level was tested at Emmaton to see if response is uniform among the models of the same network structure. The overall model fit improved with increases of network sizes and time delay. However the sensitivity to mean sea level began showing some noise when network size or time delay increased, suggesting a possibility of over-fitting (Table 4-2). The models that best balanced performance and physically meaningful sensitivity to mean sea level increase were models with 1 hidden neuron and a 120 day time delay ( $r = 0.976$ ), 2 hidden neurons with a 30 day time delay ( $r = 0.988$ ), and 3 hidden neurons with a 120 day time delay ( $r = 0.990$ ).

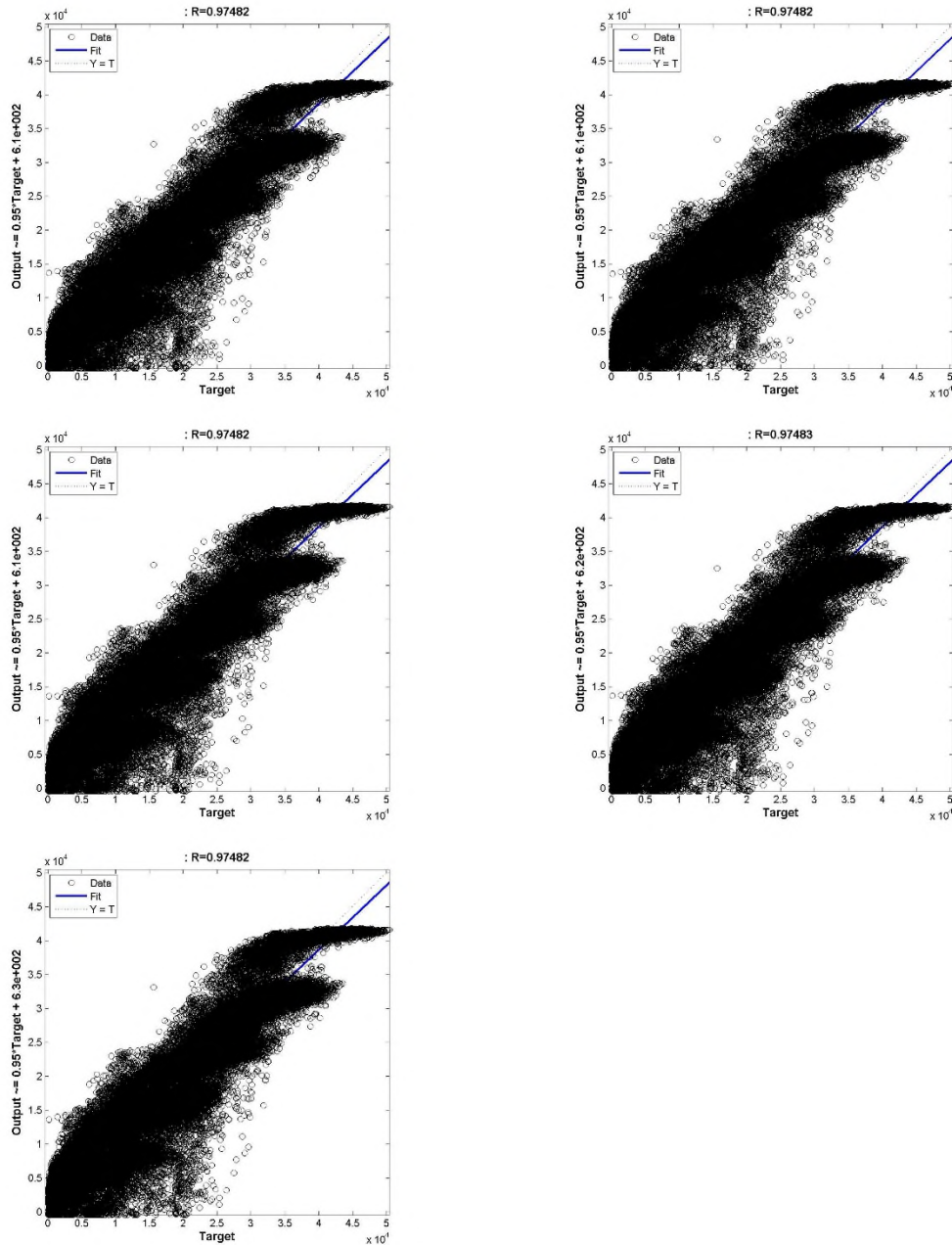


Figure 4-1 Performance of trained Sacramento River Model using Qrio, Qwest, MSL and tidal range as inputs ( $n=1$ ,  $d=60$ ). Results are shown for multiple trained ANNs, each initialized with randomized weights and biases.

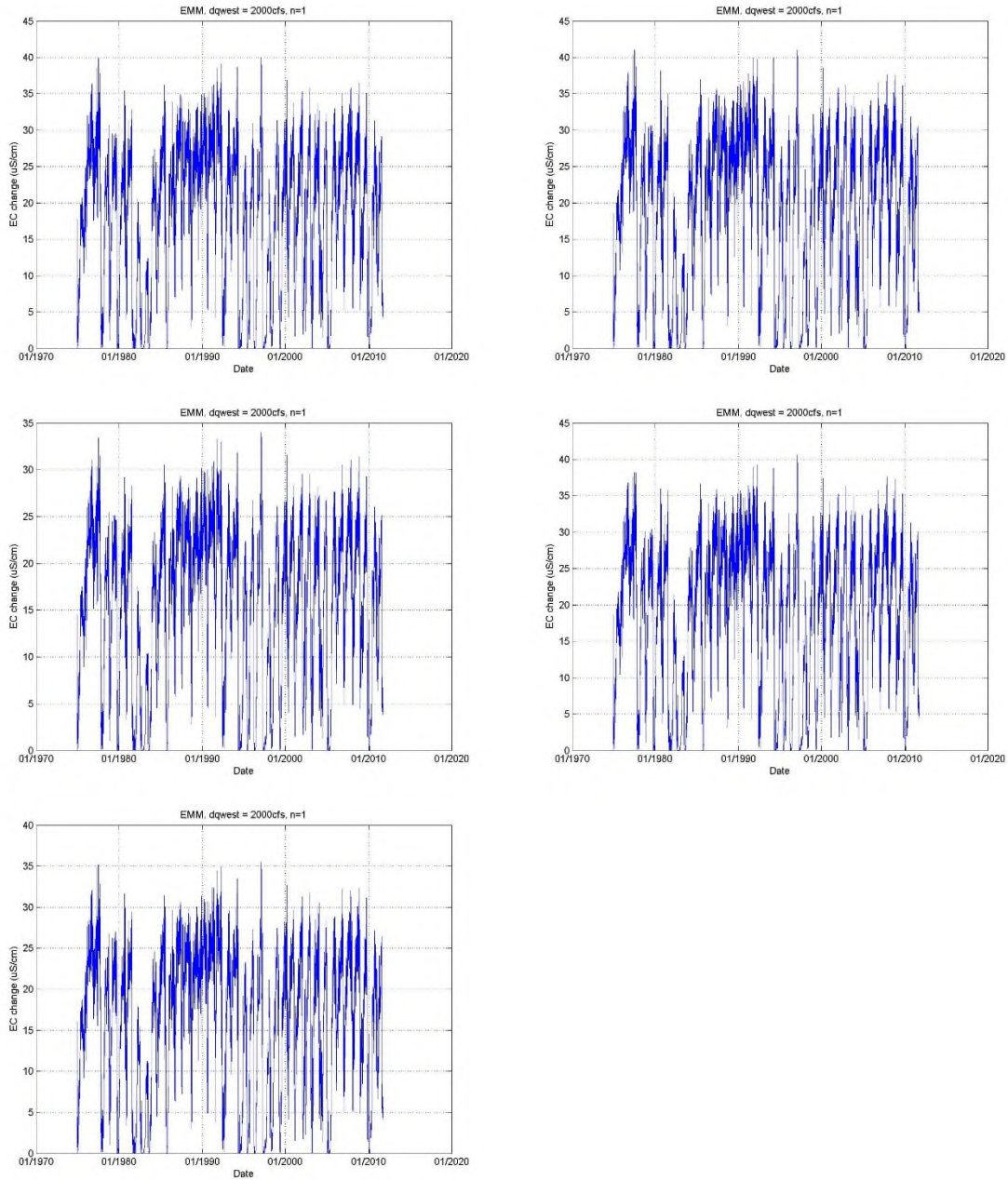


Figure 4-2 Sensitivity of trained Sacramento River Model ( $n=1$ ,  $d=60$ ) at EMM to changes in Qwest flow of 2000 cfs (+2000 cfs to Qwest flow, and -2000 cfs to Qrio flow). Results are shown for multiple trained ANNs, each initialized with randomized weights and biases.

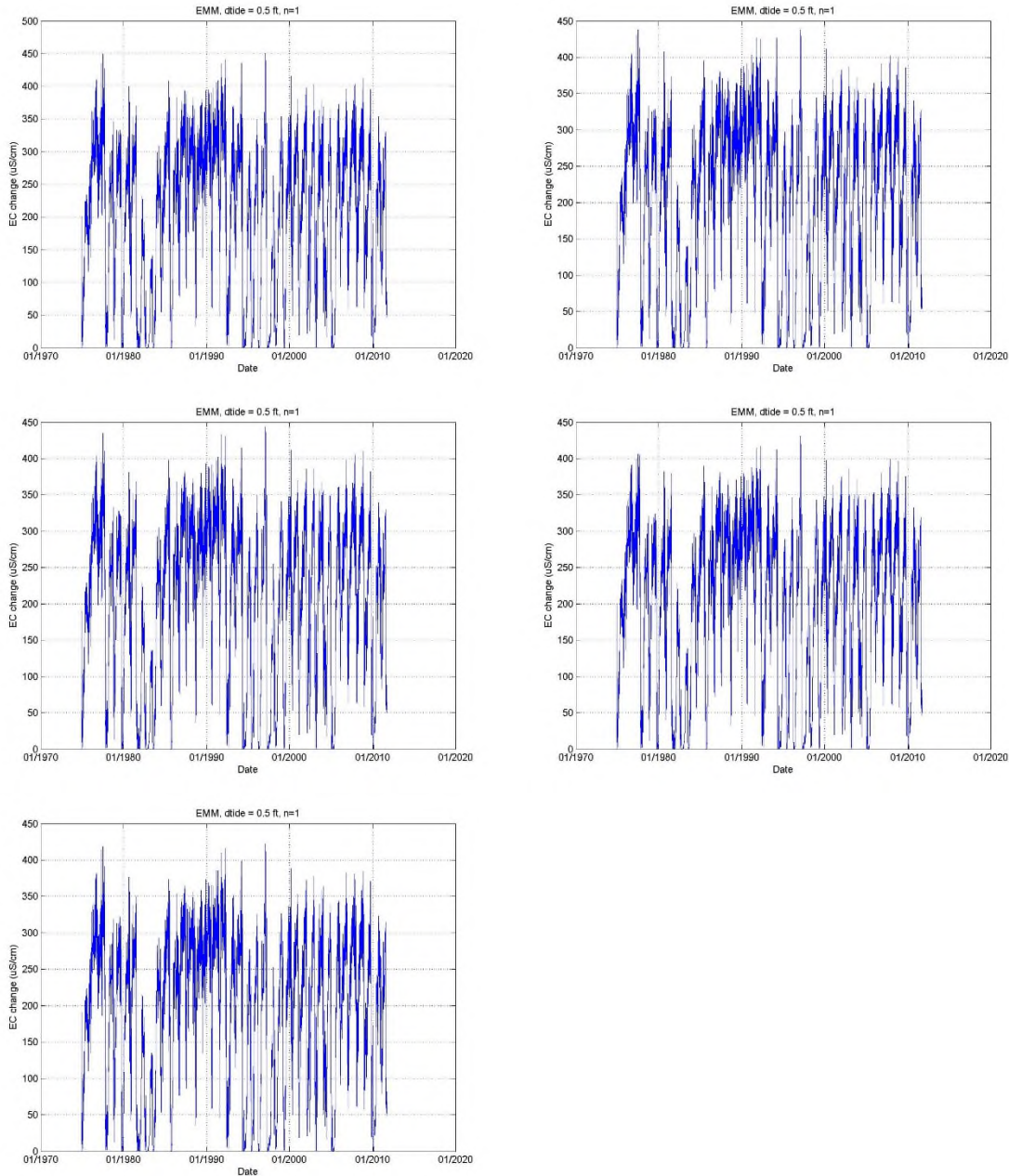


Figure 4-3 Sensitivity of trained Sacramento River Model ( $n=1$ ,  $d=60$ ) at EMM to mean sea level rise of 0.5 ft. Results are shown for multiple trained ANNs, each initialized with randomized weights and biases.

**Table 4-1 Model fit of trained ANN models at Sacramento River (in terms of r) for different network size and time delay**

Network size\time delay	d = 30	d=60	d=90	d=120
n=1	0.974	0.975	0.976	0.976
n=1	0.974	0.975	0.976	0.976
n=2	0.988	0.979	0.980	0.980
n=2	0.988	0.979	0.980	0.989
n=3	0.989	0.981	0.990	0.990
n=3	0.989	0.989	0.990	0.990

Bold means models with good fit and sensitivity.

**Table 4-2 Sensitivity range of trained ANN models at Sacramento River (in  $\mu\text{S}/\text{cm}$ ) to mean sea level increase of 0.5 ft**

Network size\time delay	d = 30	d=60	d=90	d=120
n=1	350	400	450	450
n=1	350	400	400	450
n=2	1000	x	x	600
n=2	1000	x	x	1500
n=3	900	500	900	700
n=3	x	600	x	600

x: sensitivity to mean sea level increase are not consistent. Bold means models with good fit and sensitivity.

#### **4.1.2 Model 1A-2 (Using Qout, MSL and Tidal Range as Inputs)**

The overall model fits for the five trained models (n=1, d=60 days) were generally good, with correlation coefficients of 0.975 (Figure 4-4). Sensitivity to Qout flow was tested at a station at Emmaton and was relatively uniform ranging from 0 – 250  $\mu\text{S}/\text{cm}$  (Figure 4-5). Sensitivity of EC at Emmaton to 0.5 ft mean sea level increase was also consistent, and positive, ranging from 0- 400  $\mu\text{S}/\text{cm}$  (Figure 4-6). For a time delay of 60 days, the best model had a network size of one hidden neuron (n =1, d=60 days), among the trained models with up to seven neurons (n = 1 to 7).

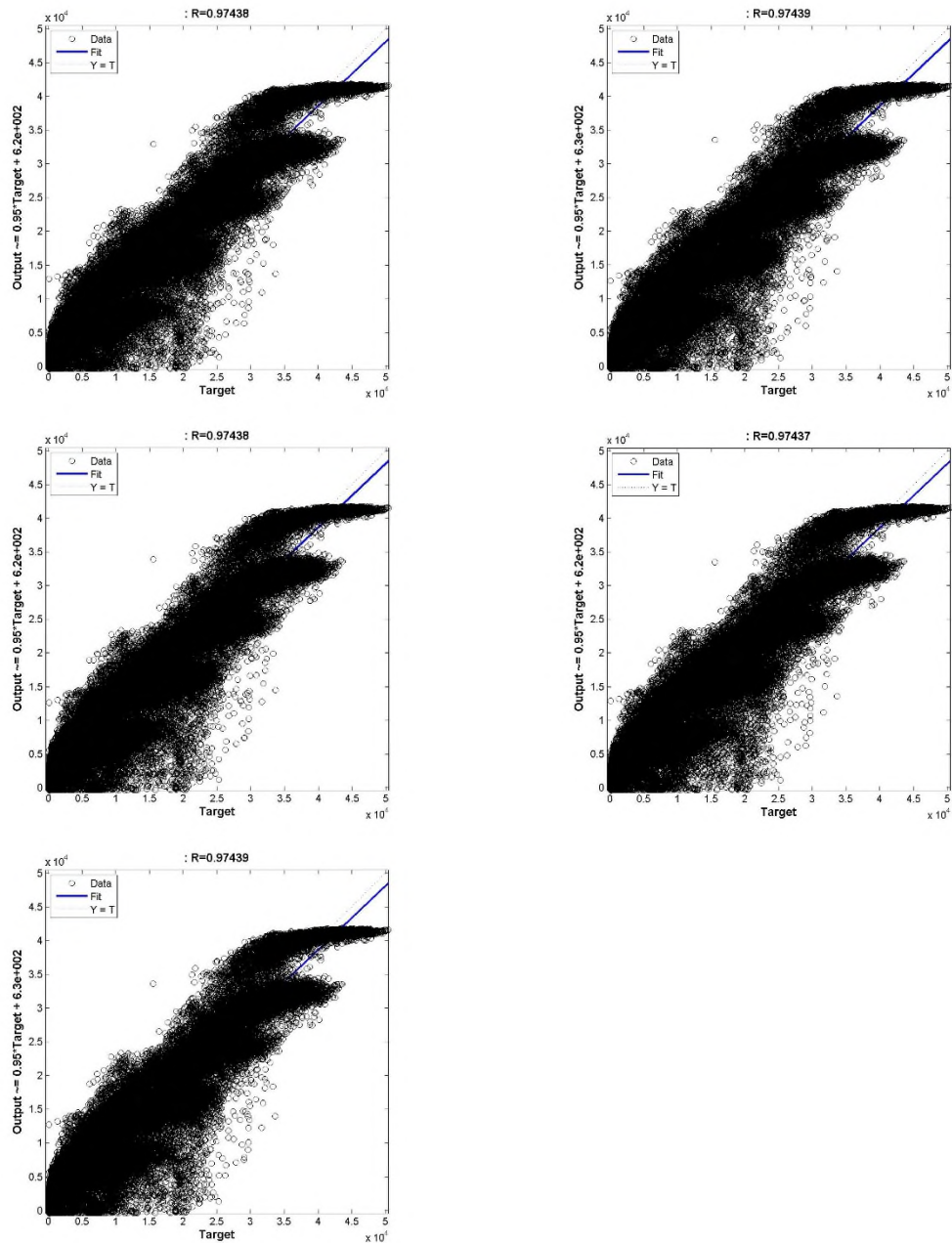


Figure 4-4 Performance of trained ANN networks at Sacramento River with Qout as input ( $n=1$ ,  $d=60$ ). Results are shown for multiple trained ANNs, each initialized with randomized weights and biases.

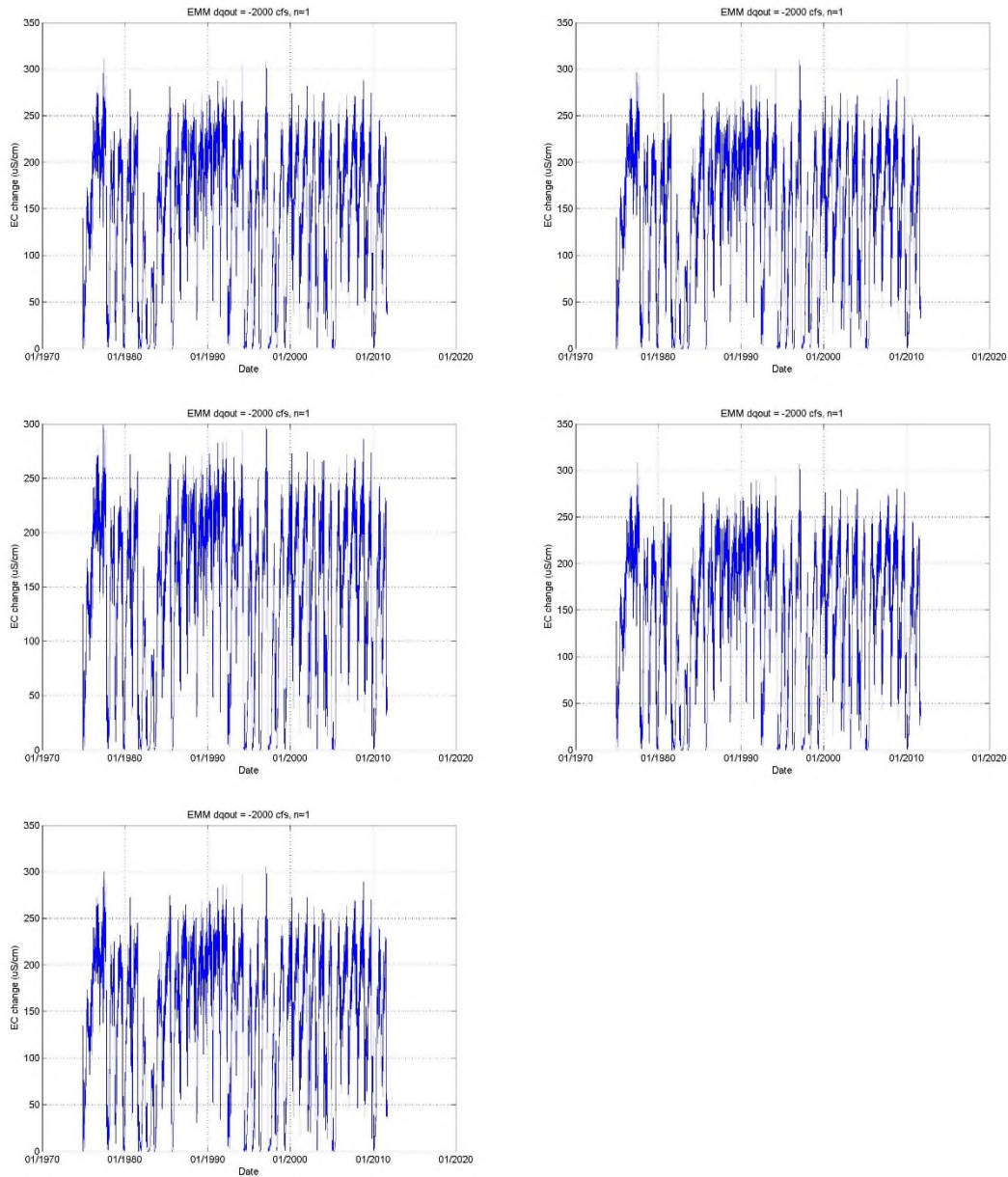


Figure 4-5 Sensitivity of trained Sacramento River model to changes in Qout flow of 2000 cfs at Emmaton ( $n = 1$ ,  $d = 60$ ). Results are shown for multiple trained ANNs, each initialized with randomized weights and biases.

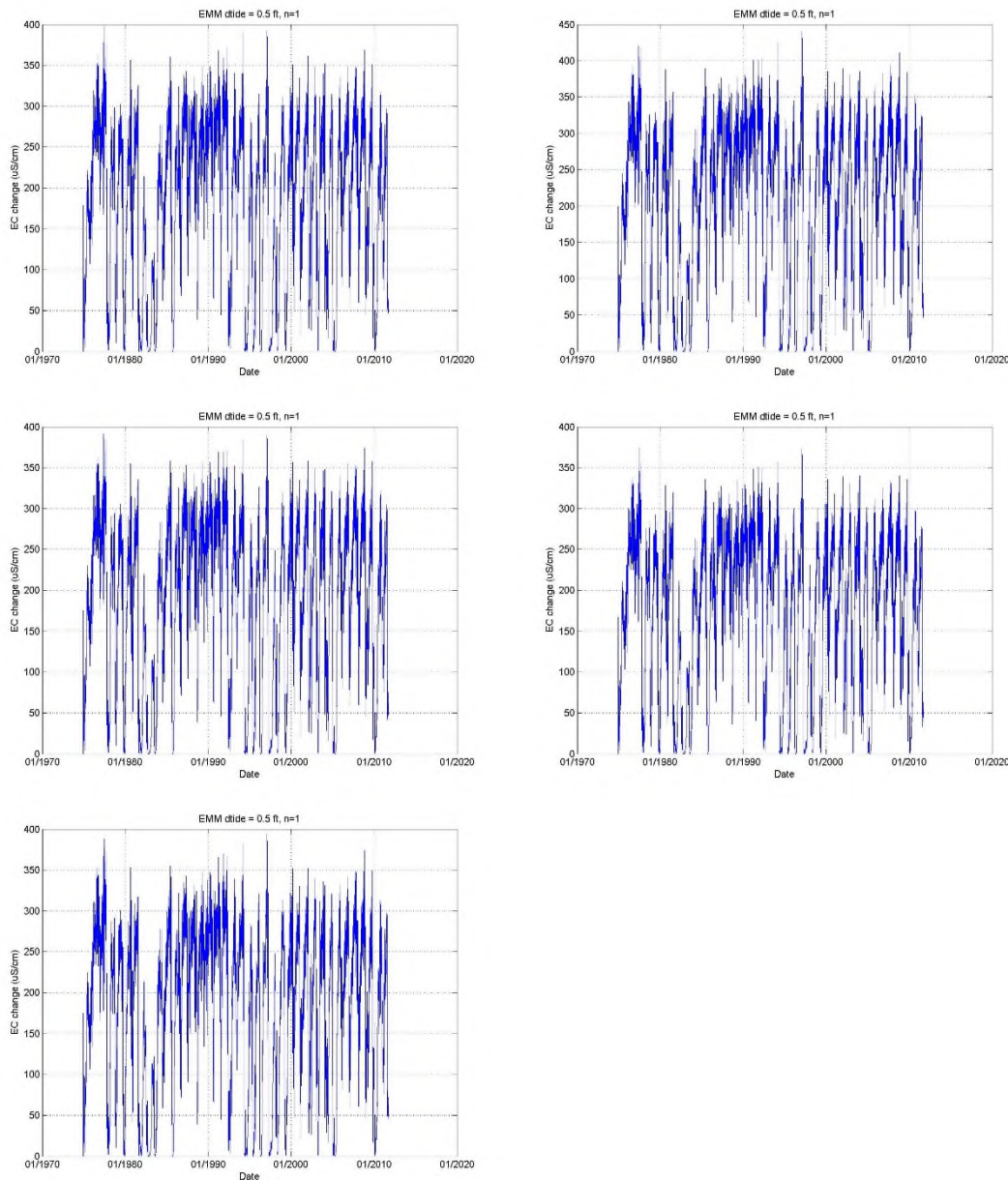


Figure 4-6 Sensitivity of trained Sacramento River model to tide increase of 0.5 ft at Emmaton ( $n=1$ ,  $d=60$ ). Results are shown for multiple trained ANNs, each initialized with randomized weights and biases.

## 4.2 DATA-DRIVEN SAN JOAQUIN RIVER ANN MODELS

### 4.2.1 Model 1B-1 (Using Qrio, Qwest, MSL and Tidal Range as Inputs)

#### A. Training using time delay of 60 days

The overall model fit for five trained models (all with  $n=1$  hidden neuron,  $d=60$  days) was generally good, with correlation coefficient of 0.977 (Figure 4-7). Sensitivity to Qwest flow was small, ranging from 0 – 40  $\mu\text{S}/\text{cm}$  at Jersey Point (Figure 4-8). Sensitivity to mean sea level increase is also consistent at Jersey Point, ranging from 0 – 300  $\mu\text{S}/\text{cm}$  (Figure 4-9).

## B. Training for different network sizes and time delay

The models were also trained using different network sizes (1 to 3 hidden neurons) and time delays (15 to 120 days; Table 4-3). Each network was trained for 2 iterations. The overall model fit improved with increases of network size and time delay, however the sensitivity to mean sea level increase started to show some physically inconsistent results when the network size exceeded 2 hidden neurons or a time delay was greater than 90 days, suggesting a possibility of over-fitting (Table 4-4). The best models included 1 hidden neuron with a 60 day time delay ( $r = 0.979$ ) and 3 neurons with 120 day time delay ( $r = 0.990$ ).

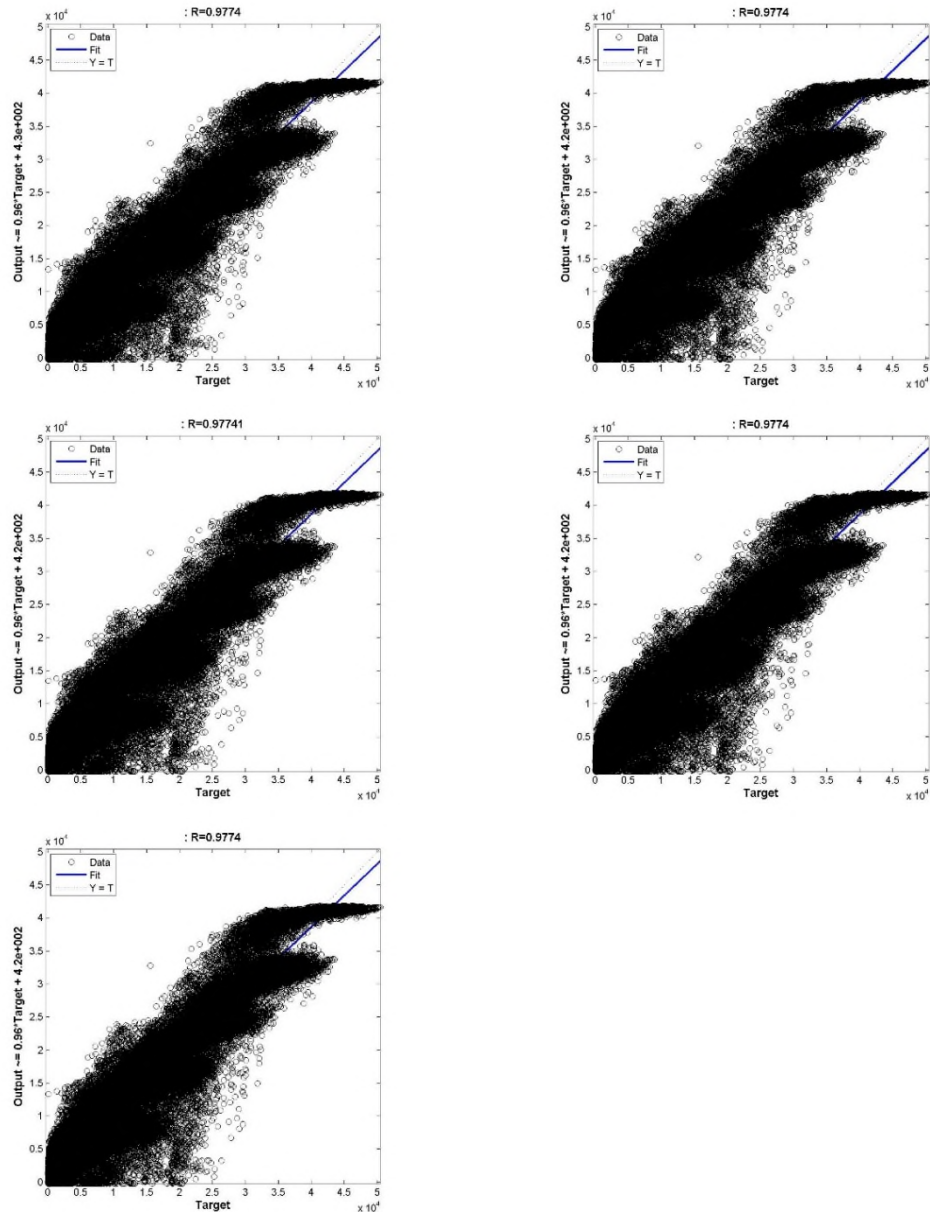


Figure 4-7 Performance of trained San Joaquin River model ( $n=1$ ,  $d=60$ ). Results are shown for multiple trained ANNs, each initialized with randomized weights and biases.

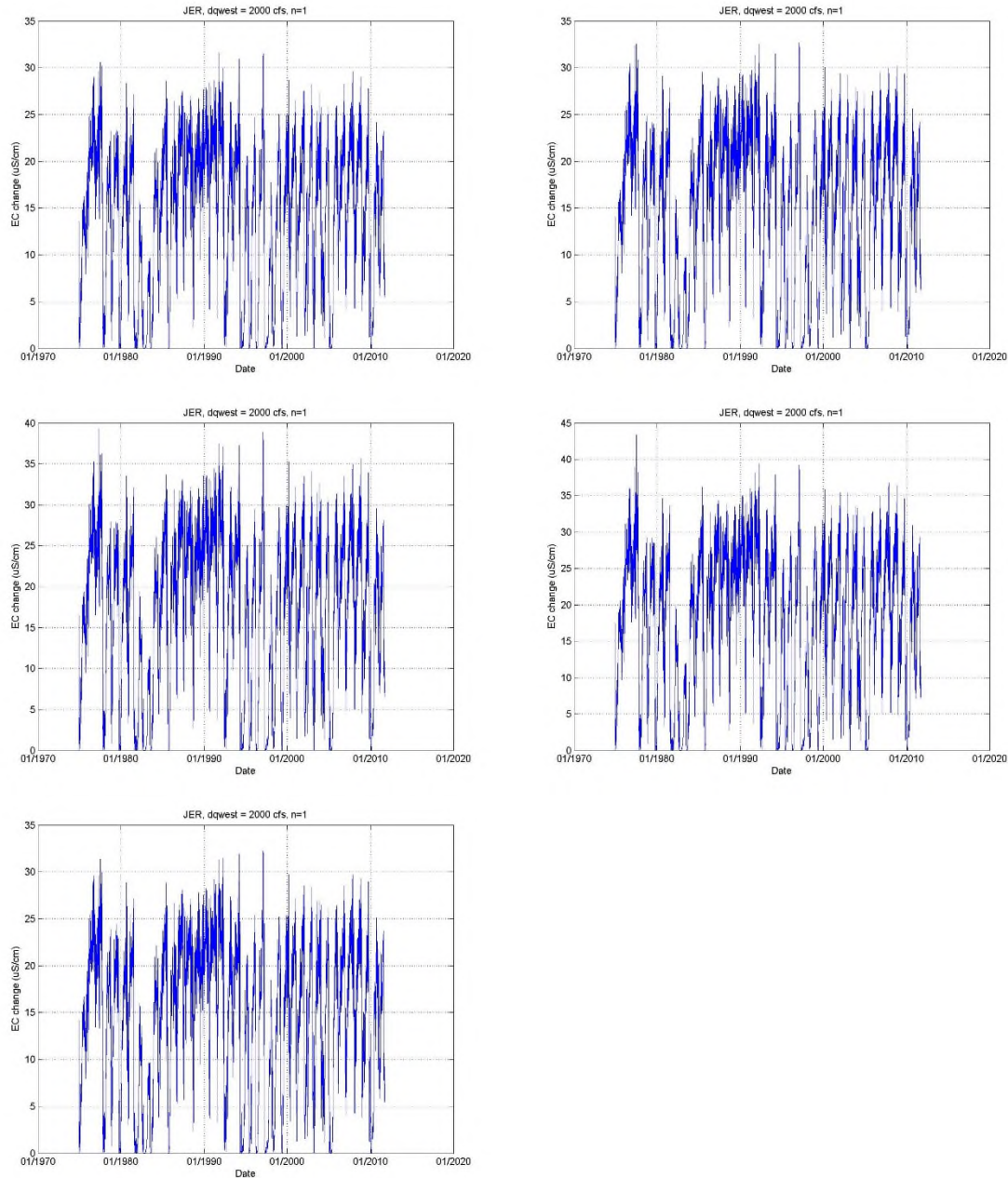


Figure 4-8 Sensitivity of trained San Joaquin River model to changes in Qwest flow of 2000 cfs at Jersey Point ( $n=1$ ,  $d=60$ ). Results are shown for multiple trained ANNs, each initialized with randomized weights and biases.

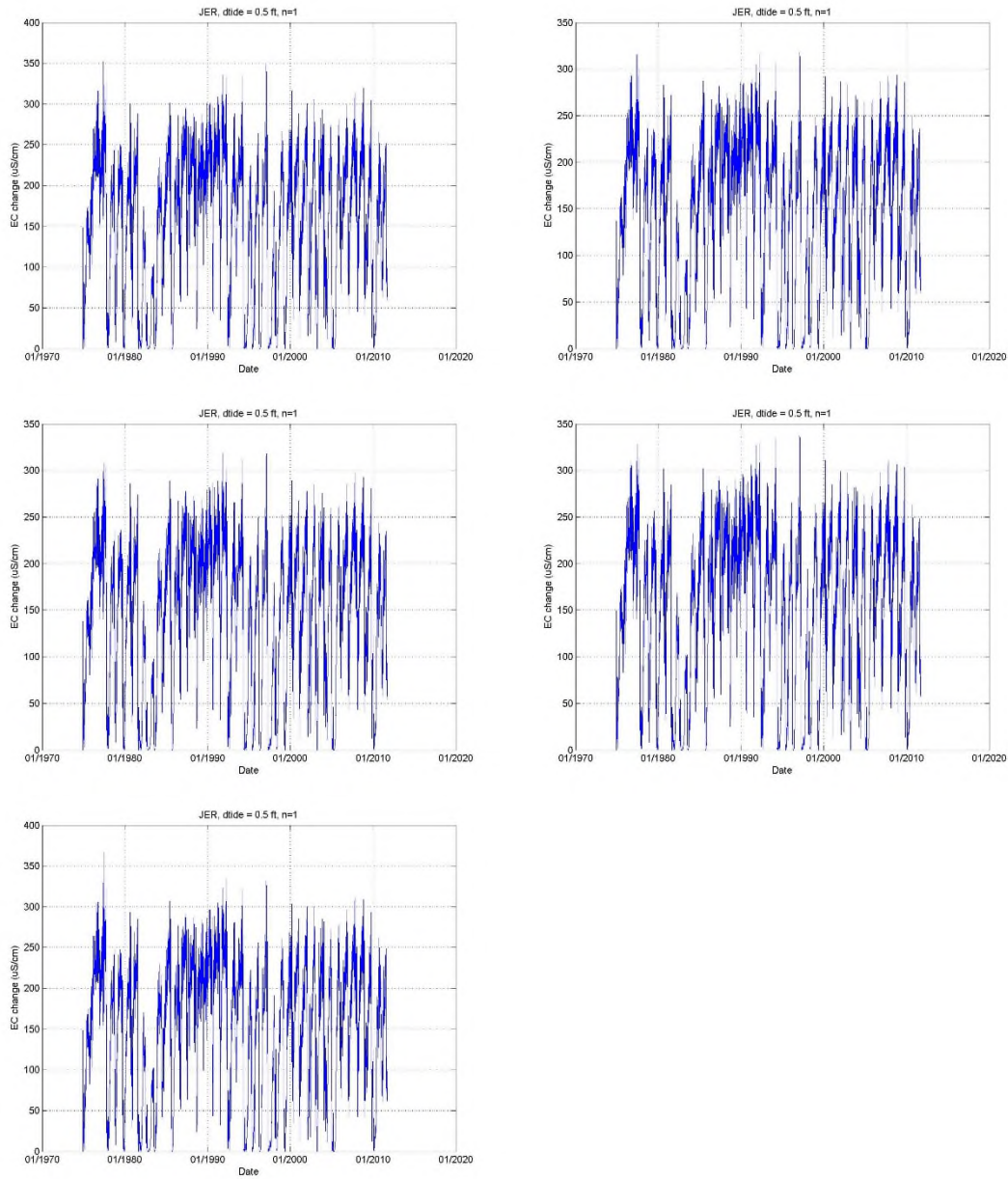


Figure 4-9 Sensitivity of trained San Joaquin River model to tide increase of 0.5 ft at Jersey Point ( $n=1$ ,  $d=60$ ). Results are shown for multiple trained ANNs, each initialized with randomized weights and biases.

**Table 4-3 Model fit of trained ANN models at San Joaquin River (in terms of r) for different network size and time delay**

Network size\time delay	d = 15	d=60	d=90	d=120
n=1	0.976	0.977	0.978	0.979
n=1	0.976	0.977	0.978	0.979
n=2	0.988	0.990	0.982	0.990
n=2	0.981	0.982	0.982	0.983
n=3	0.988	0.990	0.984	0.990
n=3	0.988	0.983	0.984	0.990

Bold means models with good fit and sensitivity.

**Table 4-4 Sensitivity range of trained ANN models at San Joaquin River (in  $\mu\text{S}/\text{cm}$ ) to mean sea level increase of 0.5 ft**

Network size\time delay	d = 15	d=60	d=90	d=120
n=1	300	320	320	350
n=1	280	300	320	350
n=2	900	700	x	1200
n=2	350	x	x	450
n=3	x	x	x	600
n=3	x	400	400	600

x: sensitivity to mean sea level increase are not consistent across networks. Bold means models with good fit and sensitivity.

#### **4.2.2 Model 1B-2 (Using Qout, MSL and Tidal Range as Inputs)**

The overall model fit for the five trained models (all with n=1 hidden neuron, d=60 days) was good, with correlation coefficient >0.97 (Figure 4-10). Sensitivity to Qout flow at Jersey Point is reasonable, ranging from 0 – 200  $\mu\text{S}/\text{cm}$  (Figure 4-11). Sensitivity of EC at Jersey Point to a 0.5 ft increase of mean sea level ranges from 0 - 300  $\mu\text{S}/\text{cm}$  (Figure 4-12). For a time delay of 60 days, the best models have one neuron, among the trained models with network size up to 5 neurons (n = 1 to 5).

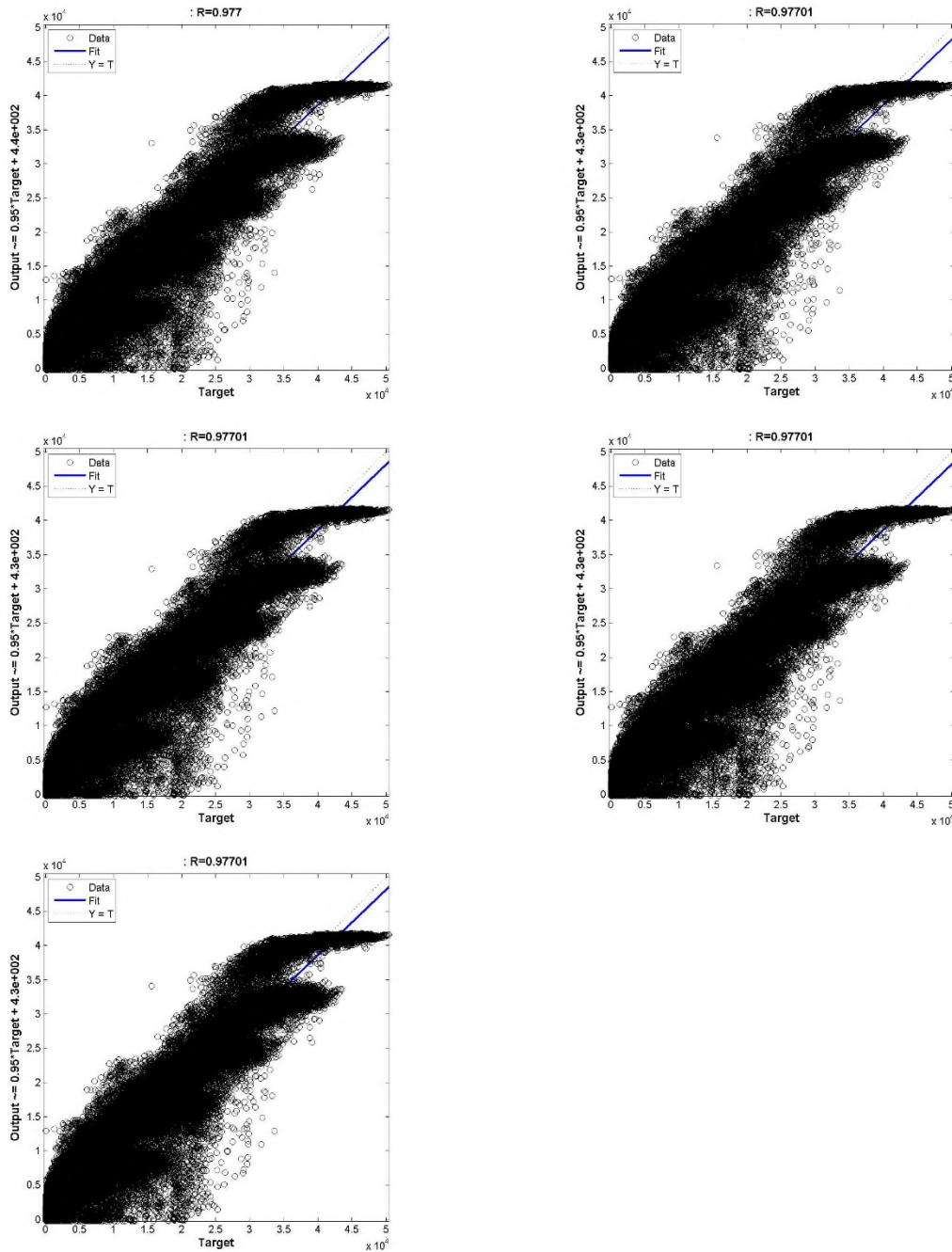


Figure 4-10 Performance of trained San Joaquin River model with Qout as input ( $n = 1, d=60$ ). Results are shown for multiple trained ANNs, each initialized with randomized weights and biases.

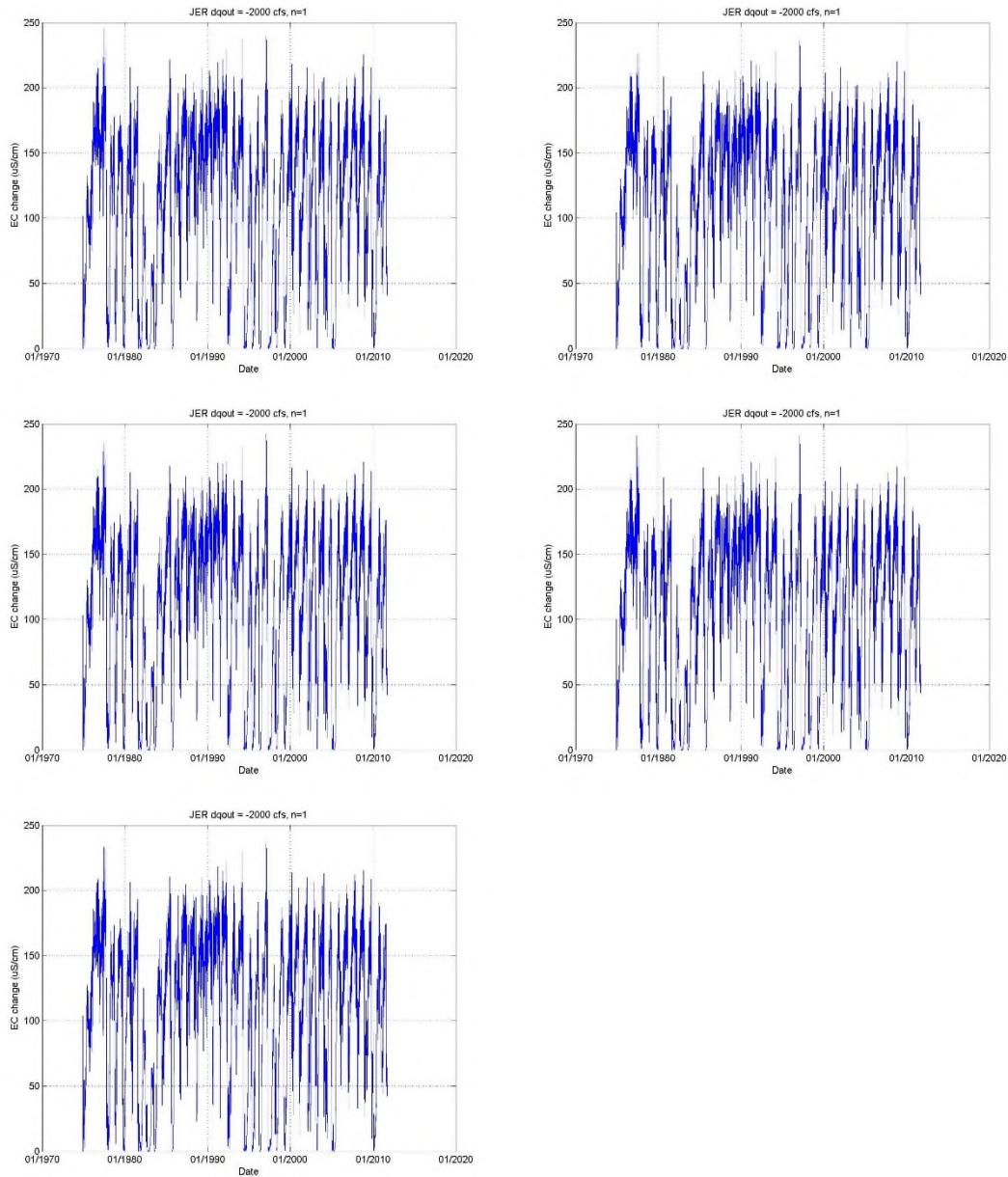


Figure 4-11 Sensitivity at Jersey Point for trained San Joaquin River model to changes in Qout flow of -2000 cfs ( $n=1$ ,  $d=60$ ). Results are shown for multiple trained ANNs, each initialized with randomized weights and biases.

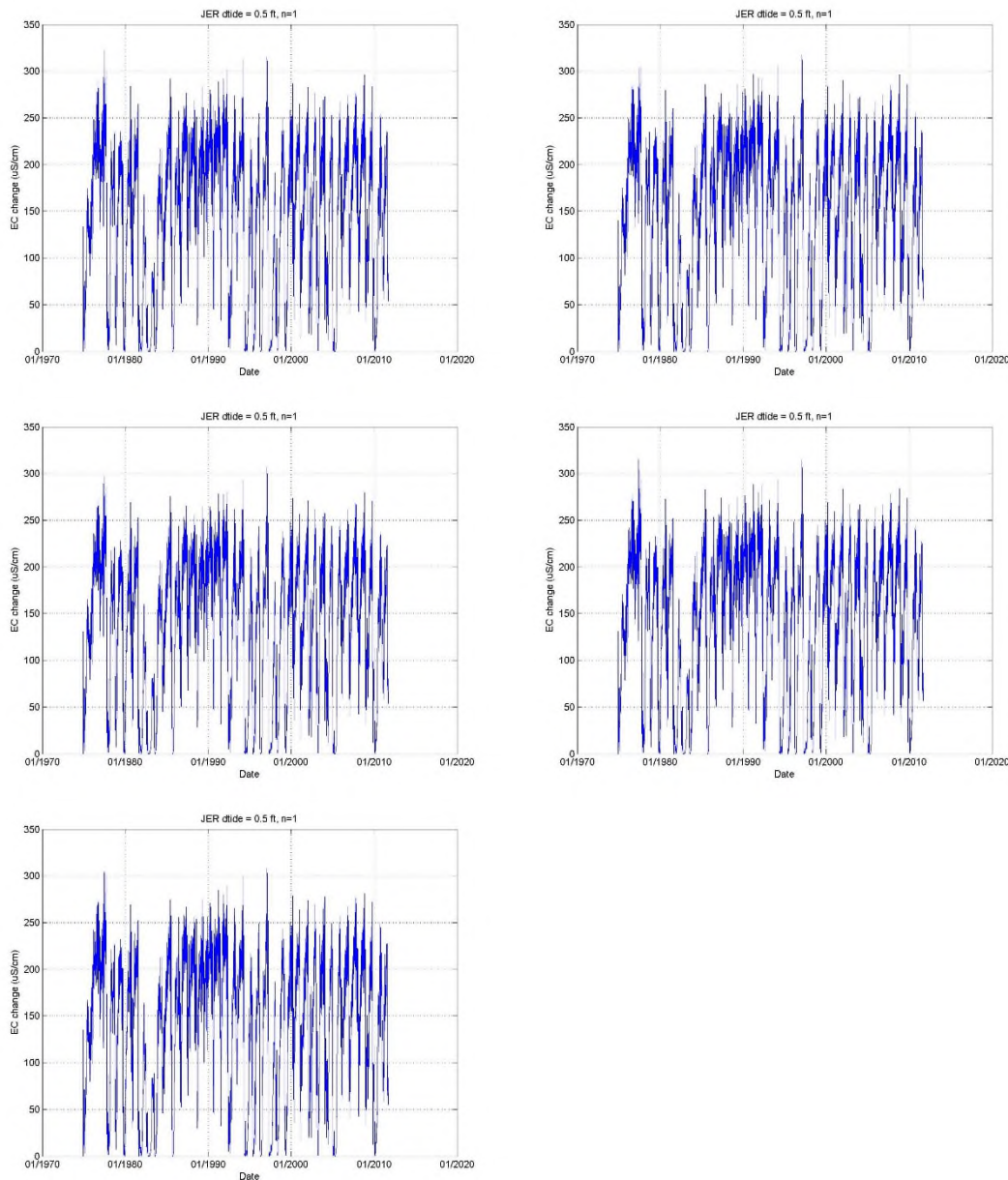


Figure 4-12 Sensitivity at Jersey Point for trained San Joaquin River model to tide increase of 0.5 ft ( $n=1$ ,  $d=60$ ). Results are shown for multiple trained ANNs, each initialized with randomized weights and biases.

#### 4.3 DATA-DRIVEN MODELS AT EMMATON (MODEL 1C-1)

The overall model fit for the six trained site-specific models at Emmaton (with 1 neuron and 60 day time delay) was good, with correlation coefficient  $>0.93$  (Figure 4-13). The models have a sensitivity to Qwest flow ranging from 0 – 1,600  $\mu\text{S}/\text{cm}$  among the six trained models (Figure 4-14). Sensitivity of EC at Emmaton to 0.5 ft increase of mean sea level was from 0 – 120  $\mu\text{S}/\text{cm}$  (Figure 4-15). For a time delay of 60 days, the best model had a network size of 1, among the trained models with network size up to 5 neurons ( $n = 1-5$ ) neurons.

Additional ANN models were trained for a set of network sizes (1 to 5 hidden neurons) and time delay (30 to 120 days; Table 4-5). Each network was trained for 3 times. The overall model fit improved with increases of network size and time delay, however, as in the previous section, the sensitivity to mean sea level is not consistent when the network size is greater than 2 hidden neurons or the time delay is greater than 90 days (Table 4-6). The models that achieve good fits and reasonable sensitivity to tide had 1 hidden neuron and a 120-day time delay and 2 hidden neurons and a 120-day time delay ( $r = 0.951$ ; Table 4-6).

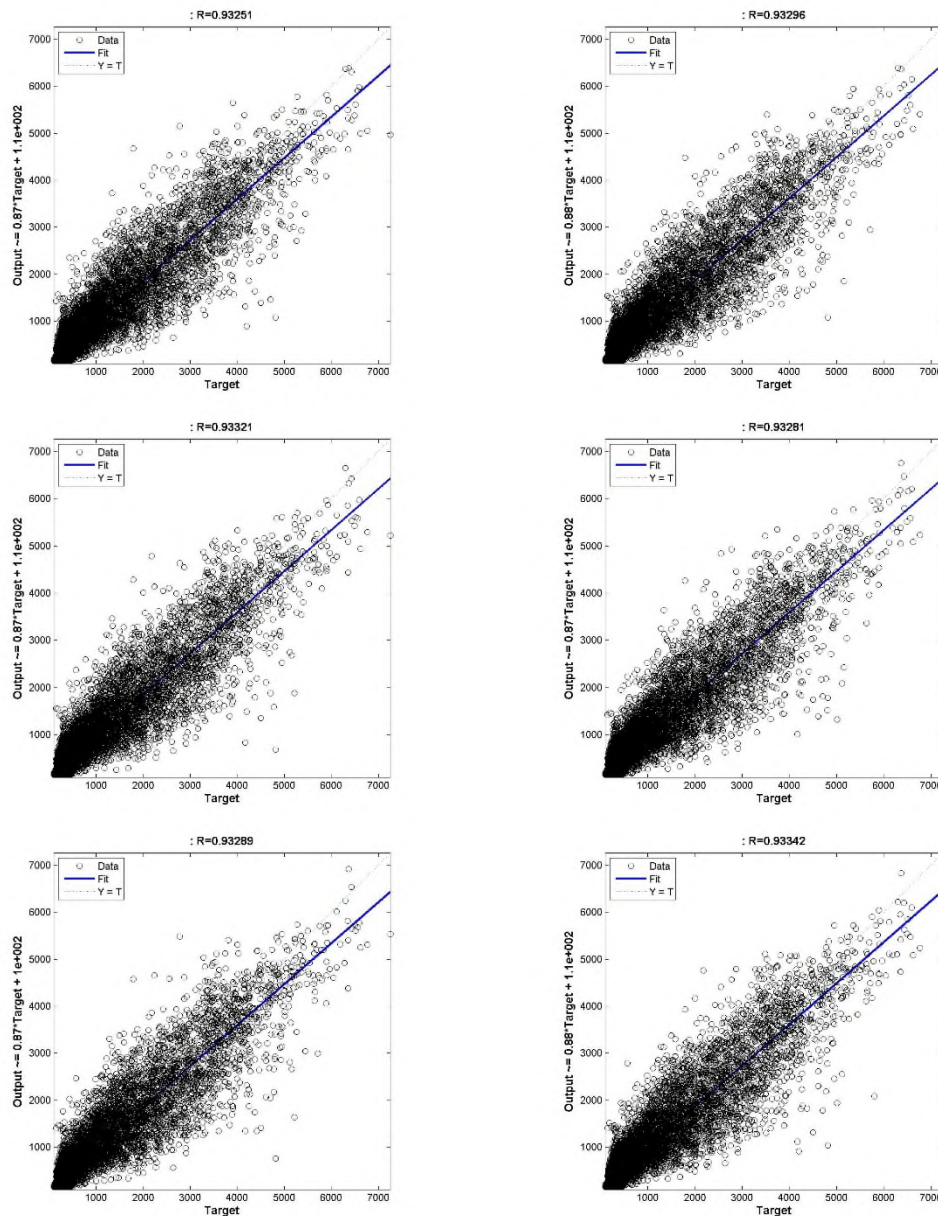


Figure 4-13 Performance of trained ANN networks at Emmaton ( $n=1$ ,  $d=60$ ). Results are shown for multiple trained ANNs, each initialized with randomized weights and biases.

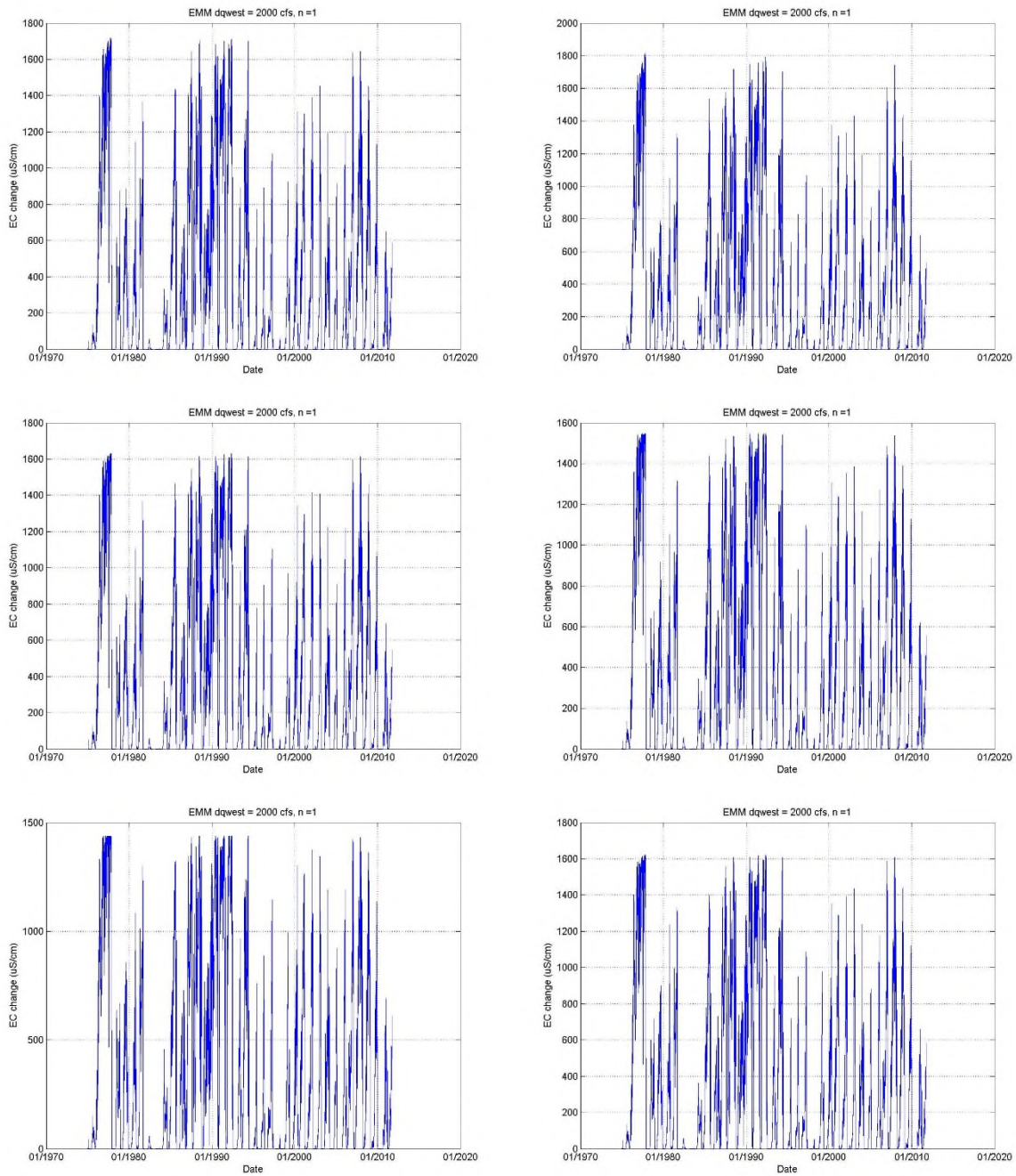


Figure 4-14 Sensitivity of trained ANN networks at Emmaton to changes in Qwest flow of 2000 cfs (+2000 cfs to Qwest flow, and -2000 cfs to Qrio flow;  $n=1$ ,  $d=60$ ). Results are shown for multiple trained ANNs, each initialized with randomized weights and biases.

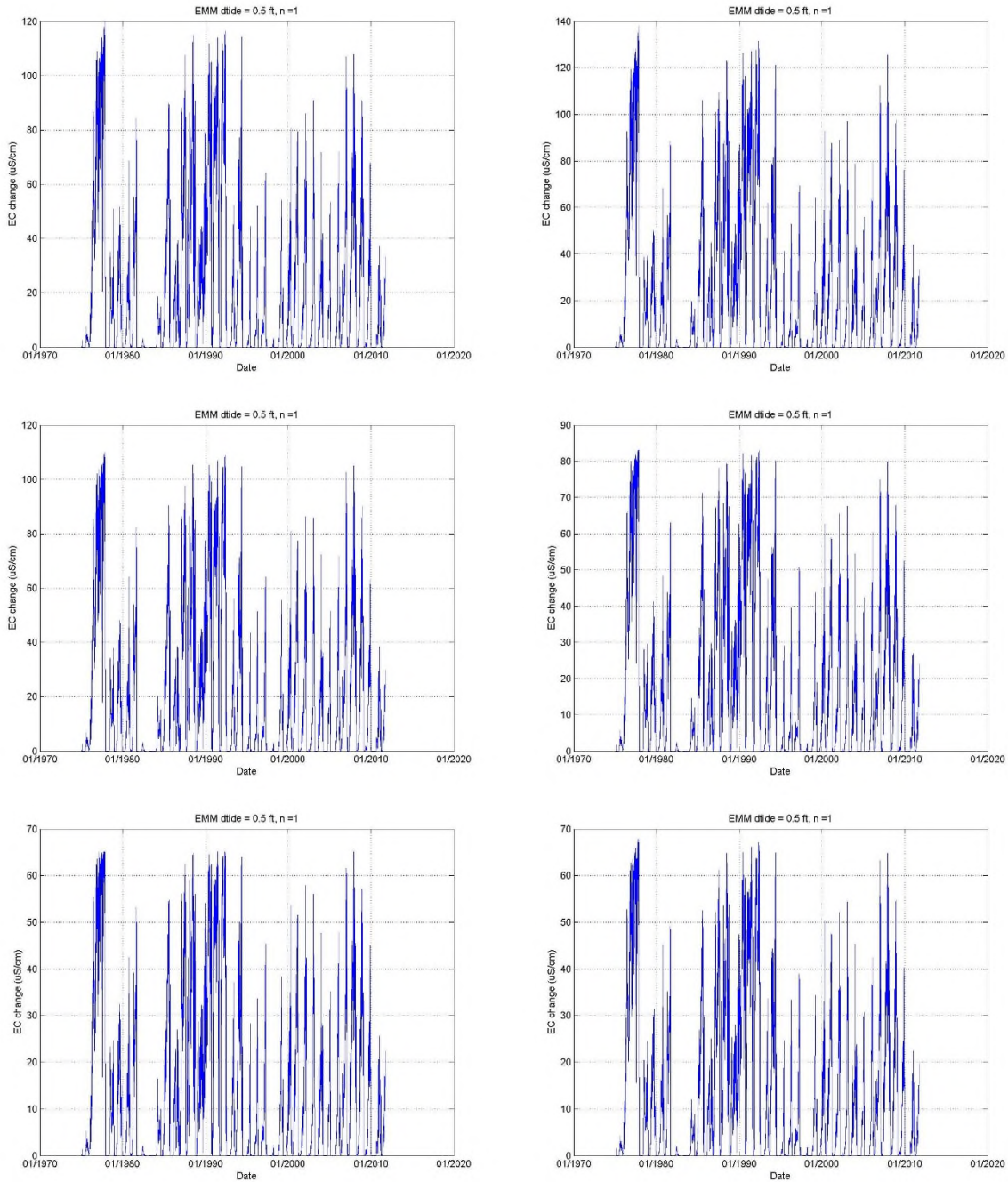


Figure 4-15 Sensitivity of trained ANN networks at Emmaton to mean sea level increase of 0.5 ft ( $n=1$ ,  $d=60$ ). Results are shown for multiple trained ANNs, each initialized with randomized weights and biases.

**Table 4-5 Model fit of trained ANN models at EMM (in terms of r) for different network size and time delay**

	d=30	d=60	d=90	d=120
n=1	0.918	0.933	0.940	<b>0.945</b>
n=1	0.918	0.933	0.149*	0.158*
n=1	0.918	0.933	0.939	<b>0.944</b>
n=2	0.923	0.924	0.944	0.836*
n=2	0.922	0.735*	0.946	<b>0.951</b>
n=2	0.932	0.936	0.834*	<b>0.951</b>
n=3	0.933	0.939	0.947	0.953
n=3	0.926	0.937	0.952	0.939
n=3	0.924	0.938	0.944	0.796*
n=4	0.849*	0.546*	0.941	0.914
n=4	0.934	0.946	0.956	0.954
n=4	0.928	0.935	0.910	0.863*
n=5	0.874*	0.892*	0.845*	0.954
n=5	0.938	0.794*	0.934	0.794*
n=5	0.927	0.925	0.939	0.944

\*model training does not converge. Bold means models with good fit and sensitivity.

**Table 4-6 Sensitivity of trained ANN models at EMM (in  $\mu\text{S}/\text{cm}$ ) to mean sea level increase of 0.5 ft**

Network size\time delay	d=30	d=60	d=90	d=120
n=1	350	95	300	<b>600</b>
n=1	300	100	x	x
n=1	300	130	270	<b>600</b>
n=2	200	x	300	x
n=2	220	x	280	<b>400</b>
n=2	600	180	x	<b>400</b>
n=3	400	300	500	600
n=3	280	500	1000	1000
n=3	220	200	x	x
n=4	1000	x	1000	3000
n=4	500	x	x	x
n=4	x	x	x	3000
n=5	x	x	x	x
n=5	x	x	x	x
n=5	250	x	x	x

x: sensitivity to mean sea level increase are not consistent. Bold means models with good fit and sensitivity.

#### 4.4 DATA-DRIVEN ANN MODELS AT JERSEY POINT (MODEL 1D-1)

The overall model fit for the five trained models at Jersey Point (with 1 neuron and 60 day time delay) was relatively good, with correlation coefficient of 0.91 (Figure 4-16). Sensitivity to Qwest flow can vary depending on the ANN version used, ranging from a positive change to a change that varies in sign over the period of record (Figure 4-17 and Figure 4-18). A time series example of the EC behavior at Jersey Point showing observed data and Qwest sensitivity is in Figure 4-19. Examination of similar patterns over different time intervals with low or zero flows confirms the complex nature of the ANN response to Qwest sensitivity. Importantly, the site specific model for Jersey Point suggests a larger EC response than does the gradient model (Model 1-B-1).

Sensitivity of EC at Jersey Point to a 0.5 ft increase of tide is negative (ranging from 0 to -250  $\mu\text{S}/\text{cm}$ ) and is inconsistent with the physical reality of the system (Figure 4-20). A different model is proposed for use in this case, as noted below.

The models were trained for a set of network sizes (1 to 4 hidden neurons) and time delay (15 to 90 days; Table 4-7). As in previous cases, the model fit improved with increases of network sizes and time delay, however the sensitivity to mean sea level increase starts to show inconsistencies when the network size exceeded 2 and a time delay was greater than 30 days (Table 4-8). The best models are those with 2 neurons and a 90-day delay ( $r > 0.93$ ), in preference to the model shown in Figure 4-20.

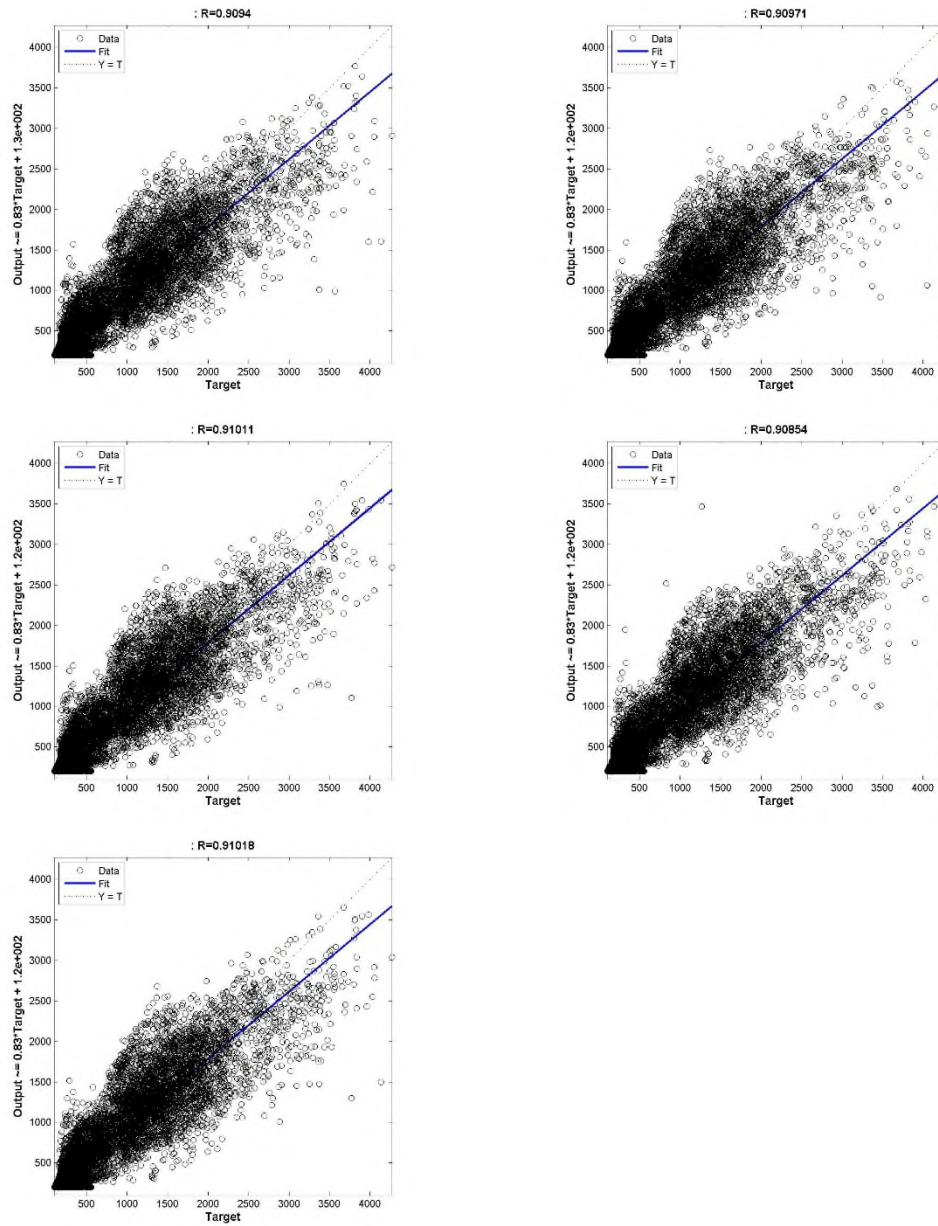


Figure 4-16 Performance of trained ANN networks at Jersey Point (JER;  $n=1$ ,  $d=120$ ). Results are shown for multiple trained ANNs, each initialized with randomized weights and biases.

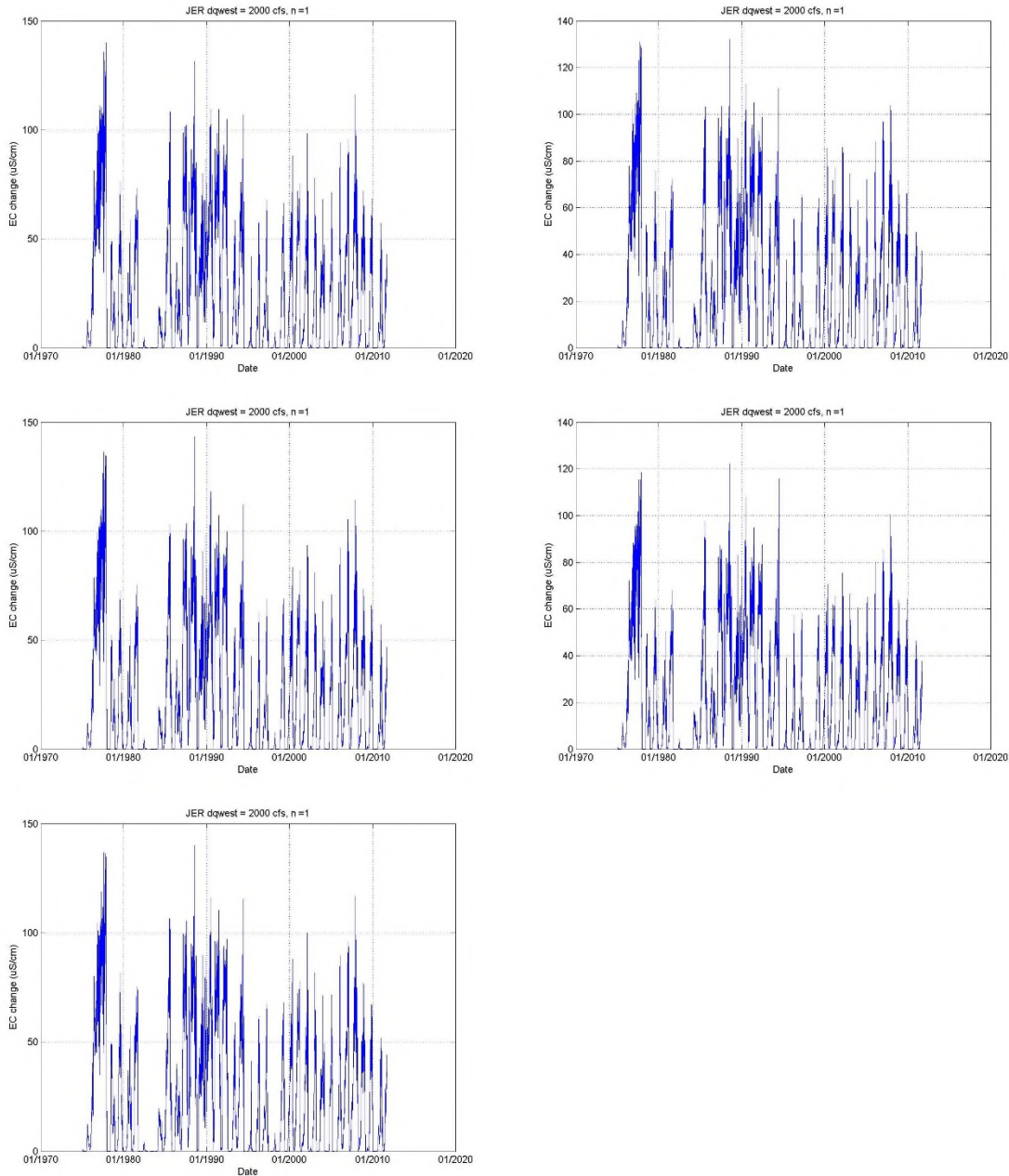


Figure 4-17 Sensitivity of trained ANN networks at Jersey Point (JER) to changes in Qwest flow of 2000 cfs (+2000 cfs to Qwest flow, and -2000 cfs to Qrio flow;  $n=1$ ,  $d=120$ ). Results are shown for multiple trained ANNs, each initialized with randomized weights and biases.

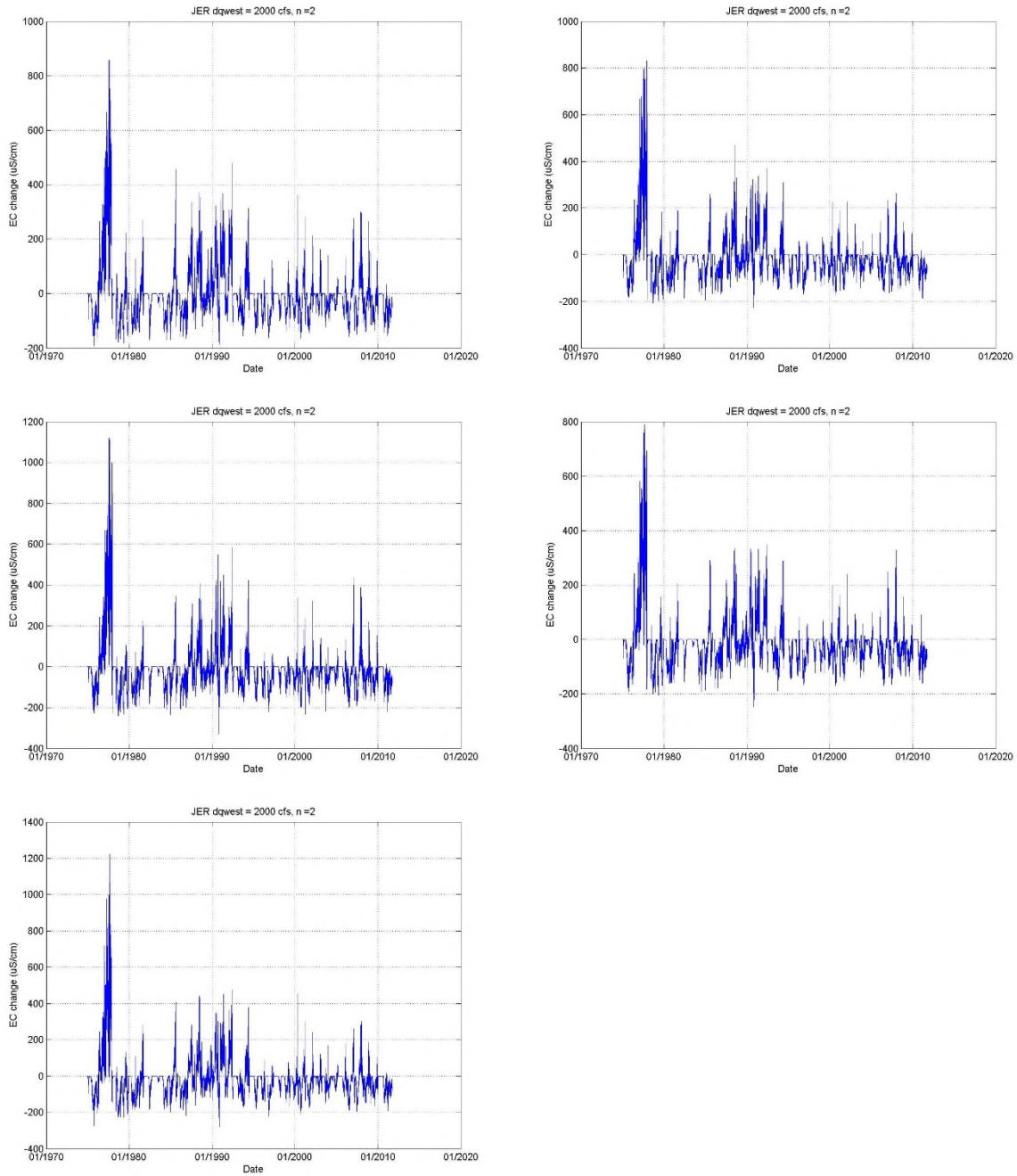


Figure 4-18 Sensitivity of trained ANN networks at Jersey Point (JER) to changes in Qwest flow of 2000 cfs (+2000 cfs to Qwest flow, and -2000 cfs to Qrio flow; n=2, d=90). Results are shown for multiple trained ANNs, each initialized with randomized weights and biases.

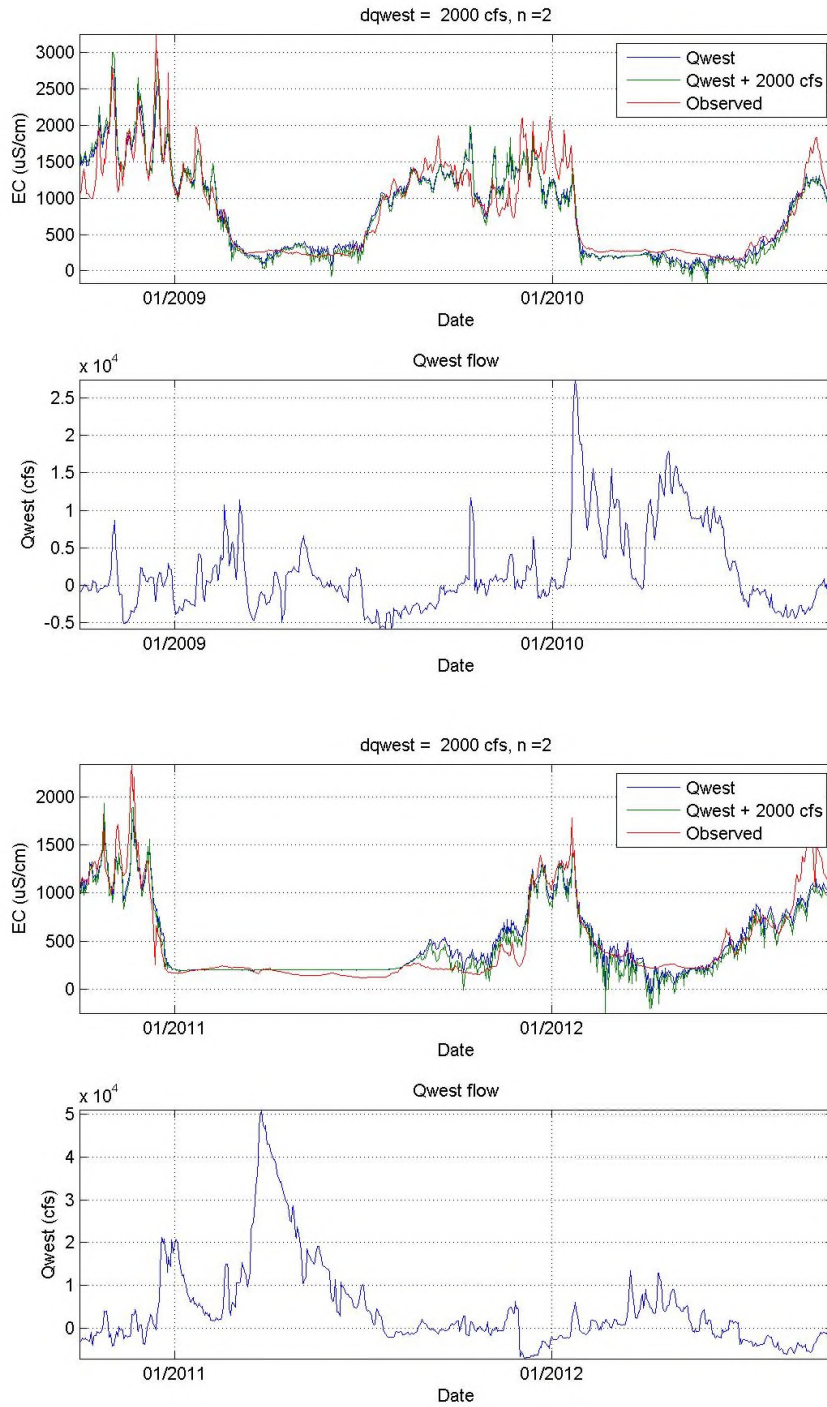


Figure 4-19 Time series example of ANN response at Jersey Point (JER) to changes in Qwest flow of 2000 cfs (+2000 cfs to Qwest flow, and -2000 cfs to Qrio flow;  $n=2$ ,  $d=90$ ).

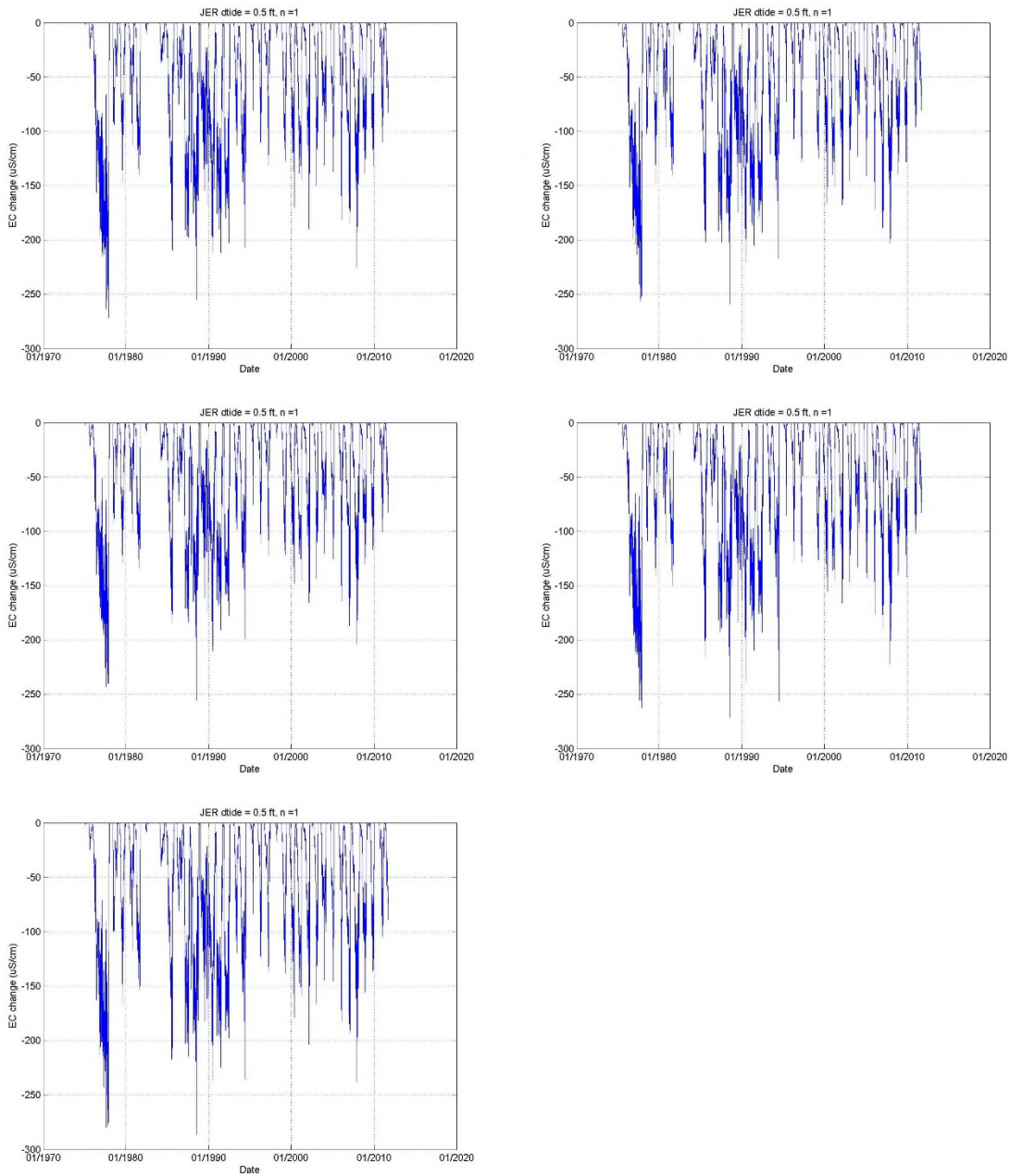


Figure 4-20 Sensitivity of trained ANN networks at Jersey Point (JER) to mean sea level increase of 0.5 ft ( $n=1$ ,  $d=120$ ). Results are shown for multiple trained ANNs, each initialized with randomized weights and biases.

**Table 4-7 Model fit of trained ANN models at JER (in terms of r) for different network size and time delay**

Network size\time delay	d=15	d=30	d=45	d=60	d=75	d=90
n=1	0.821	0.869	0.896	0.910	0.916	0.923
n=1	0.821	0.869	0.895	0.909	0.916	0.923
n=1	0.821	0.868	0.896	0.910	0.916	0.923
n=2	0.833	0.882	0.908	0.922	0.921	<b>0.936</b>
n=2	0.834	0.881	0.823	0.921	0.929	<b>0.934</b>
n=2	0.834	0.881	0.909	0.888	0.931	<b>0.936</b>
n=3	0.852	0.876	0.909	0.935	0.937	0.931
n=3	0.837	0.896	0.839	0.934	0.928	0.937
n=3	0.851	0.887	0.869	0.913	0.928	0.943
n=4	0.861	0.903	0.925	0.938	0.926	0.915
n=4	0.855	0.900	0.919	0.929	0.939	0.944
n=4	0.836	0.903	0.917	0.929	0.938	0.904

Bold means models with good fit and sensitivity.

**Table 4-8 Sensitivity of trained ANN models at JER (in  $\mu\text{S}/\text{cm}$ ) to mean sea level increase of 0.5 ft (maximum change in EC from base case with no sea level change)**

Network size\time delay	d=15	d=30	d=45	d=60	d=75	d=90
n=1	160	x	x	x	x	x
n=1	150	x	x	x	x	x
n=1	160	x	x	x	x	x
n=2	120	ok	ok	ok	x	<b>400</b>
n=2	120	x	x	x	x	<b>400</b>
n=2	120	ok	ok	x	x	<b>400</b>
n=3	x	180	x	x	x	ok
n=3	180	x	x	x	x	x
n=3	x	x	x	x	x	x
n=4	x	x	x	x	x	x
n=4	x	x	x	x	x	x
n=4	ok	x	x	x	x	x

x: sensitivity to mean sea level increase are not physically plausible. Bold means models with good fit and sensitivity.

#### 4.5 DATA-DRIVEN ANN MODEL SUMMARY

The results shown above are for models trained with different numbers of hidden neurons and time delays. In general there was a tradeoff between network size and sensitivity, with larger networks being better at fitting the data, although often showing inconsistent responses during sensitivity evaluation. Going forward, this work suggests keeping the networks small, particularly when model sensitivity is an important aspect of the proposed analysis. However, it is possible that there are future applications where ANNs are primarily used for prediction, say for near term operational forecasts, in which case larger ANN models may be acceptable. In such cases one would need to acknowledge the limitations associated with the sensitivity response.

## **4.6 DSG-BASED ANN MODELS (MODELS 2A-1, 2A-2, 2B-1, 2B-2)**

### **4.6.1 Training for DSG Parameters**

This model framework required the evaluation of the parameters in the DSG model, allowing them to vary for each day. This is in contrast with the typical application of the DSG model where these constants are set at fixed values. The ranges of fitted values for the parameters associated with Eq 2.5 ( $S_o$ ,  $S_b$ , and  $\Phi_2$ ) are shown in Figure 4-21 and Figure 4-22 along with the ranges of  $Q_{west}$  and  $Q_{rio}$ . No simple relationship between these variables emerges, although it appears that the pre-Project conditions (water year 1922-1967) are different from the post-Project conditions (water year 1968-2012).

ANN models yielded relatively good fit and reasonable sensitivity. An evaluation of different network sizes suggested reasonable sensitivity using a network with 1 hidden neuron and a time delay of 60 days. Performance of models 2A-2 and 2B-2 are summarized by station in Table 4-9. The sensitivity of model 2A-2 at Emmatton is shown in Figure 4-23 and 4-20. The sensitivity of model 2B-2 at Jersey Point is shown in Figures 4-21 and 4-22.

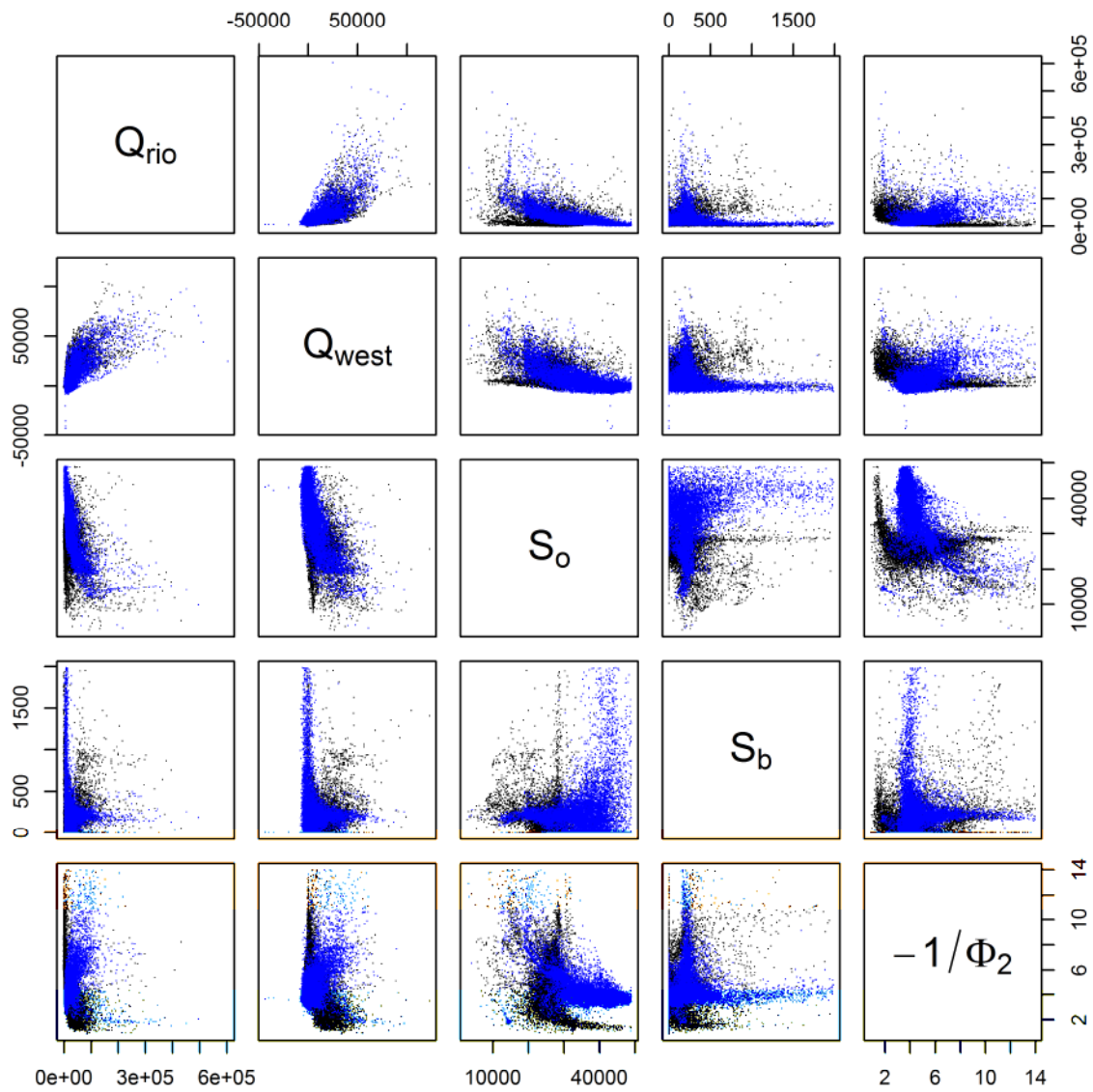


Figure 4-21 DSG parameter ranges for the Sacramento River model fit (Model 2A-1). Black points are pre-Project conditions (1922-1967), and blue points are post-Project conditions (1968-2012).

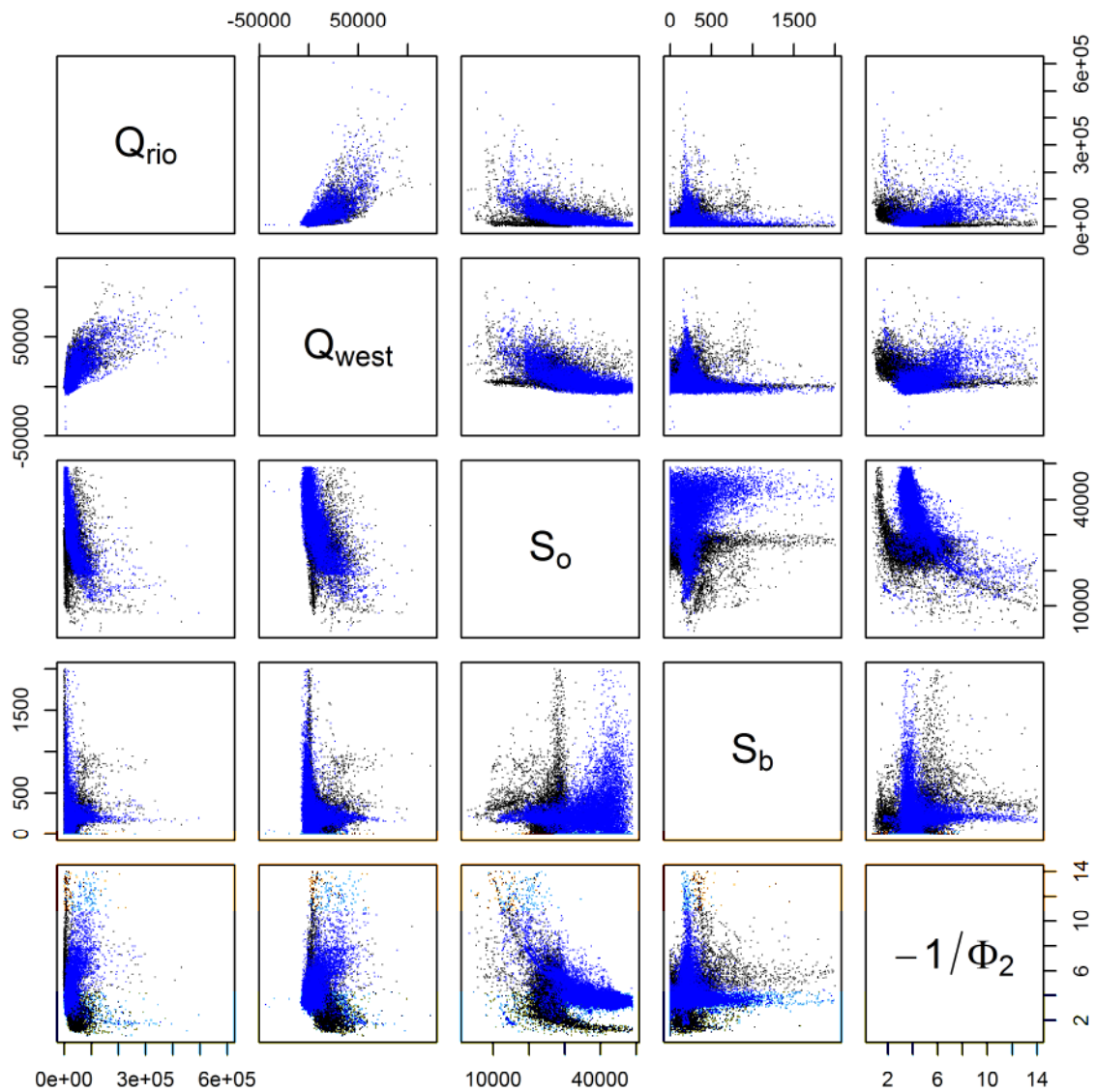


Figure 4-22 DSG parameter ranges for the San Joaquin River model fit (Model 2B-1). Black points are pre-Project conditions (1922-1967), and blue points are post-Project conditions (1968-2012).

**Table 4-9**  
**Performance of Trained Salinity ANN Model (Model 2A-1)**  
**ANN Salinity ( $\mu\text{S/cm}$ ) =  $C1 + C2 \cdot \text{Observed Salinity } (\mu\text{S/cm})$**

Station	Distance (km)	Daily		
		C2	C1	r <sup>2</sup>
Sacramento River Model				
PTO	19.8	1.043	-1740.9	0.836
PTD	40.6	0.987	-742.1	0.895
CRK	44.6	0.959	-146.8	0.909
BEN	52.3	0.934	180.4	0.935
MRZ	52.6	0.934	179.0	0.935
BHP	54.7	0.933	158.4	0.941
WSN	59.5	0.934	93.0	0.95
BPT	64.2	0.938	61.2	0.955
PCT	66.0	0.941	56.8	0.957
OAF	74.8	0.957	61.6	0.962
CLL	81.8	0.968	70.1	0.966
EMM	92.8	0.977	54.8	0.954
TSB	96.6	0.986	44.1	0.933
RVB	102.2	1.013	28.3	0.878
ITB	110.6	1.055	9.3	0.694
WNG	124.6	1.149	-17.2	0.226
PSP	22.0	1.05	-2041.6	0.842
CAR	45.5	0.954	-56.0	0.912
MRZ	54.0	0.933	167.2	0.939
MBR	55.0	0.933	154.6	0.941
PCT	64.0	0.938	61.9	0.955
MAL	75.0	0.957	61.8	0.962
CLL	81.0	0.967	69.6	0.966
EMM	92.0	0.976	57.2	0.957
RVB	101.0	1.006	31.4	0.893

**Table 4-9 (continued)**  
**Performance of Trained Salinity ANN Model (Model 2A-2)**  
**ANN Salinity ( $\mu\text{S}/\text{cm}$ ) =  $C1 + C2 \cdot \text{Observed Salinity } (\mu\text{S}/\text{cm})$**

Station	Distance (km)	Daily		
		C2	C1	r <sup>2</sup>
San Joaquin River model				
PTO	19.8	1.119	-4023.2	0.841
PTD	40.6	1.005	-1048.0	0.901
CRK	44.6	0.978	-432.2	0.917
BEN	52.3	0.954	-40.1	0.943
MRZ	52.6	0.953	-35.0	0.944
BHP	54.7	0.951	-10.9	0.949
WSN	59.5	0.949	12.1	0.957
BPT	64.2	0.951	28.1	0.963
PCT	66.0	0.953	36.3	0.964
OAF	74.8	0.959	85.1	0.97
ANH	88.4	0.927	116.2	0.978
ANB	93.7	0.897	102.9	0.969
JER	98.8	0.873	85.1	0.952
FRV	101.2	0.866	77.3	0.942
OPT	108.1	0.855	58.7	0.912
SAL	113.1	0.856	48.2	0.882
WBP	115.9	0.859	43.2	0.861
MIP	128.6	0.907	22.0	0.682
KIP	135.5	0.97	6.5	0.523
SCC	146.1	1.17	-36.5	0.282
SCT	152.6	1.394	-83.4	0.178
PSP	22.0	1.123	-4190.8	0.846
CAR	45.5	0.973	-342.3	0.921
MRZ	54.0	0.951	-17.6	0.947
MBR	55.0	0.951	-8.7	0.949
PCT	64.0	0.951	27.2	0.962
MAL	75.0	0.959	85.9	0.97
PTS	77.0	0.959	95.2	0.971
ANH	85.8	0.94	117.7	0.978
BLP	92.9	0.902	105.5	0.971
JER	95.8	0.887	95.7	0.963
TSL	100.4	0.868	79.9	0.945
SAL	109.2	0.854	56.3	0.906

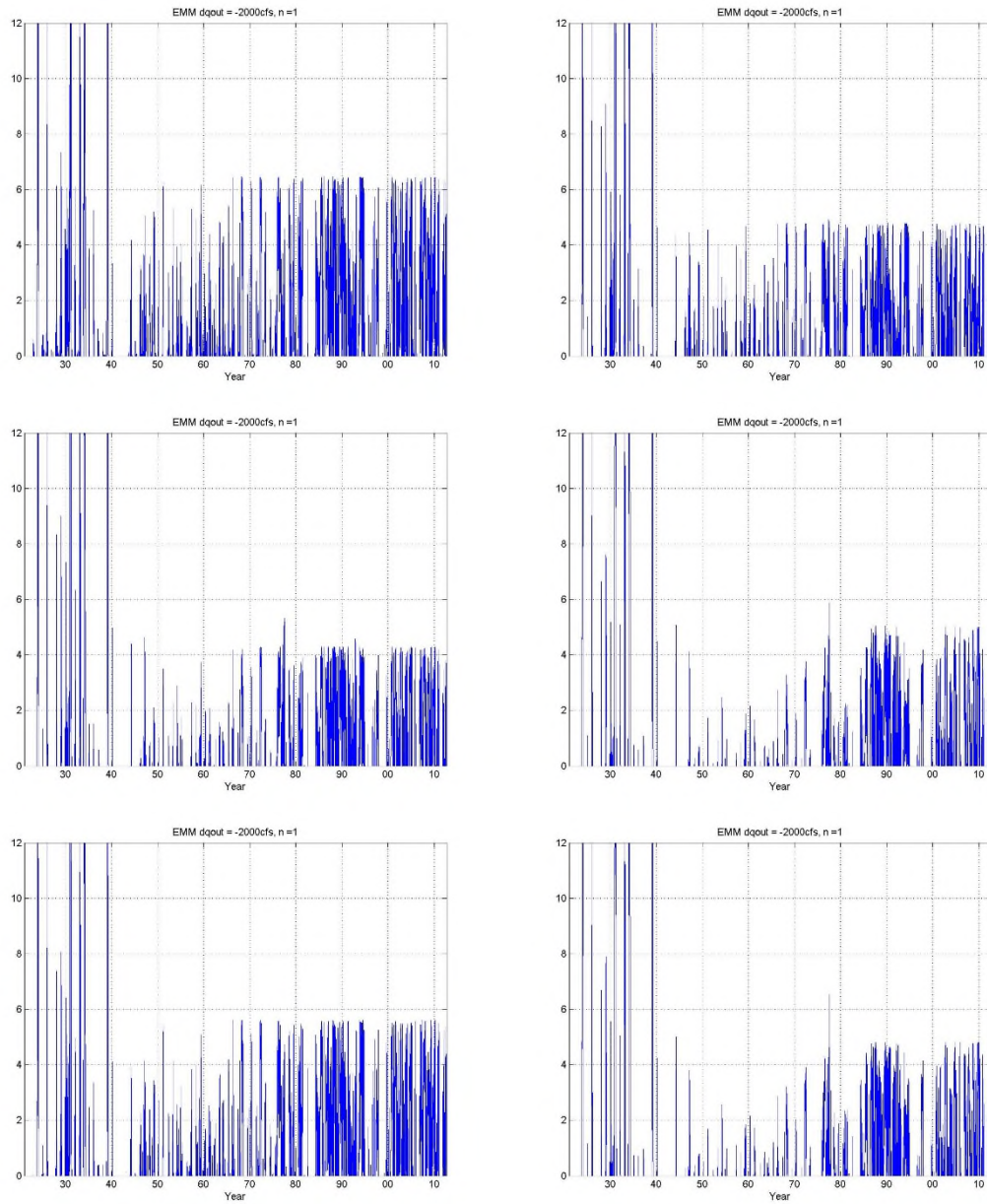


Figure 4-23 Sensitivity in EC ( $\mu\text{S}/\text{cm}$ ) of Sacramento River fitted DSG model to changes in delta outflow (-2000 cfs). Results are shown for multiple trained ANNs, each initialized with randomized weights and biases.

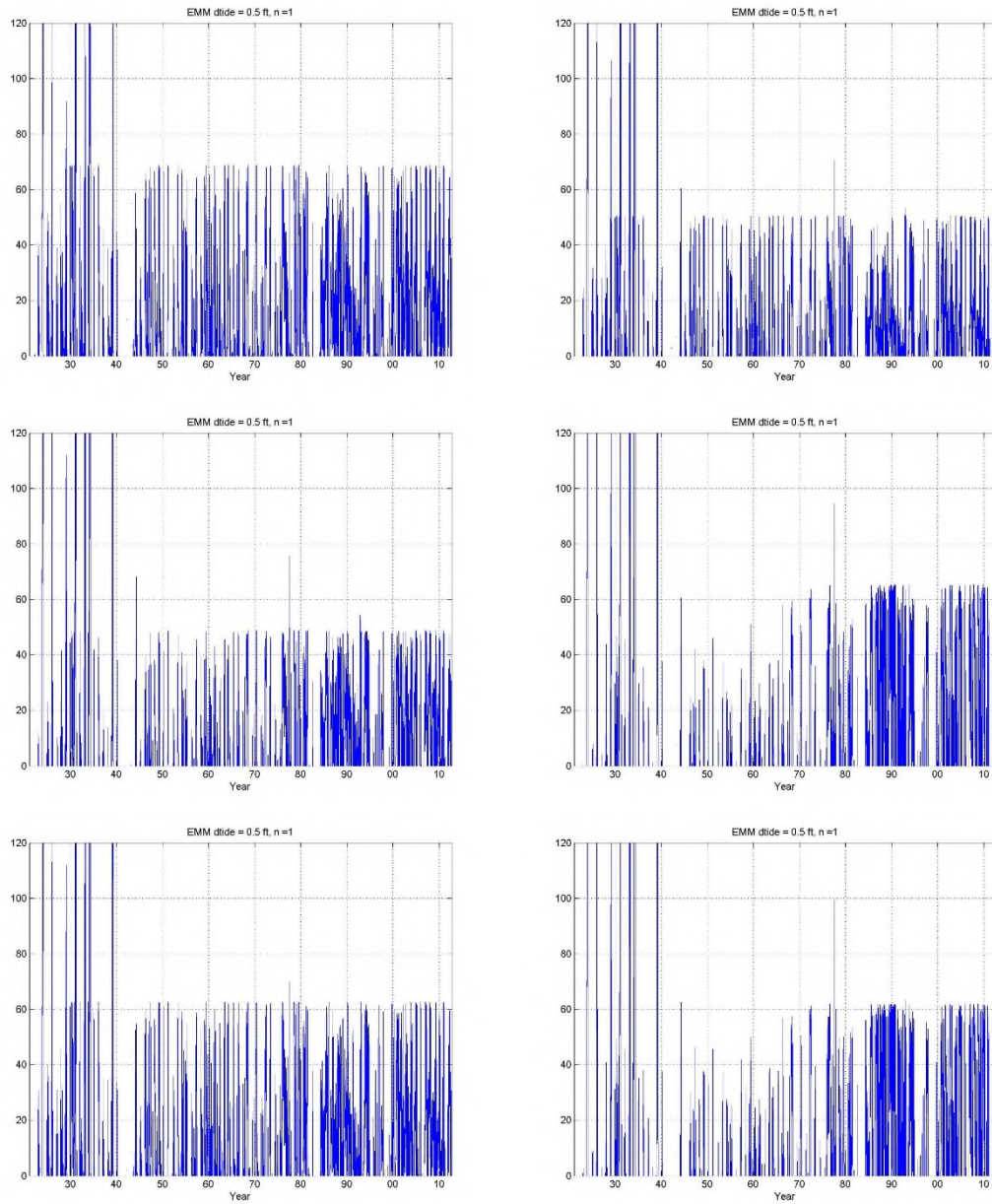


Figure 4-24 Sensitivity in EC ( $\mu\text{S}/\text{cm}$ ) of Sacramento River fitted DSG model to changes in mean sea level (0.5 ft). Results are shown for multiple trained ANNs, each initialized with randomized weights and biases.

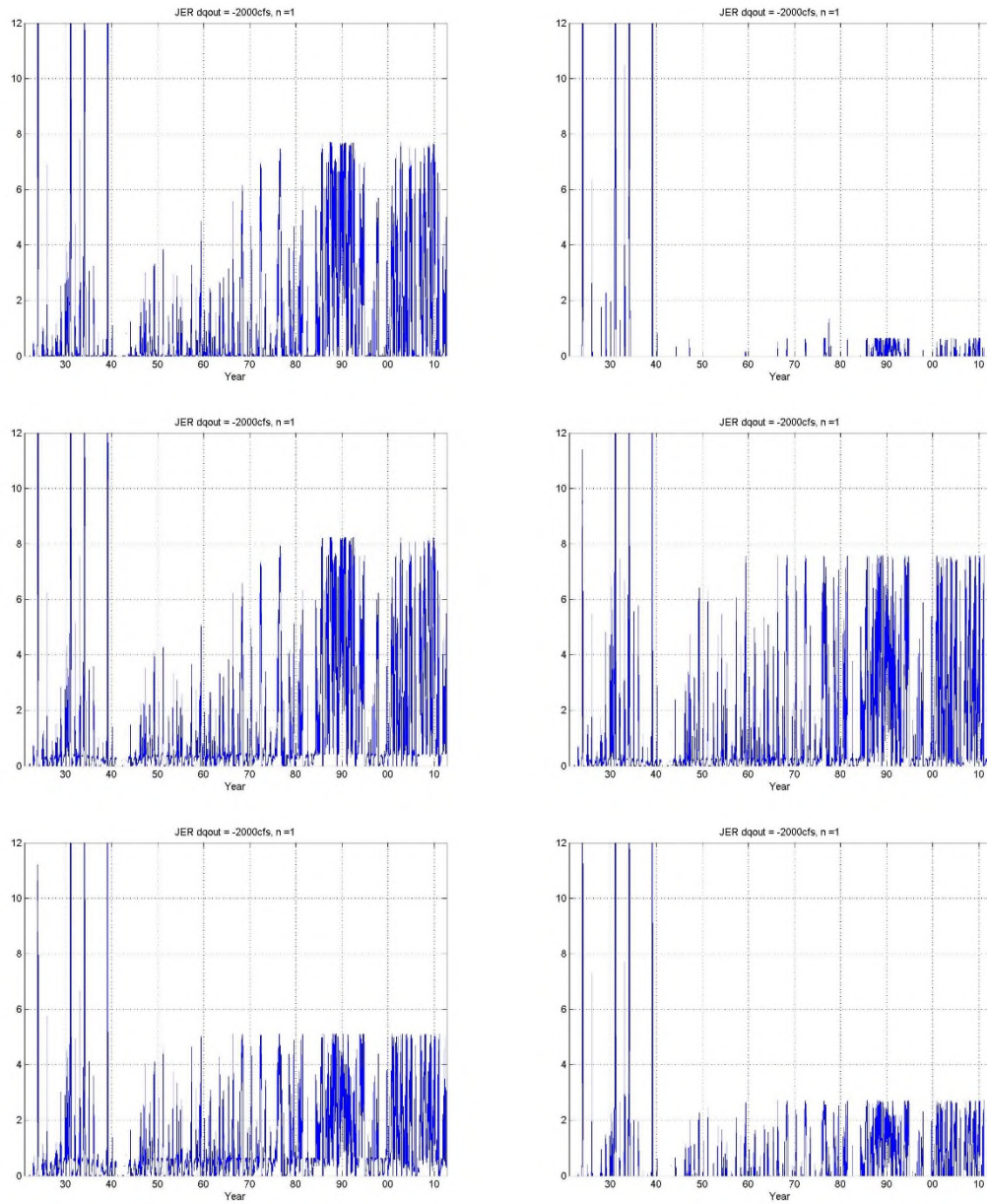


Figure 4-25 Sensitivity in EC ( $\mu\text{S}/\text{cm}$ ) of San Joaquin River fitted DSG model to changes in Delta outflow (-2000 cfs). Results are shown for multiple trained ANNs, each initialized with randomized weights and biases.

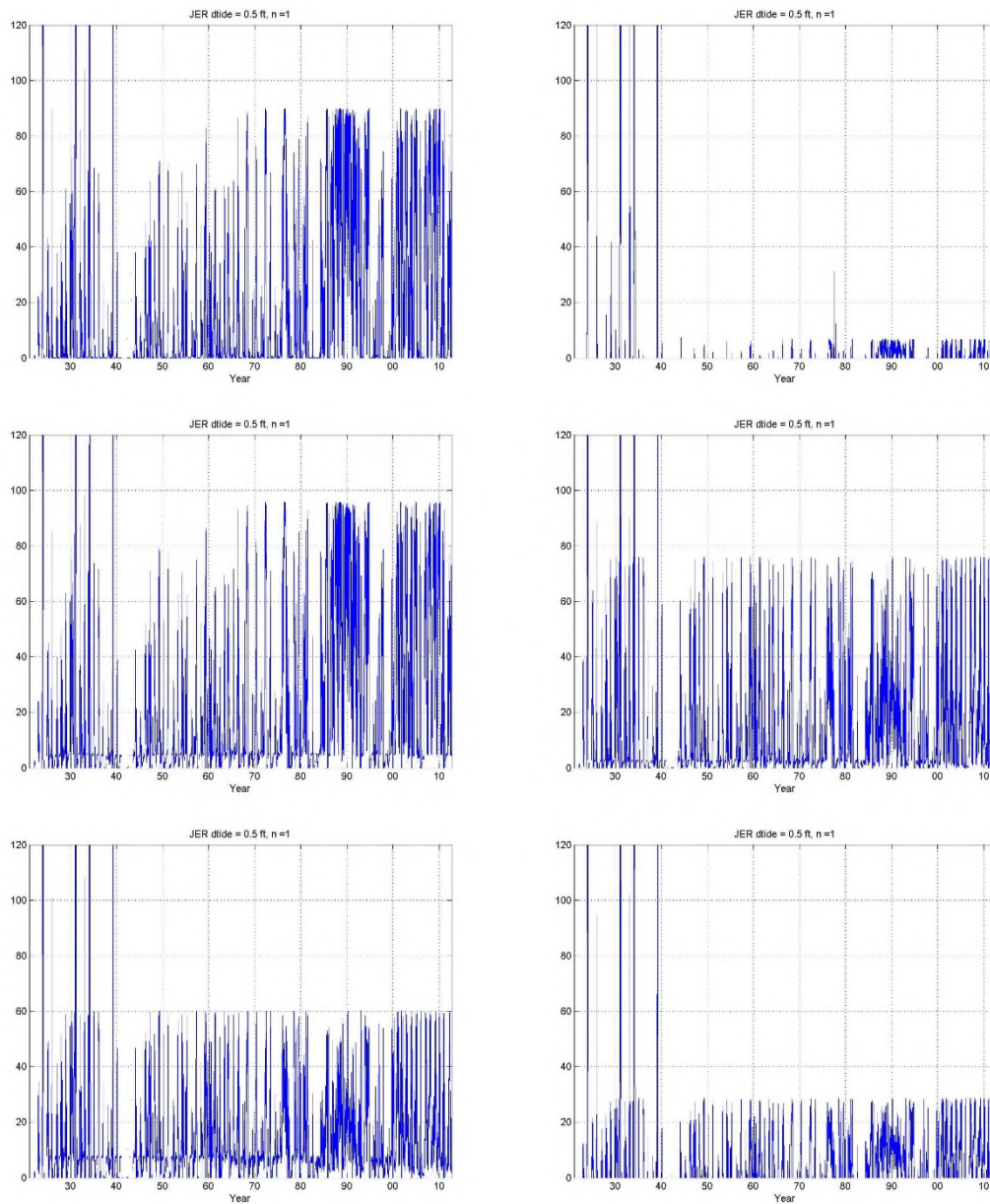


Figure 4-26 Sensitivity in EC ( $\mu\text{S}/\text{cm}$ ) of San Joaquin River fitted DSG model to changes in mean sea level (0.5 ft). Results are shown for multiple trained ANNs, each initialized with randomized weights and biases.

## 4.6.2 Training for X2

Intermediate ANN models were trained to predict X2 position for the Sacramento and San Joaquin River reaches.

### 4.6.2.1 Model 2A-1 (Training using Qrio, Qwest, MSL and Tidal Range as Inputs)

The ANN models were trained using a network size of 2, 5, and 10 hidden neurons and a time delay of 15, 30 and 60 days. Model fit for the different network sizes and time delays is shown in

Figure 4-27. The sensitivity to Qwest flow (+2000 cfs) and a sea level increase of 0.5 ft is shown in Figure 4-28 to Figure 4-29. The sensitivity to Qwest flow and mean sea level started to show inconsistencies when the network size exceeded 2 ( $n = 5, 10$ ). The best model had  $n = 2$  hidden neurons with  $d = 60$  days ( $r > 0.955$ ).

ANN models were trained for selected network sizes (1 to 5 hidden neurons) and time delay (30 to 120 days; Table 4-10) to identify the best model. Each network structure was trained for 2 iterations. The overall model fit improved with increases of network sizes and time delay, as in all prior tests. However, the sensitivity to mean sea level increase showed inconsistent results when the network size exceeded 3 (Table 4-11). The models with 1-3 hidden neurons showed reasonable fit and sensitivity to mean sea level. The best models were found at  $n = 4$  hidden neurons with  $d = 120$  days ( $r = 0.976$ ) and  $n = 3$  hidden neurons with  $d = 90$  days ( $r = 0.979$ ).

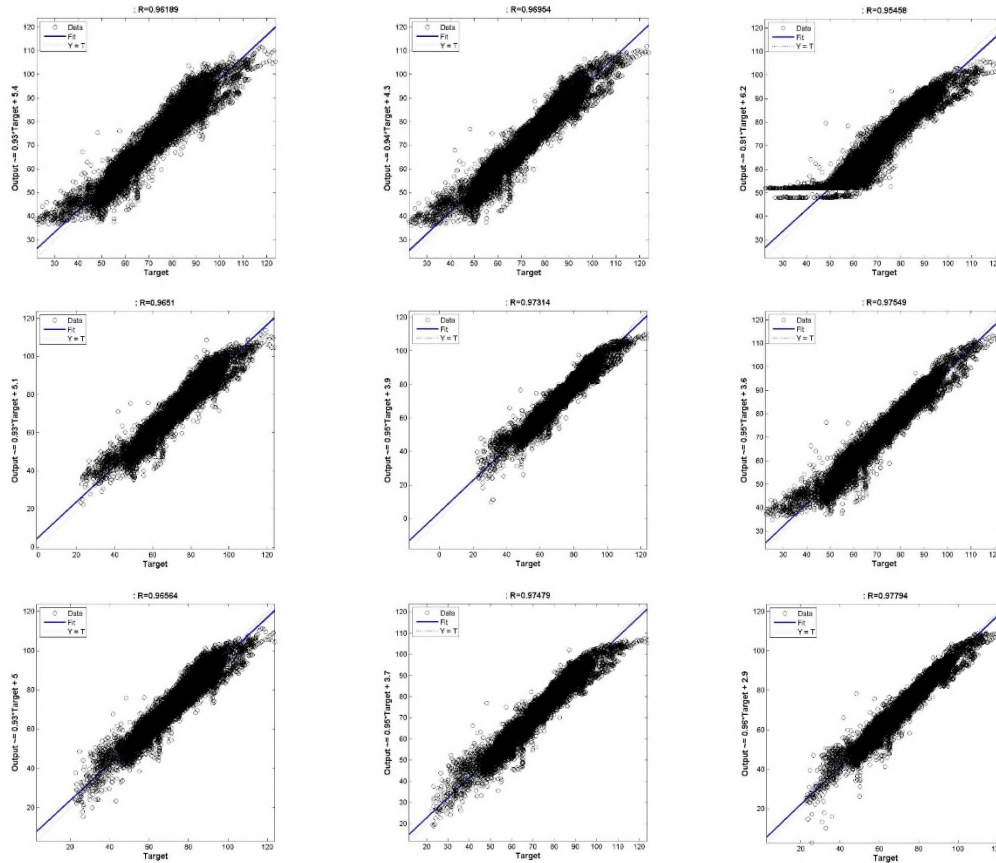


Figure 4-27 X2 model fit for the Sacramento River (n = 2, 5, 10) with time delay of 15, 30 and 60 days.

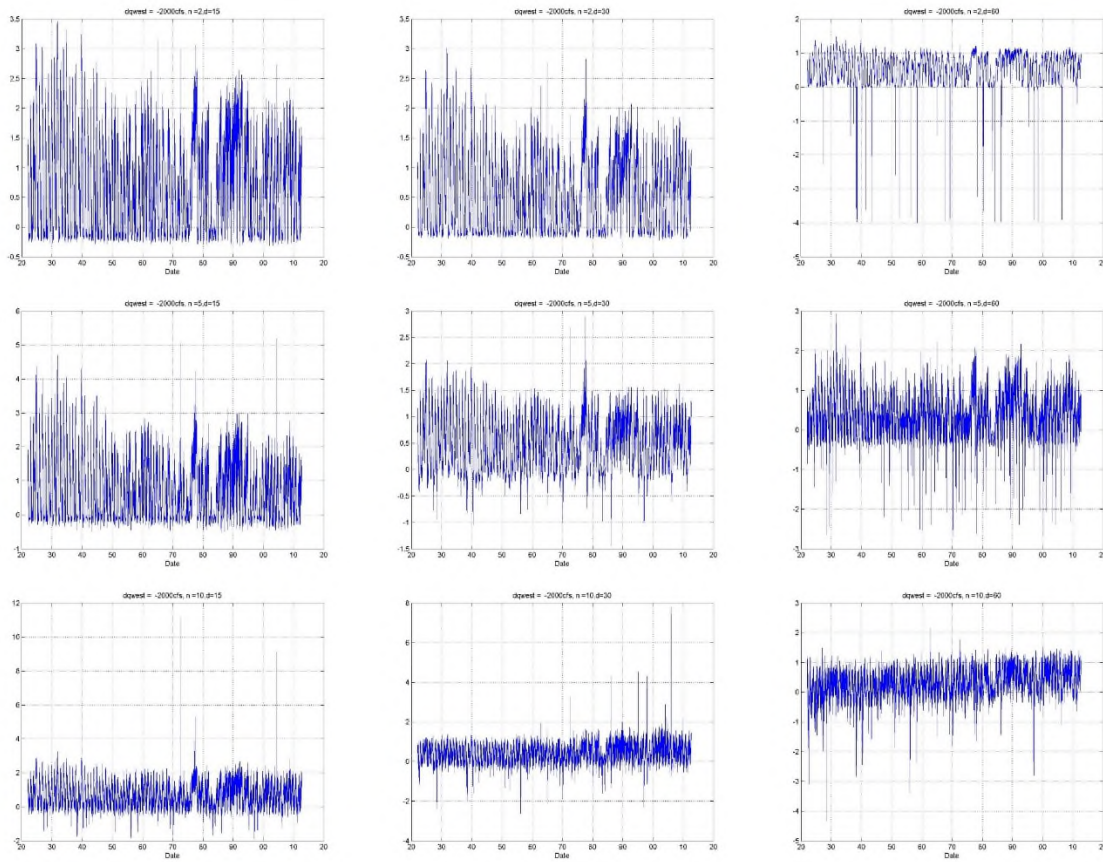


Figure 4-28 Sensitivity of fitted X2 model to Qwest flow change (Sacramento River model,  $n = 2, 5, 10$ ) with time delay of 15, 30 and 60 days.

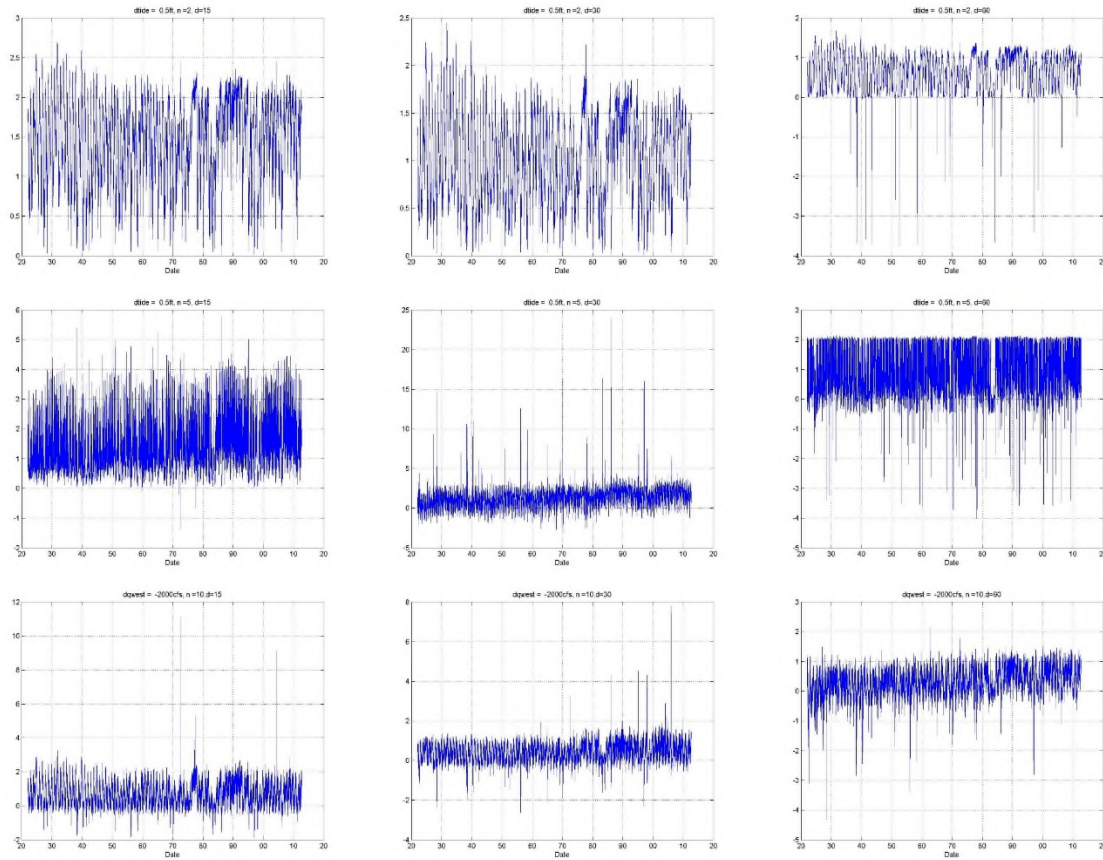


Figure 4-29 Sensitivity of fitted X2 model to mean sea level increase of 0.5 ft (Sacramento River model,  $n = 2, 5, 10$ ) with time delay of 15, 30 and 60 days.

Table 4-10 Model fit of trained ANN models at Sacramento River (in terms of r) for different network size and time delay

Network size \ time delay	d = 30	d=60	d=90	d=120
n=1	0.951	0.955	0.955	0.956
n=1	0.951	0.955	0.955	0.956
n=2	0.970	0.974	0.974	0.957
n=2	0.970	0.974	0.955	0.976
n=3	0.972	0.975	0.979	0.975
n=3	0.971	0.976	0.976	0.966
n=4	0.973	0.975	0.976	0.977
n=4	0.970	0.977	0.977	0.976
n=5	0.970	0.977	0.977	0.979
n=5	0.975	0.975	0.977	0.978

Bold means models with good fit and sensitivity.

**Table 4-11 Sensitivity of trained ANN models at Sacramento to mean sea level increase of 0.5 ft River (change X2 from base case, in km)**

Network size\time delay	d = 30	d=60	d=90	d=120
n=1	1.4	1.4	1.6	2
n=1	1.4	1.4	1.5	1.5
n=2	2	1.2	1.2	3.2
n=2	2	1.2	1.5	1.5
n=3	x	1.5	1.8	1.5
n=3	2	1.5	1.8	x
n=4	x	x	2.5	2.5
n=4	x	x	x	2.8
n=5	x	x	3.5	3
n=5	4	1.5	x	x

x: sensitivity to mean sea level increase is not physically plausible. Bold means models with good fit and sensitivity.

#### 4.6.2.2 Model 2A-2 (Training using Qout, MSL and Tidal Range as Inputs)

ANN model fits are shown in Figure 4-30 and Figure 4-31. The sensitivity to flow and tide are shown in Figure 4-32 through Figure 4-35. For two neuron models, when the r value of the fit is greater than 0.97, the sensitivity to mean sea level change was not physically plausible.

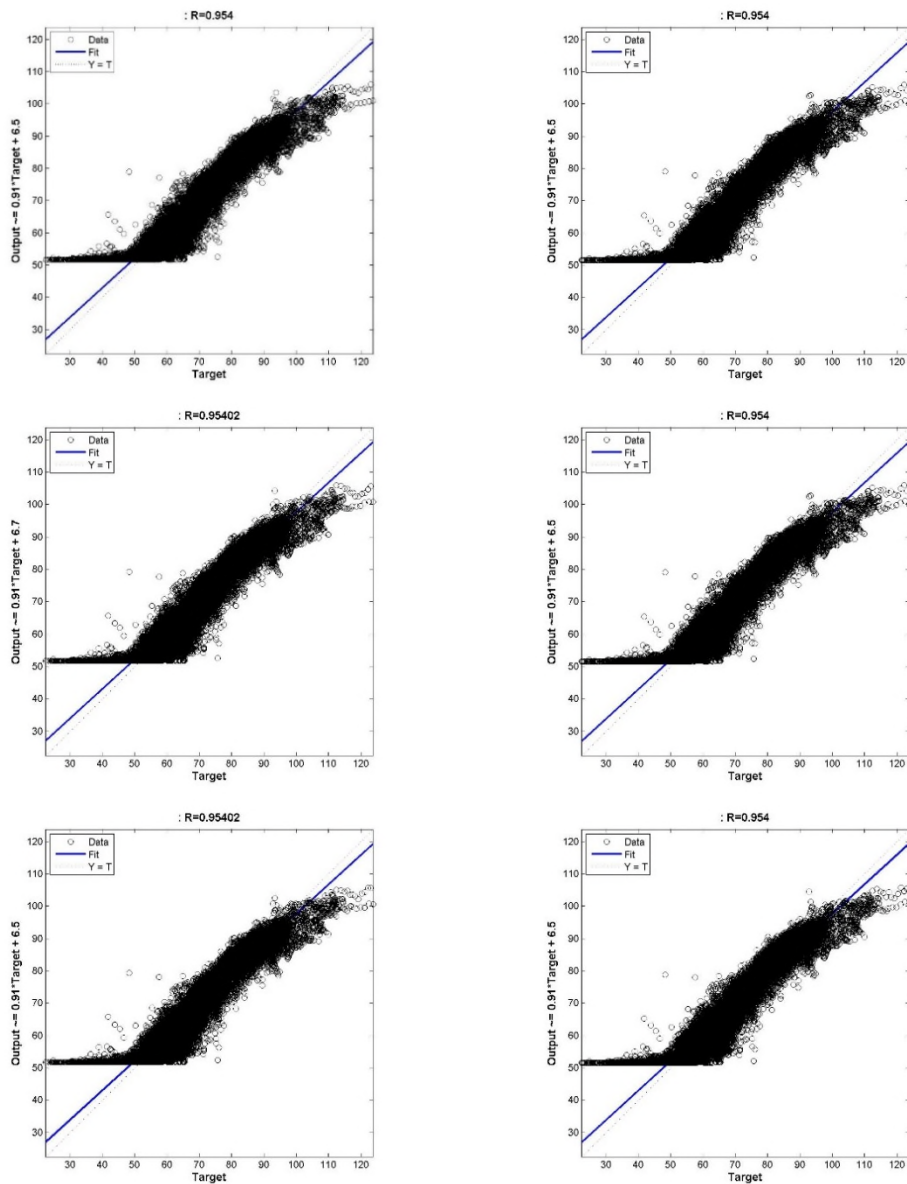


Figure 4-30 X2 model fit for the Sacramento River model ( $n=1, d=120$ ). Results are shown for multiple trained ANNs, each initialized with randomized weights and biases.

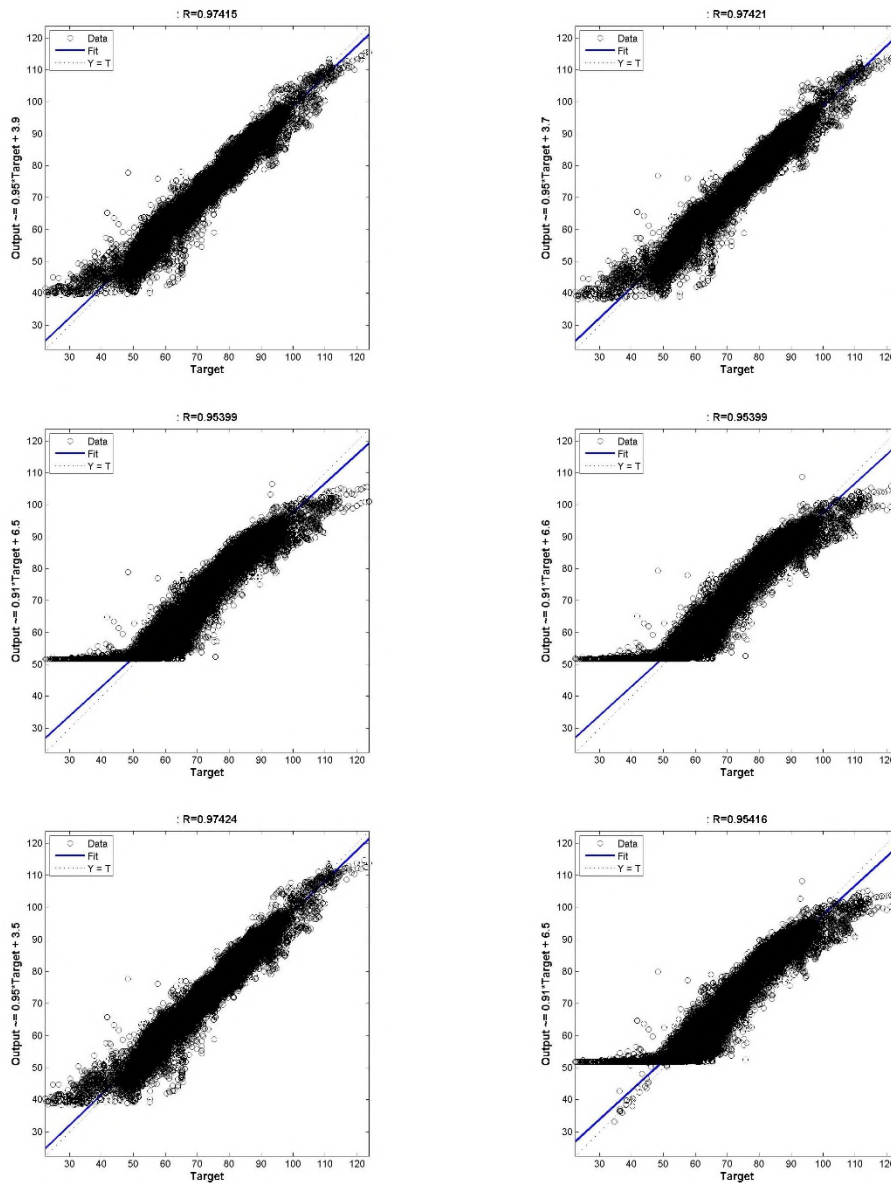


Figure 4-31 X2 model fit for the Sacramento River model ( $n=2$ ,  $d=120$ ). Results are shown for multiple trained ANNs, each initialized with randomized weights and biases.

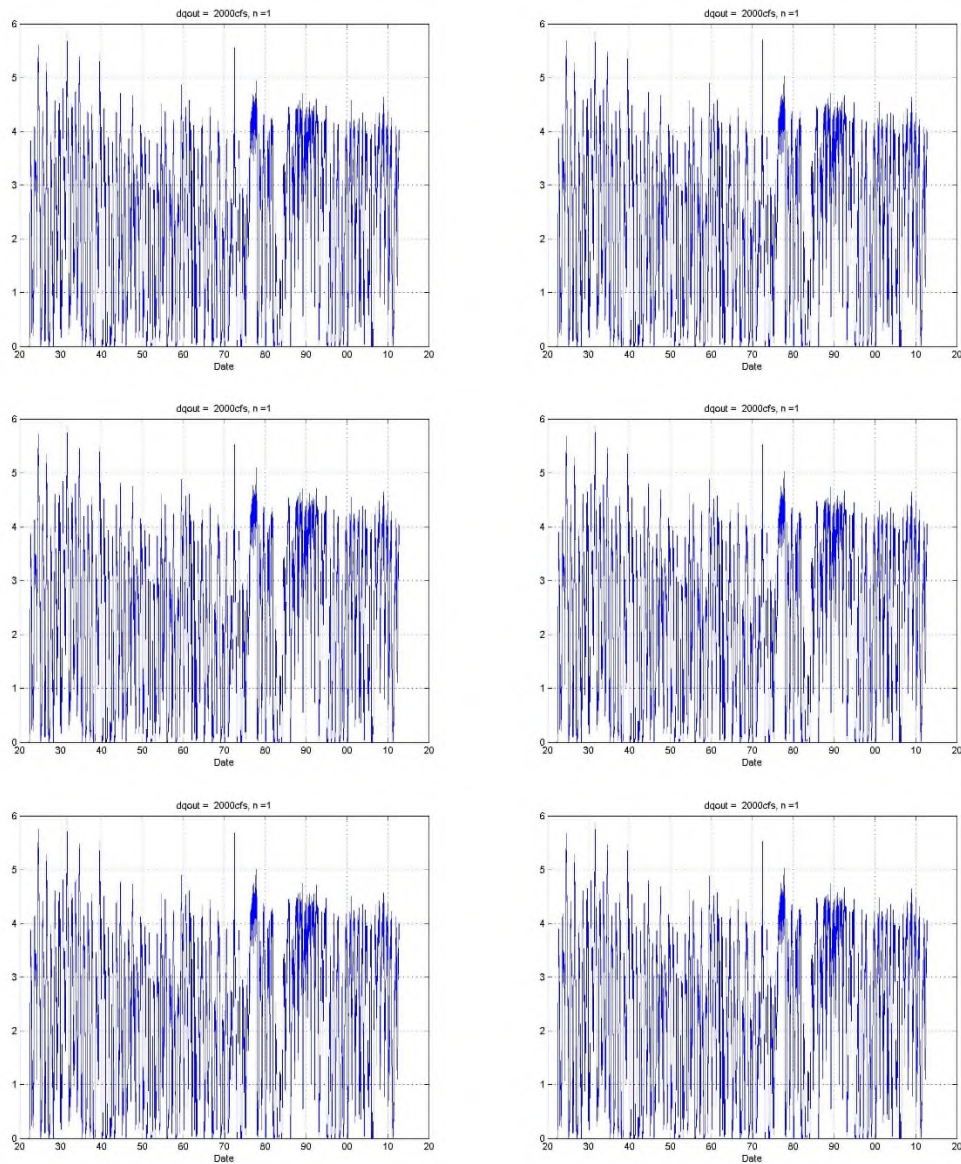


Figure 4-32 Sensitivity of fitted X2 (km) model to delta outflow change (Sacramento River model,  $n=1$ ,  $d=120$ ). Results are shown for multiple trained ANNs, each initialized with randomized weights and biases.

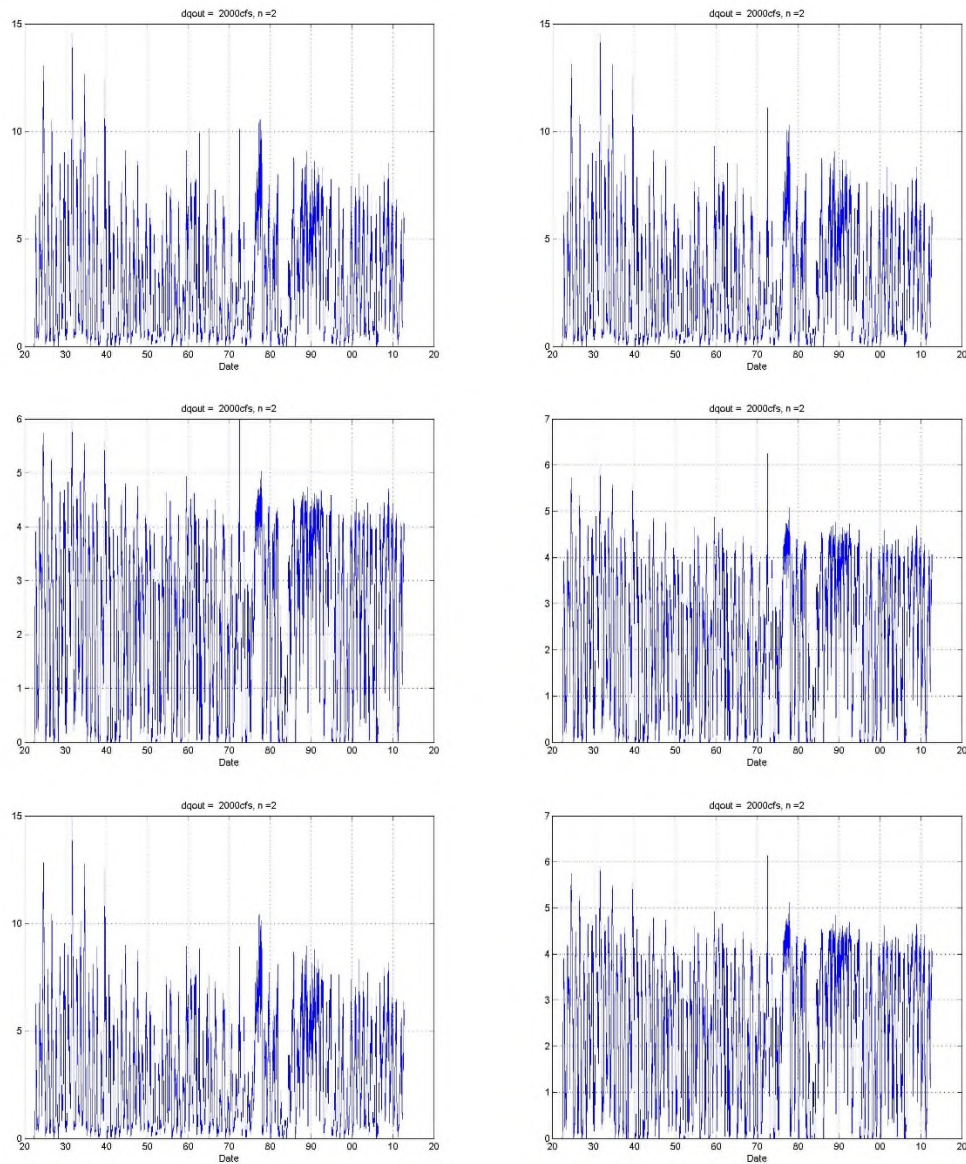


Figure 4-33 Sensitivity of fitted X2 model to delta outflow change (Sacramento River model,  $n=2$ ,  $d=120$ ). Results are shown for multiple trained ANNs, each initialized with randomized weights and biases.

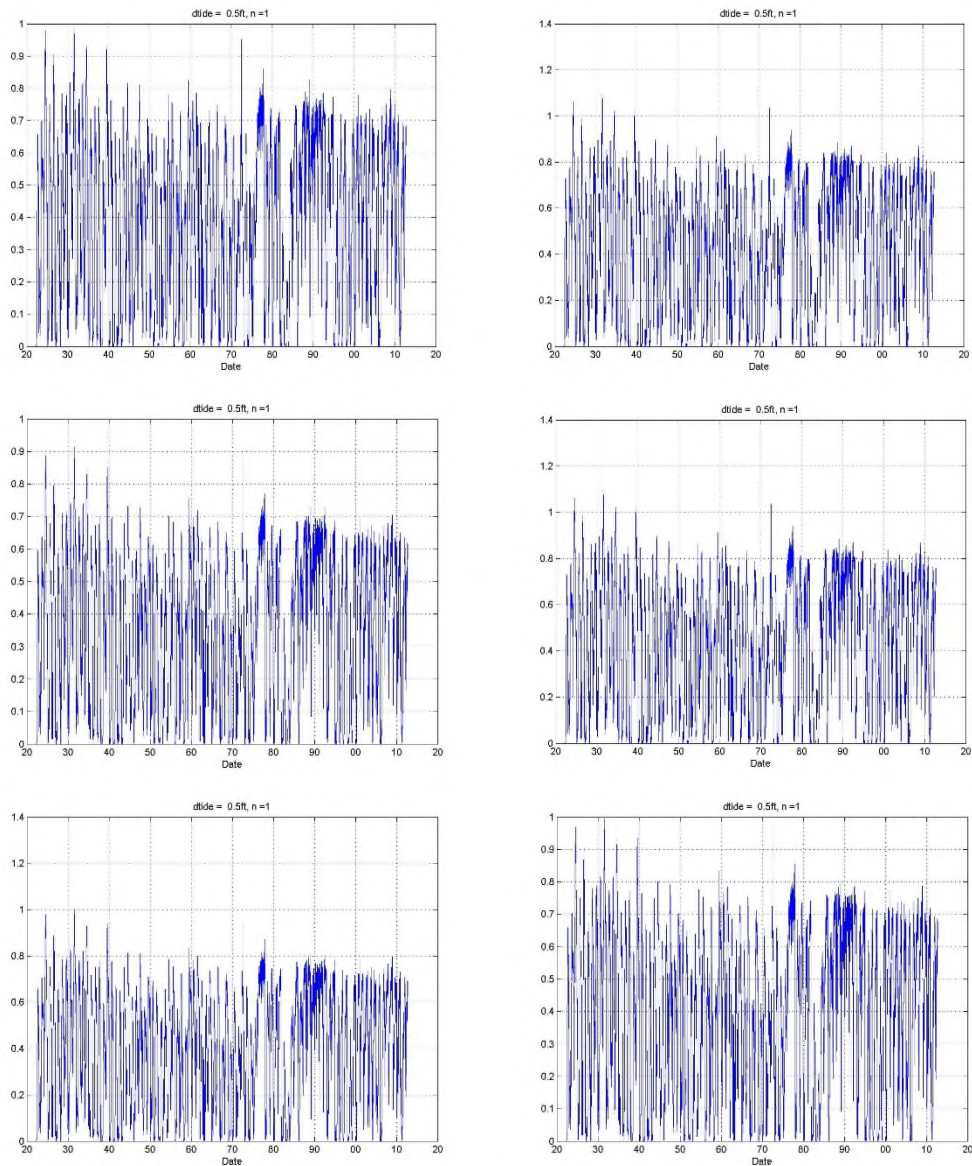


Figure 4-34 Sensitivity of fitted X2 model to mean sea level increase of 0.5 ft (Sacramento River model,  $n=1$ ,  $d=120$ ). Results are shown for multiple trained ANNs, each initialized with randomized weights and biases.

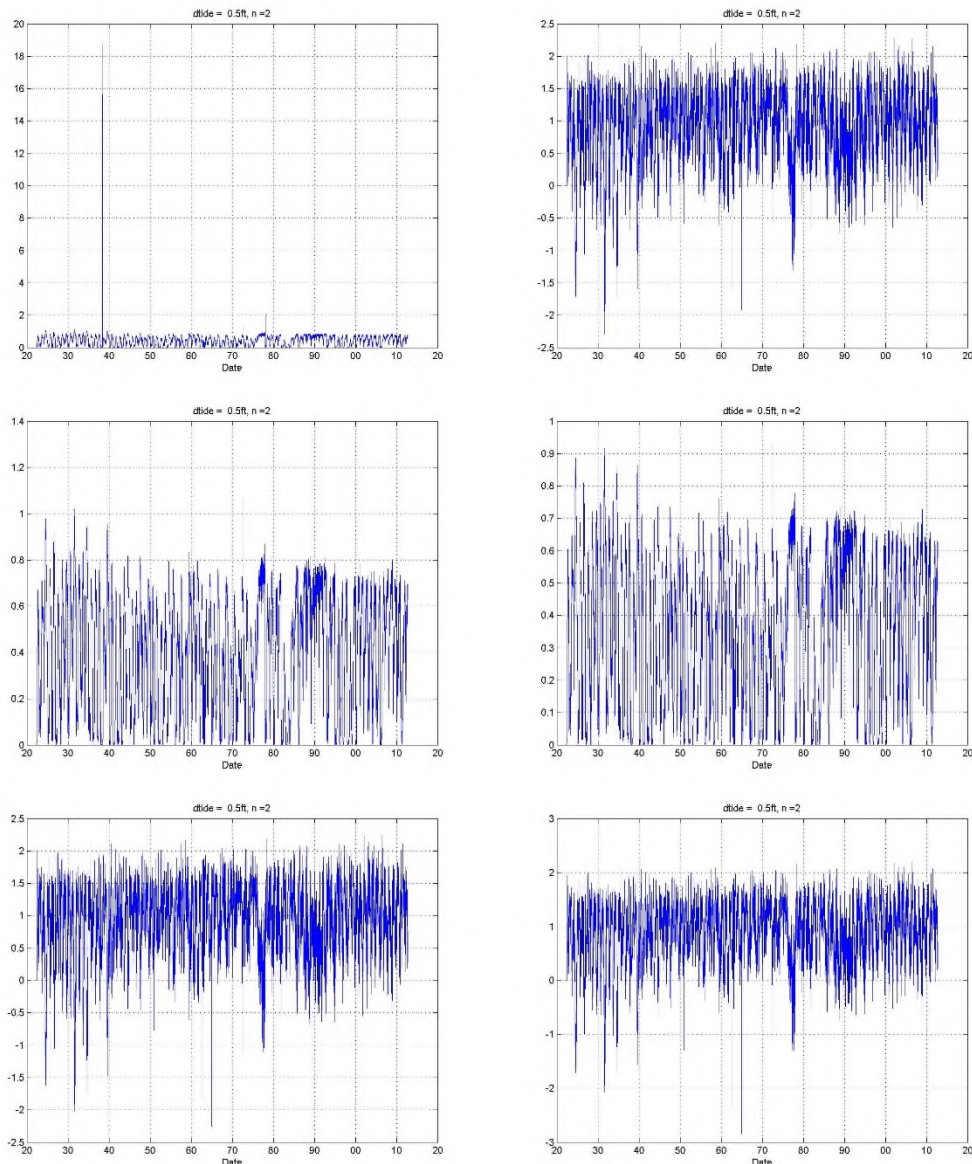


Figure 4-35 Sensitivity of fitted X2 model to mean sea level increase of 0.5 ft (Sacramento River model,  $n=2$ ,  $d=120$ ). Results are shown for multiple trained ANNs, each initialized with randomized weights and biases.

#### 4.6.2.3 Model 2B-1 (Training using Qrio, Qwest, MSL and Tidal Range as Inputs)

The ANN models were trained using a network size of 1, 2, 5, and 10 neurons and a time delay of 2, 15, and 30 days. The model fit for the different network sizes and time delays is shown in Figure 4-36. The sensitivity to Qwest flow (+2000 cfs) and mean sea level increase of 0.5 ft is shown in Figure 4-37 and Figure 4-38. The sensitivity test for network sizes of 1-10 hidden neurons and time delays of 2-30 days suggested the sensitivity becomes inconsistent when the hidden neurons exceed 2. The best model has  $n = 2$  hidden neurons and  $d = 15$  days ( $r = 0.947$ ).

The models were also trained for selected range of network sizes (1 to 3 neurons) and time delay (15 to 90 days; Table 4-12). The overall model fit increased with increases of network sizes and time delay, however the sensitivity to mean sea level increase started to show inconsistent behavior when the network size exceeded 1 hidden neuron or the time delay was greater than 15 days (Table 4-13). Best models were for  $n = 3$  hidden neurons with  $d = 15$  days ( $r = 0.948$ ) and  $n = 1$  hidden neuron with  $d = 90$  days ( $r = 0.941$ ).

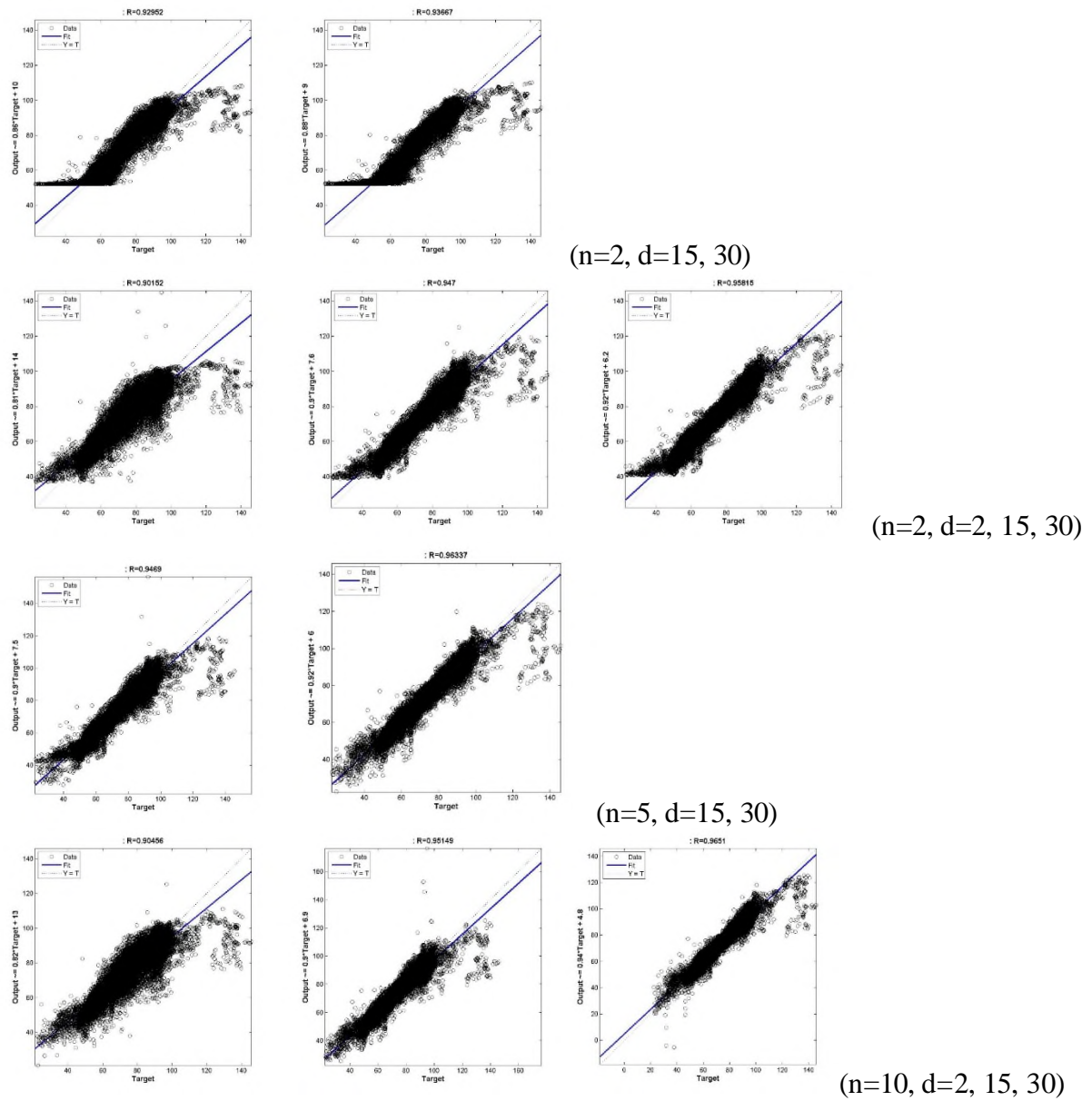


Figure 4-36 X2 model fit for the San Joaquin River ( $n = 1, 2, 5, 10$ ) with time delay of 2, 15 and 30 days.

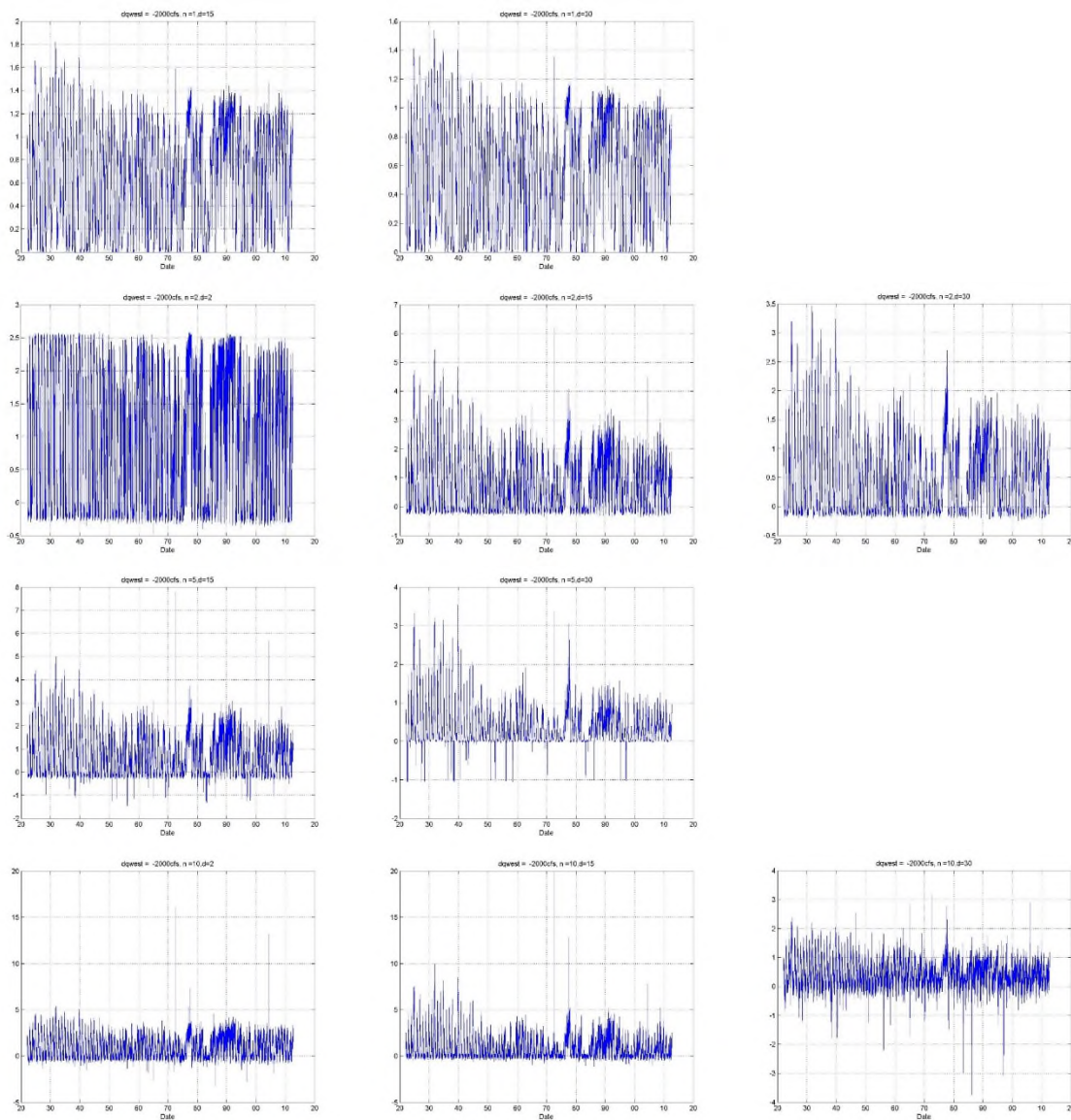


Figure 4-37 Sensitivity of fitted X2 model to Qwest flow change (San Joaquin River model,  $n=1, 2, 5, 10$ ) with time delay of 2, 15, and 30 days.

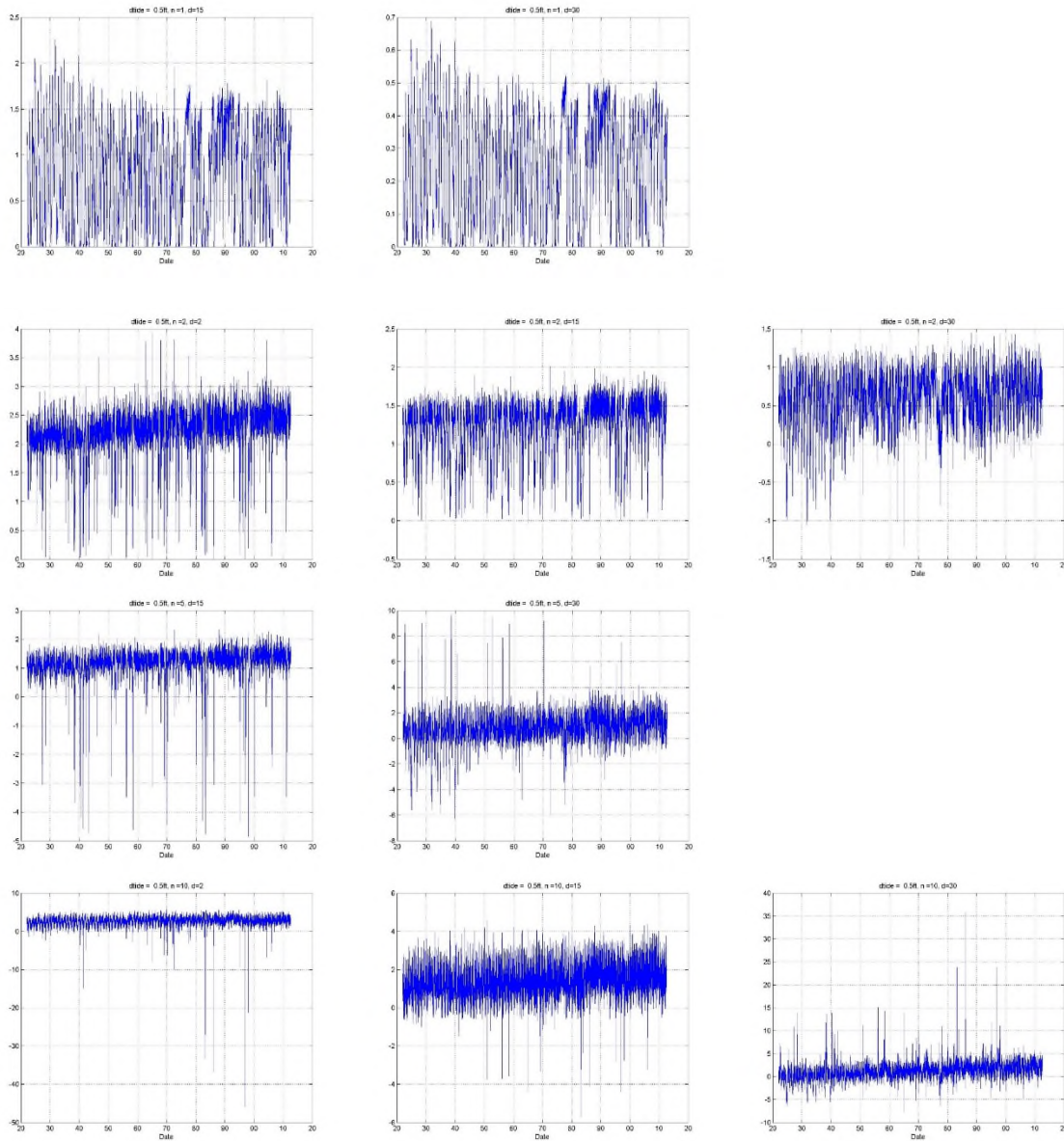


Figure 4-38 Sensitivity of fitted X2 model to sea level increase of 0.5 ft (San Joaquin River model,  $n = 1, 2, 5, 10$ ) with time delay of 2, 15 and 30 days.

**Table 4-12 Model fit of trained ANN models at San Joaquin River (in terms of r) for different network size and time delay**

Network size\time delay	d=15	d=30	d=45	d=60	d=75	d=90
n=1	0.930	0.937	0.939	0.940	0.941	0.941
n=1	0.930	0.937	0.938	0.940	0.941	0.941
n=2	0.947	0.955	0.963	0.961	0.005*	0.966
n=2	0.947	0.958	0.963	0.948	0.966	0.966
n=3	0.947	0.958	0.963	0.965	0.932	0.969
n=3	0.948	0.964	0.964	0.967	0.966	0.966

\*training did not converge. Bold means models with good fit and sensitivity.

**Table 4-13 Sensitivity of trained ANN models at San Joaquin River to mean sea level increase of 0.5 ft (change in X2 from base case, in km)**

Network size\time delay	d=15	d=30	d=45	d=60	d=75	d=90
n=1	2	0.5	x	0.04	x	0.12
n=1	2	0.5	x	x	x	0.15
n=2	2	0.7	x	x	x	x
n=2	1.8	x	x	x	x	x
n=3	1.8	x	x	x	0.4	x
n=3	2	x	x	x	x	x

x: sensitivity to mean sea level increase is not physically plausible. Bold means models with good fit and sensitivity.

**4.6.2.4 Model 2B-2 (Training using Qout, MSL and Tidal Range as Inputs)**

ANN model fit and sensitivity are shown in Figure 4-39 to Figure 4-41. Model sensitivity concerns occur when the time delay was greater than 30 days. Therefore, a shorter time delay of 14 days was used in the model.

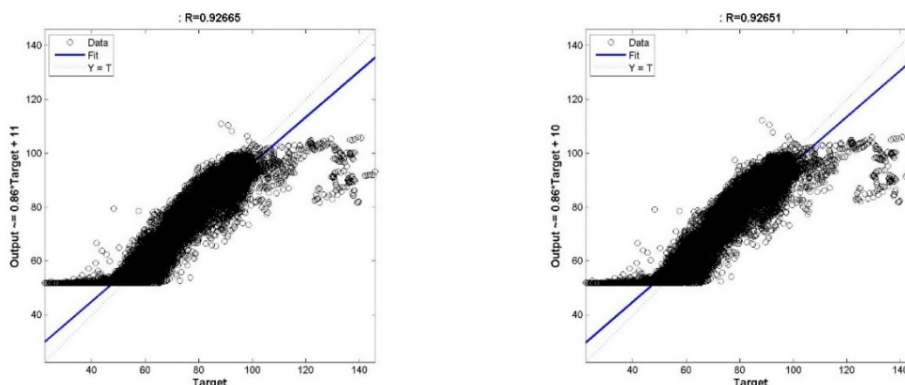


Figure 4-39 X2 model fit for the San Joaquin River model (n =1, n =2) with a time delay of 14 days

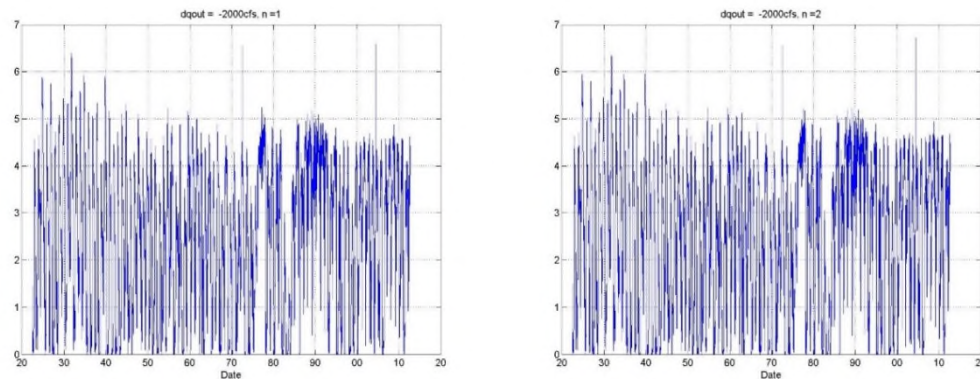


Figure 4-40 Sensitivity of fitted X2 model to delta outflow (San Joaquin River model,  $n = 1$ ,  $n = 2$ )

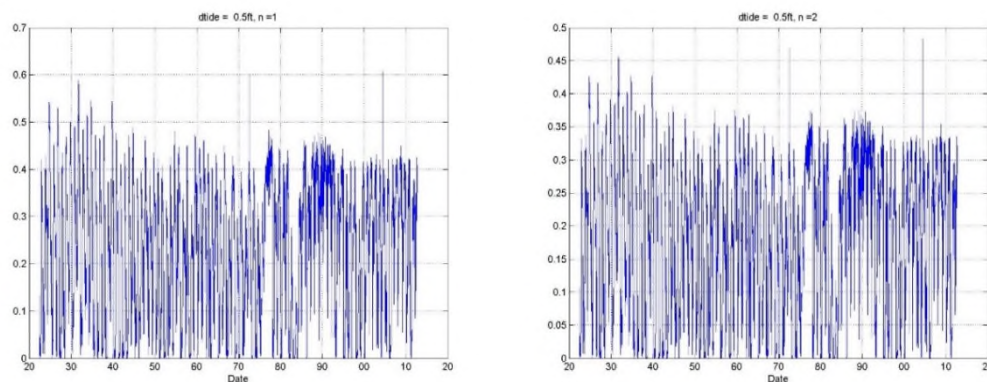


Figure 4-41 Sensitivity of fitted X2 model to mean sea level of 0.5 ft (San Joaquin River model,  $n = 1$ ,  $n = 2$ )

## 4.7 DSG RESIDUAL-BASED ANN MODELS

### 4.7.1 Model 3A (Sacramento River)

The intermediate ANN model generally fits the X2 training data well (Figure 4-42 and Figure 4-43). The model over-predicts X2 position under very high flows ( $X2 < 50\text{km}$ ). Performance is slightly worse in the higher-flow winter months (January–April) and slightly better in the dry, summer months (June–September). The fitted model has similar performance relative to the entire dataset (Figure 4-44 and Figure 4-45) and a similar pattern of seasonal performance variation. The residuals from the DSG model and from the combined DSG-ANN model are shown in Figure 4-46, indicating that there is a slight improvement in the residuals (closer to a mean of zero and narrower range), although there still remains noise that is not explained by the combined DSG-ANN model.

Sensitivity to sea level rise was assessed by adding a constant 0.5 ft to the mean sea level input while leaving all other inputs the same and comparing model predictions (Figure 4-47 to Figure 4-50). Figure 4-47 and Figure 4-49 show that X2 change is dependent on the magnitude of G-flow, and the X2 values in Figure 4-48 and Figure 4-50 show the overriding effects of Delta outflow on X2 position with symbol colors highlighting the

change in X2. X2 position shifts between 0 and 3km upstream, depending on the other inputs. The sea level rise effect appears to be suppressed under high flow conditions.

The use of a slightly improved X2 from the DSG-ANN model on the calculation of EC can also be examined. The model is able to meet the observed targets fairly well in most cases (Figure 4-51). Directly comparing the predictions to the targets (Figure 4-52 and Figure 4-53) shows good agreement on average, but there is a degree of variability around the mean. The targets at some stations further inland (modern RVB and EMM, ITB, WNG) are harder for the model to predict.

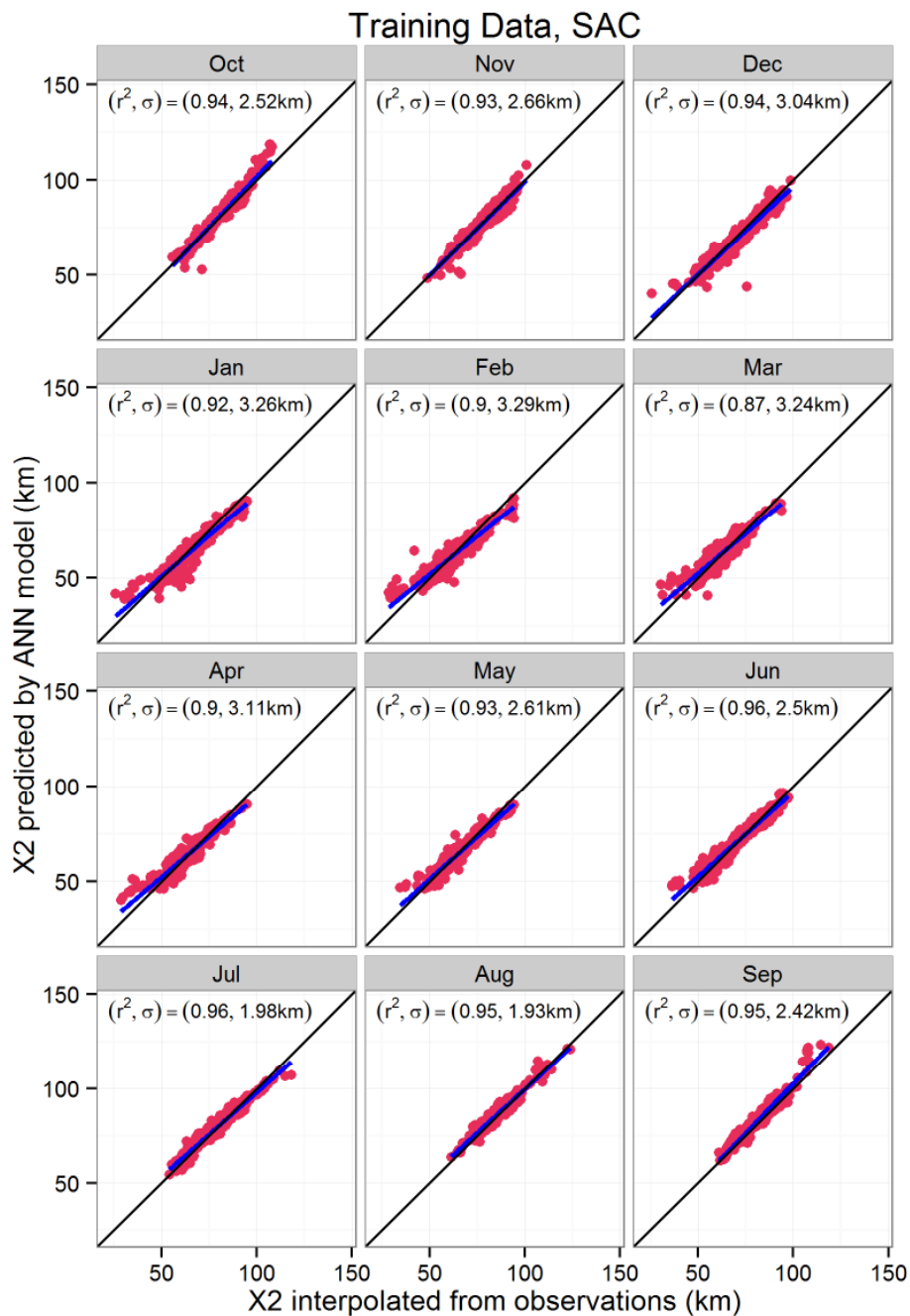


Figure 4-42

Sacramento River X2 targets interpolated from observed EC data against ANN predictions for the subset of data used to train the model, separated by month. The black line is  $y = x$ , and the blue line is a linear regression of the plotted points. Each panel's regression  $r^2$  and standard error,  $\sigma$ , are also shown.

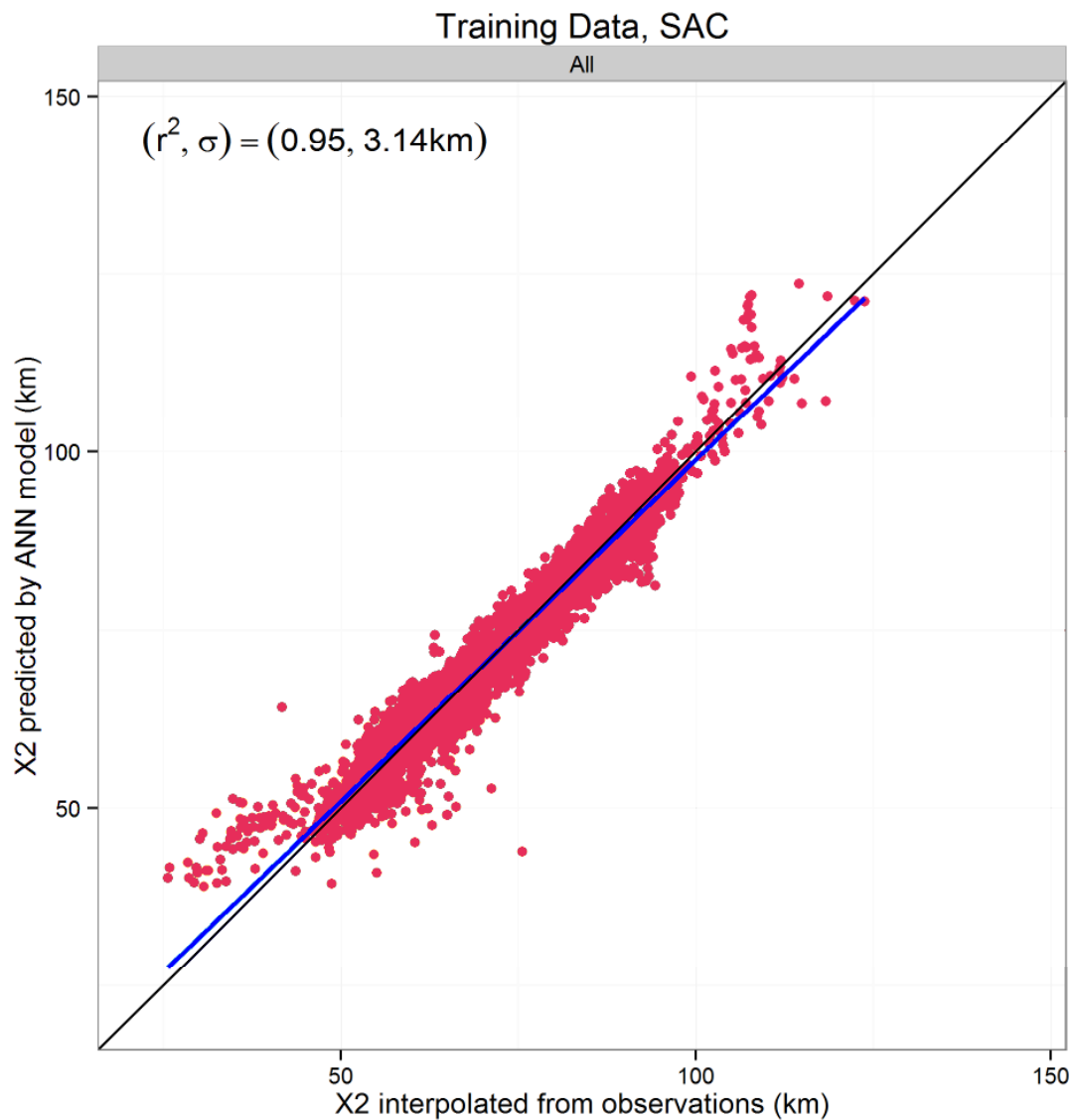


Figure 4-43 Sacramento River X2 targets interpolated from observed EC data against ANN predictions for the subset of data used to train the model, all months. The black line is  $y = x$ , and the blue line is a linear regression of the plotted points. Each panel's regression  $r^2$  and standard error,  $\sigma$ , are also shown.

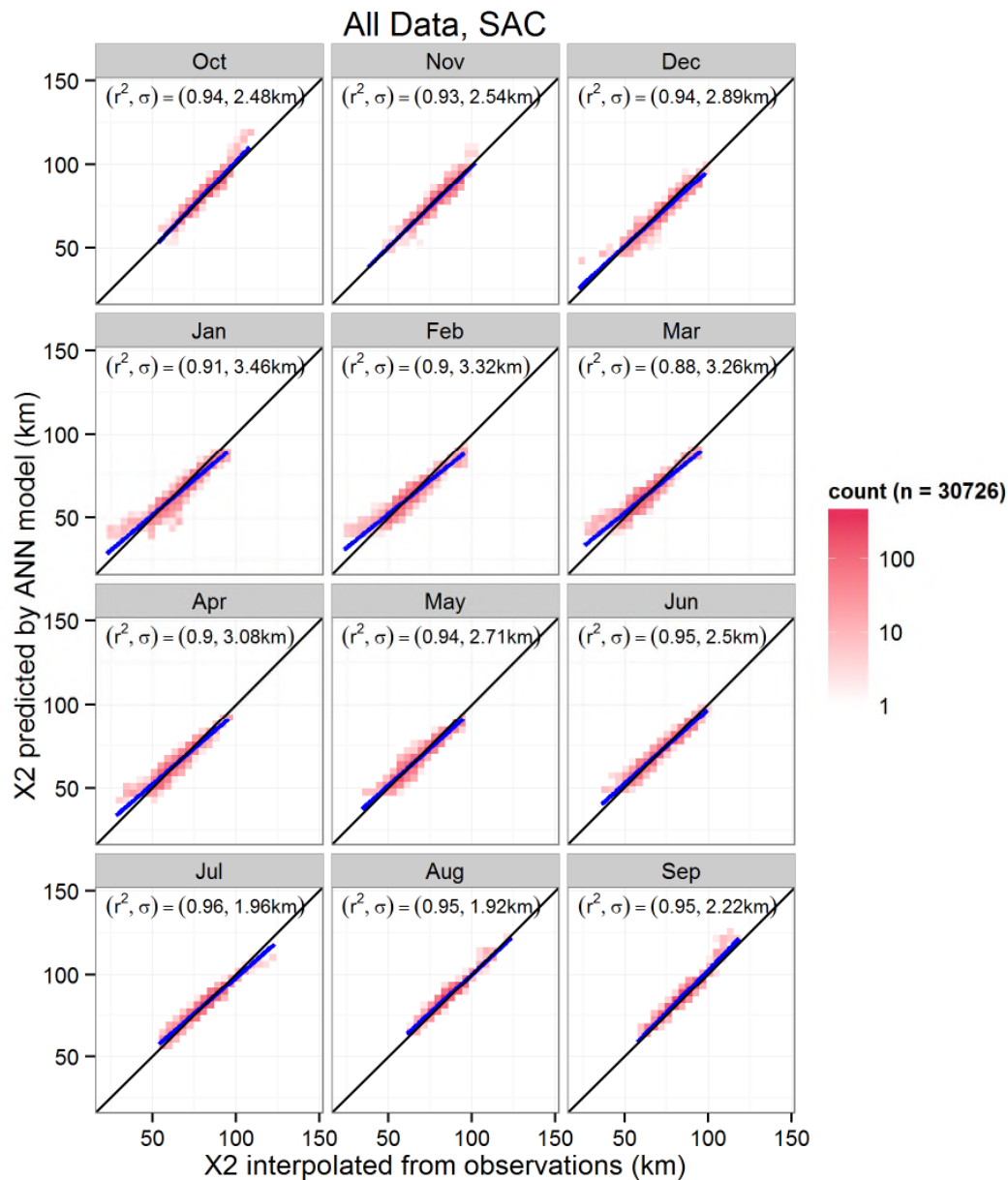


Figure 4-44

Sacramento River X2 targets interpolated from observed EC data against ANN predictions for all available data, separated by month. The black line is  $y = x$ , and the blue line is a linear regression of the plotted points. Each panel's regression  $r^2$  and standard error,  $\sigma$ , are also shown. Plots are displayed as binned counts of points to prevent overplotting.

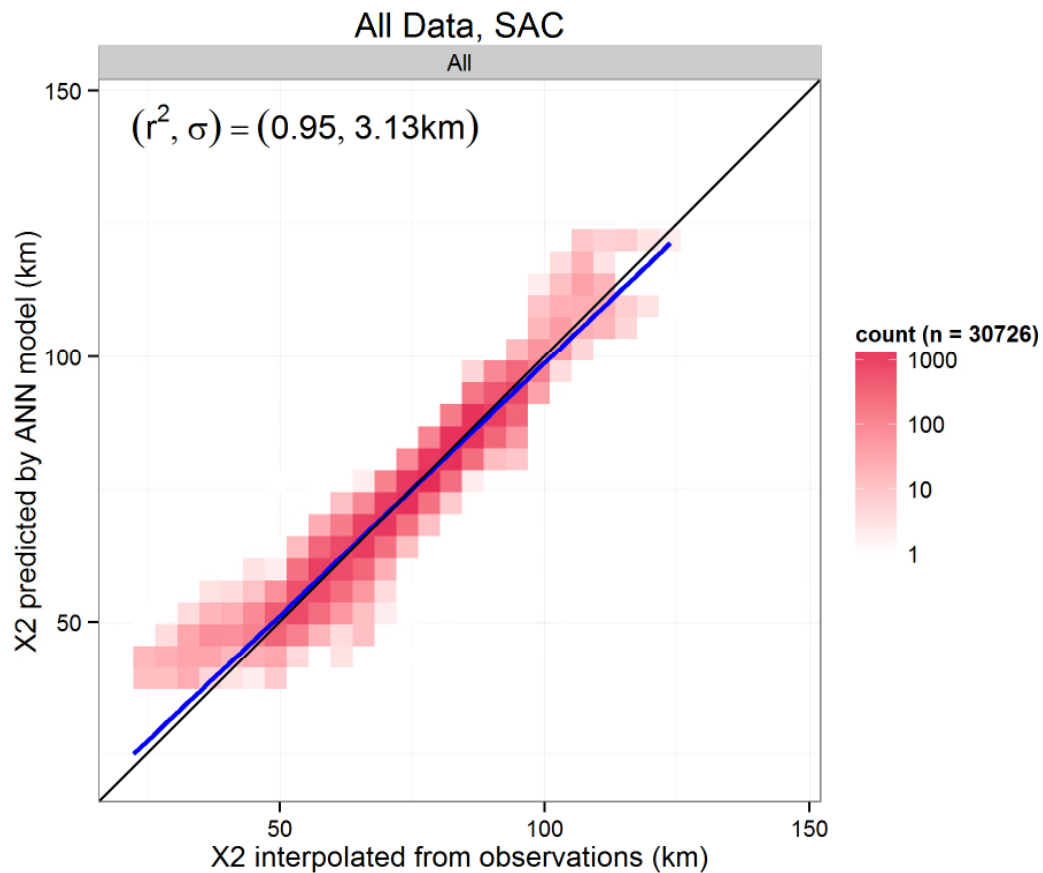


Figure 4-45 Sacramento River X2 targets interpolated from observed EC data against ANN predictions for all available data, all months combined. The black line is  $y = x$ , and the blue line is a linear regression of the plotted points. Each panel's regression  $r^2$  and standard error,  $\sigma$ , are also shown. The plot is displayed as binned counts of points to prevent overplotting.

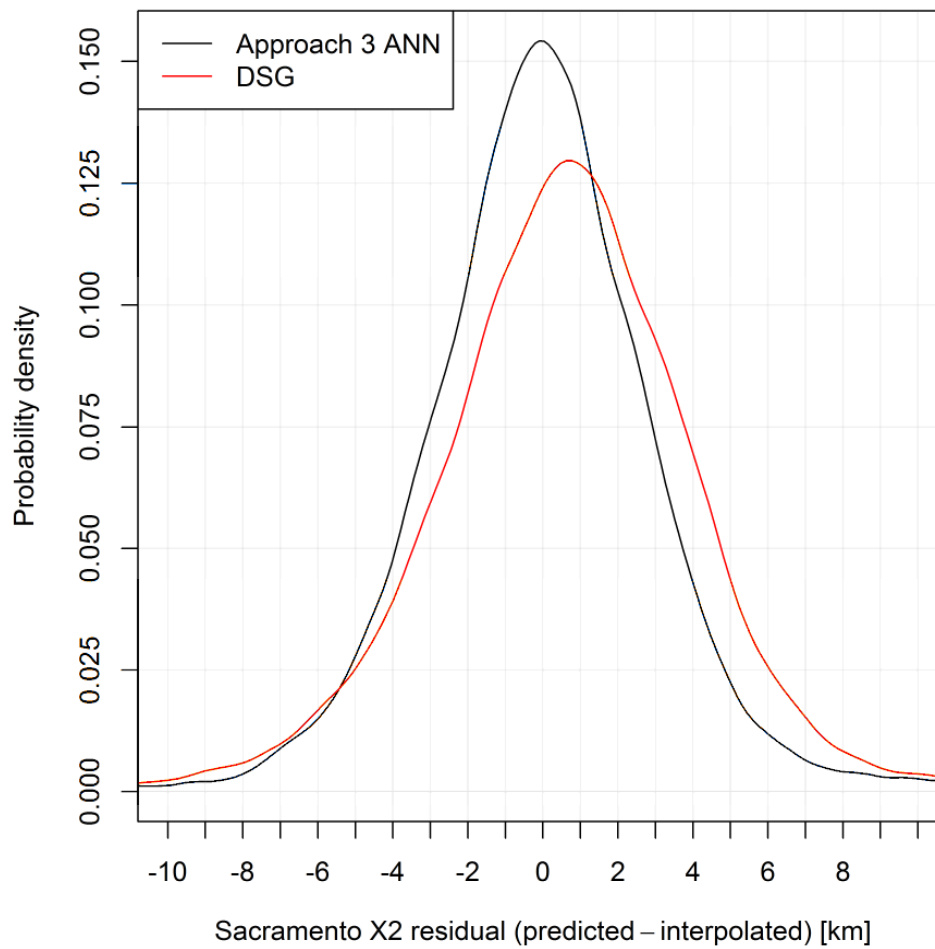


Figure 4-46 Distribution of residuals from the DSG model compared to the residuals from the ANN model for the Sacramento River.

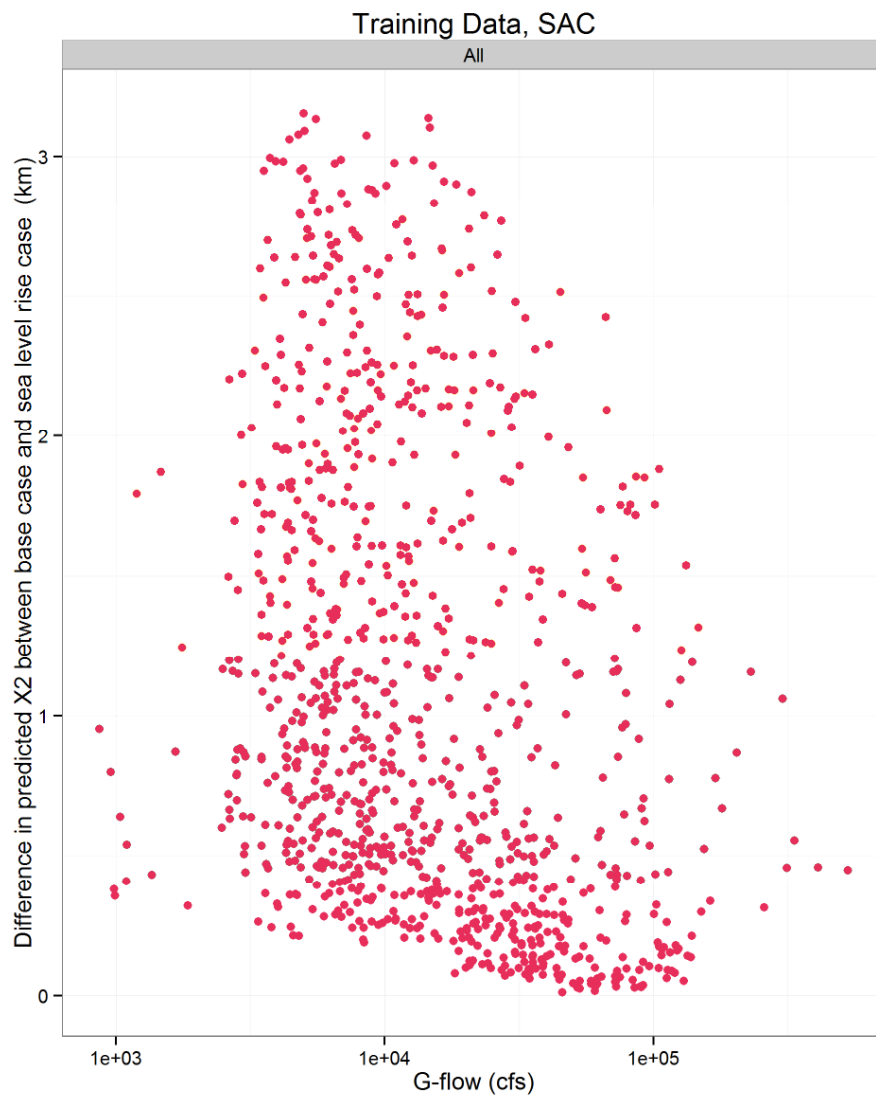


Figure 4-47 Increase in Sacramento River X2 position due to uniform increase of 0.5 ft to mean sea level input for Approach 3 ANN model, conditioned on G-flow, for the subset of data used to train the model.

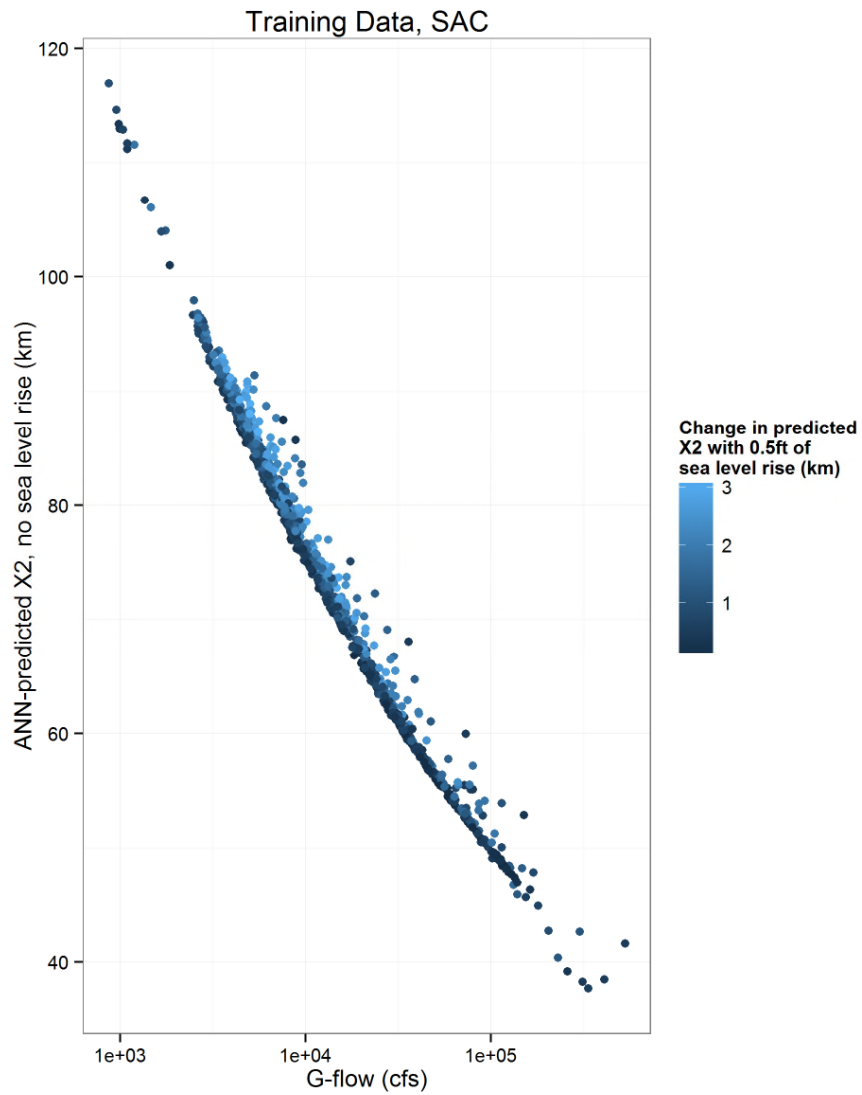


Figure 4-48 Increase in Sacramento River X2 position due to uniform increase of 0.5 ft to mean sea level input for Approach 3 ANN model, conditioned on G-flow and predicted X2 position, for the subset of data used to train the model.

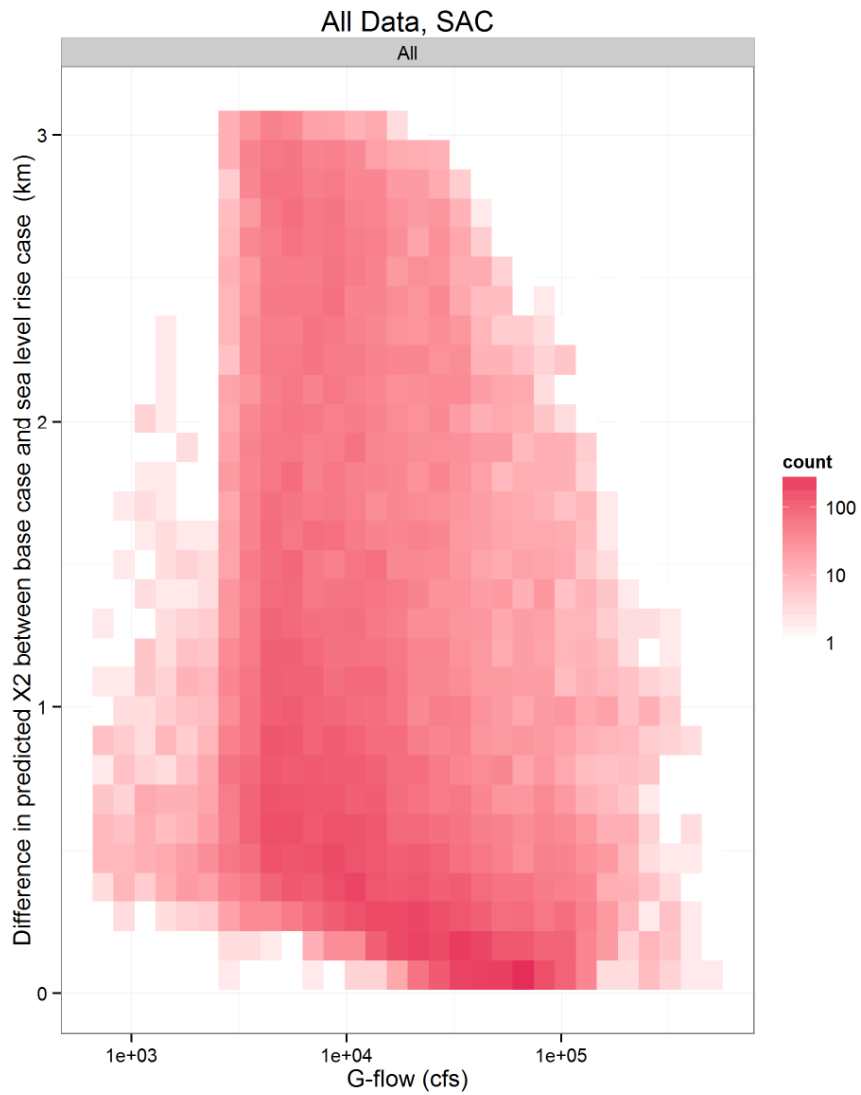


Figure 4-49 Increase in Sacramento River X2 position due to uniform increase of 0.5 ft to mean sea level input for Approach 3 ANN model, conditioned on G-flow, for all available data. The plot is displayed as binned counts of points to prevent overplotting.

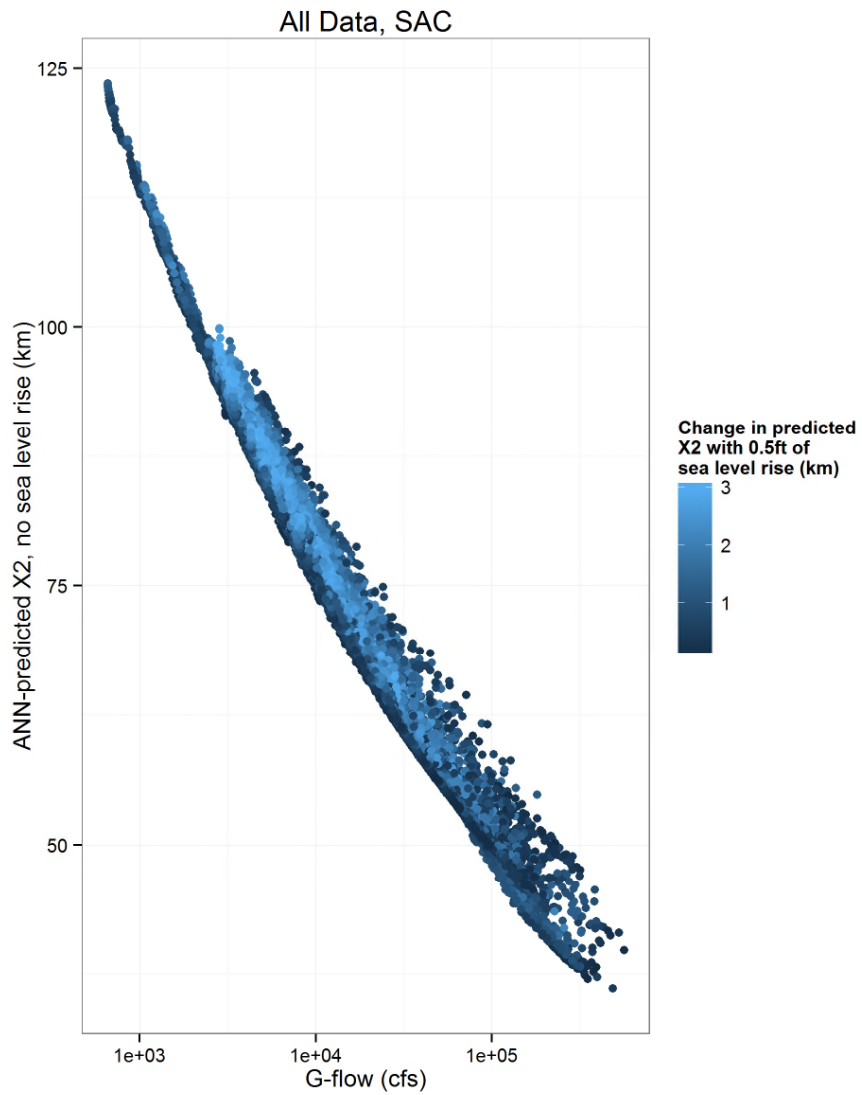


Figure 4-50 Increase in Sacramento River X2 position due to uniform increase of 0.5 ft to mean sea level input for Approach 3 ANN model, conditioned on G-flow and predicted X2 position, for all available data.

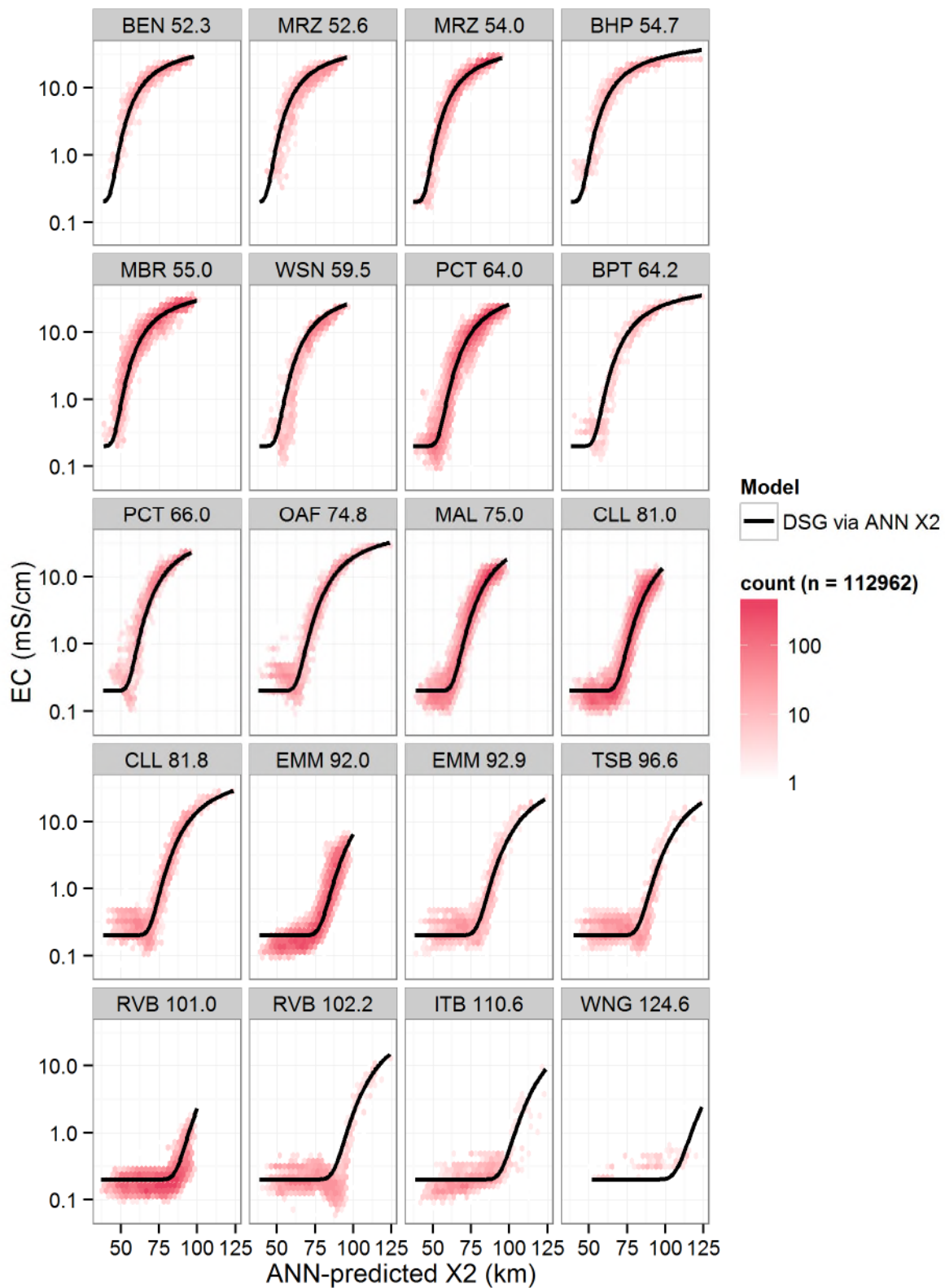


Figure 4-51 DSG-ANN model (black) at each station (with channel distance in km) on the Sacramento River. Observed data are plotted as binned counts to prevent overplotting.

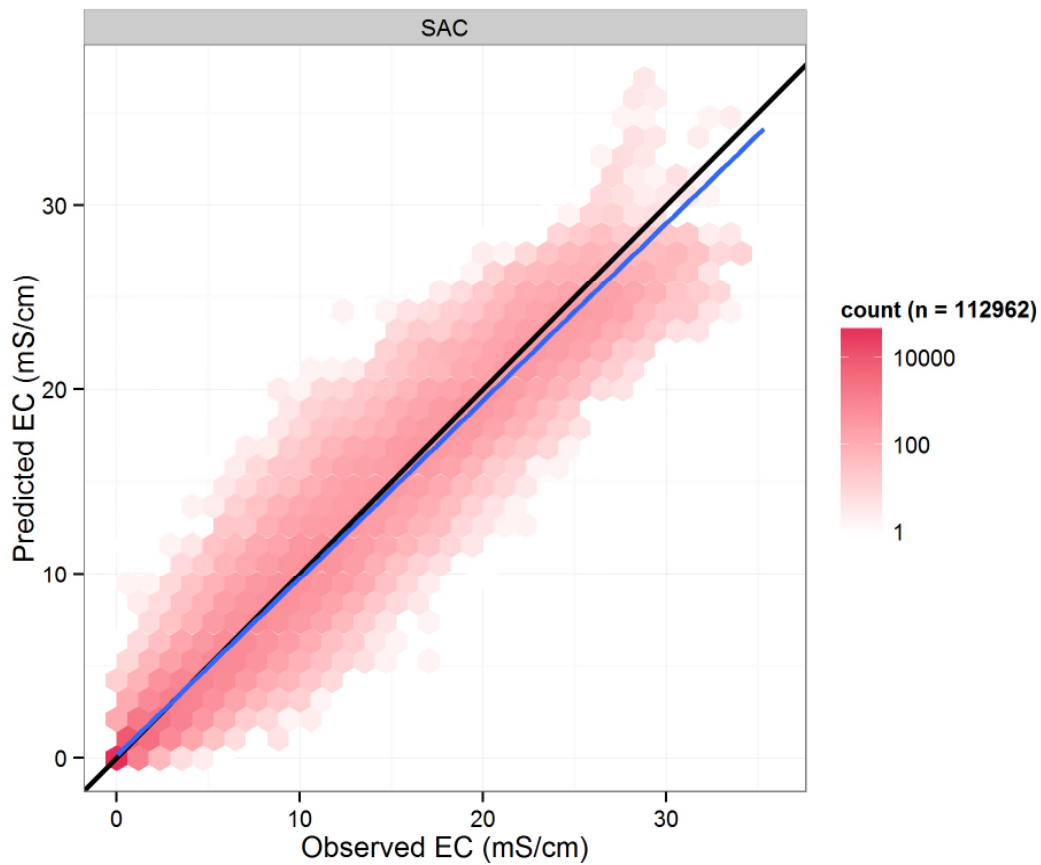


Figure 4-52 Sacramento River observed EC targets against EC predictions from DSG model using ANN X2. Points are displayed as binned counts to prevent overplotting. The black line is  $y = x$ , and the blue line is a linear regression of the underlying points.

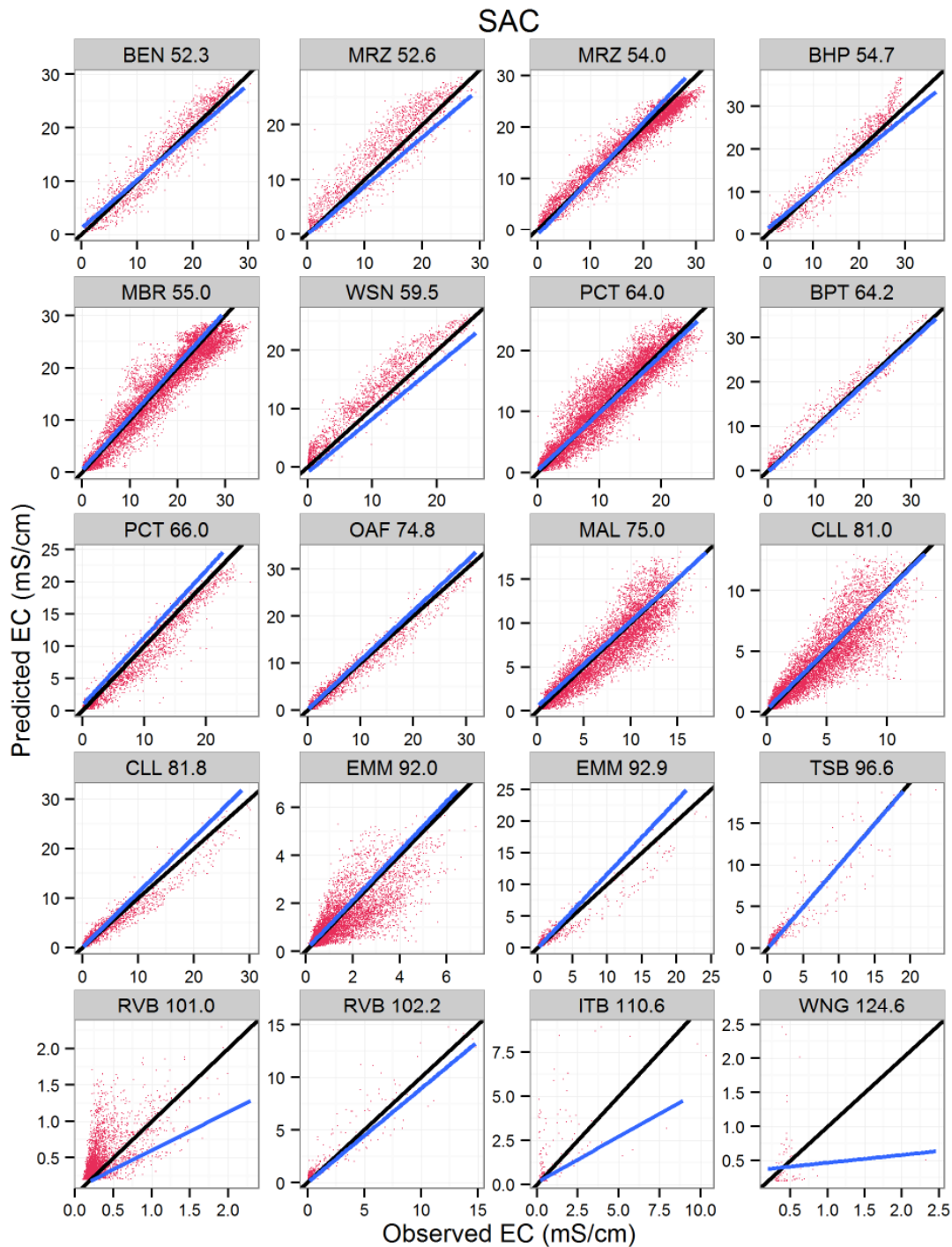


Figure 4-53 Observed EC targets against EC predictions from DSG model using ANN X2, at each station along the Sacramento River. Each black line is  $y = x$ , and each blue line is a linear regression of the underlying points. Duplicated station names at different distances come from combining Bulletin 23 and CDEC datasets.

#### 4.7.2 **Model 3B (San Joaquin River)**

The DSG-ANN model generally fits the X2 training data well (Figure 4-54 and Figure 4-55). The model over-predicts X2 position under very high flows ( $X2 < 50\text{km}$ ) and under-predicts under very low flows ( $X2 > 100\text{ km}$ ). The low-flow under-prediction here is distinct from the Sacramento River model (Model 3A), and one might hypothesize that agricultural runoff into the San Joaquin River affects the salinity data in ways that are not represented in the seawater intrusion-focused input data. Evaluating the model on the entire dataset gives similar performance characteristics compared to the subsample used for training (Figure 4-56 and Figure 4-57).

Sensitivity to sea level rise is assessed by adding 0.5 ft to the mean sea level input while leaving all other inputs the same and comparing model predictions (Figure 4-58 to Figure 4-61). The X2 position shifts between 0 and 2 km upstream, depending on the other inputs. The sea level rise effect appears to be suppressed under high flow conditions.

The central DSG component in the EC model is able to meet the observed targets fairly well in most cases. The nonparametric adjustment needs to make the largest adjustments for stations very far inland and under more atypical X2 conditions. See Figure 4-62. Directly comparing the predictions to the targets (Figure 4-63 and Figure 4-64) shows good agreement on average, but there is a degree of variability around the mean. The targets at some stations further inland (TSL and SAL) are harder for the model to predict. Estimates for the Bulletin 23 stations very far inland ( $> 120\text{ km}$ ) are based on a small amount of data and should be used with more caution.

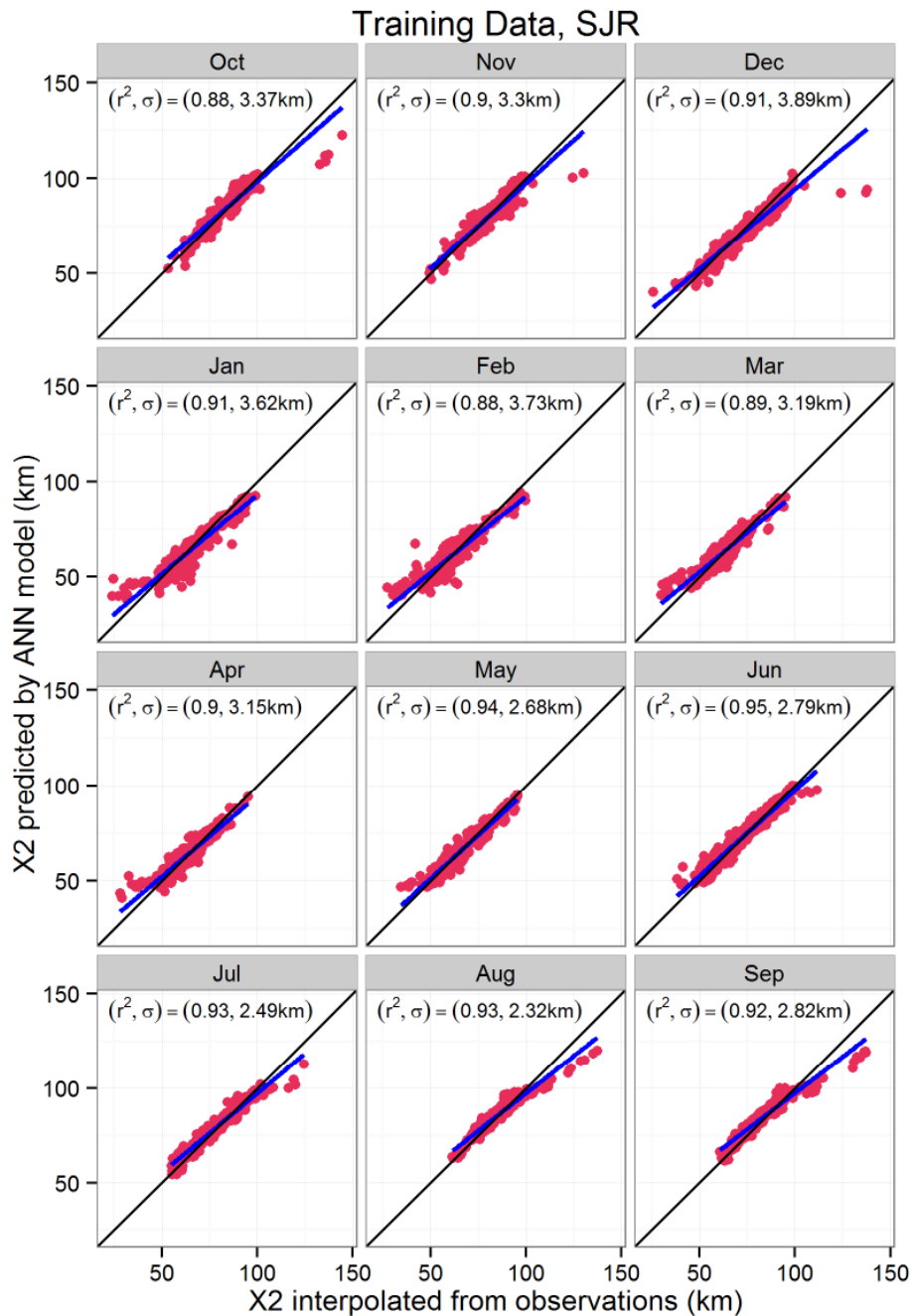


Figure 4-54

San Joaquin River X2 targets interpolated from observed EC data against ANN predictions for the subset of data used to train the model, separated by month. The black line is  $y = x$ , and the blue line is a linear regression of the plotted points. Each panel's regression  $r^2$  and standard error,  $\sigma$ , are also shown.

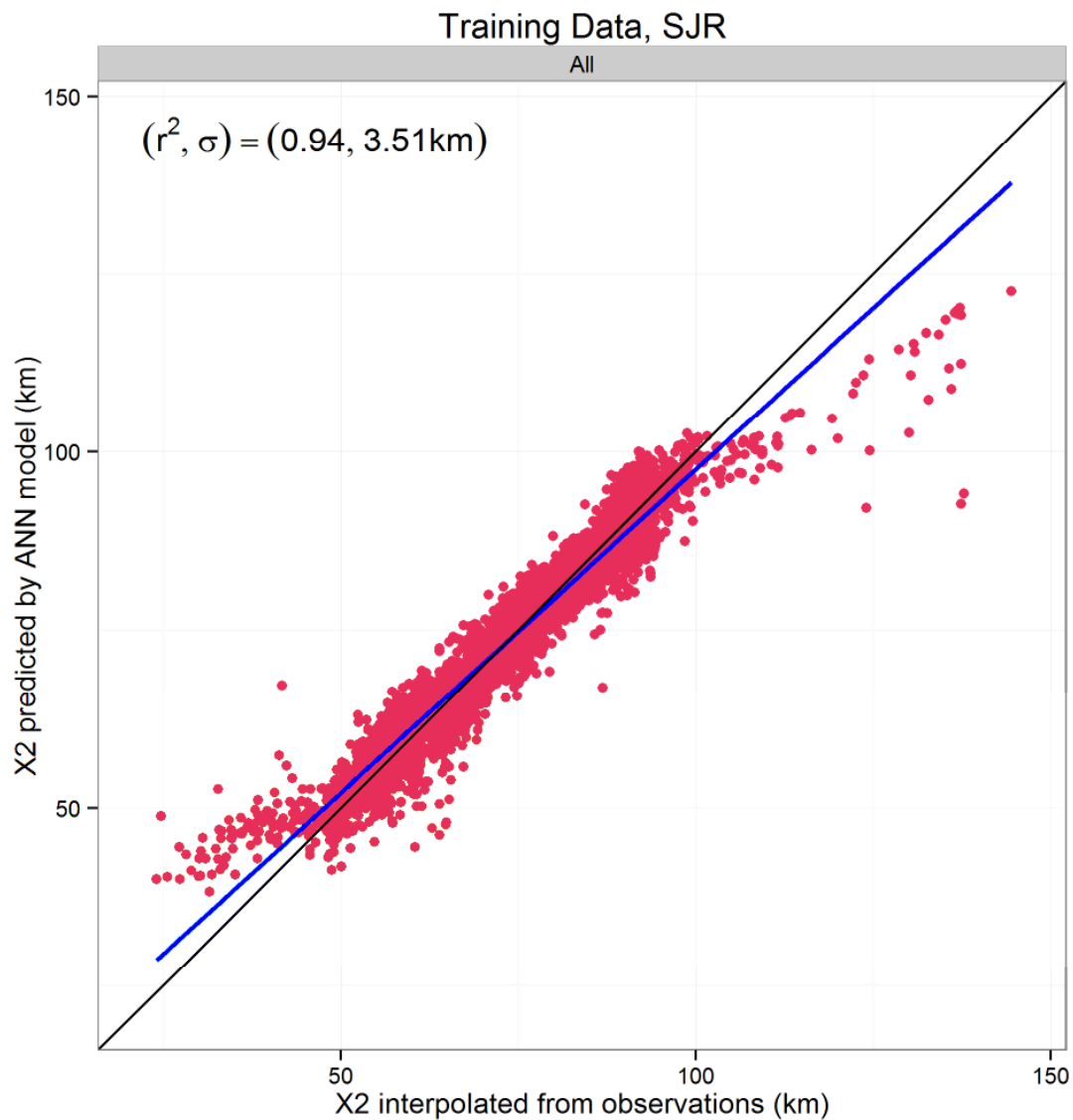


Figure 4-55

San Joaquin River X2 targets interpolated from observed EC data against ANN predictions for the subset of data used to train the model, all months. The black line is  $y = x$ , and the blue line is a linear regression of the plotted points. Each panel's regression  $r^2$  and standard error,  $\sigma$ , are also shown.

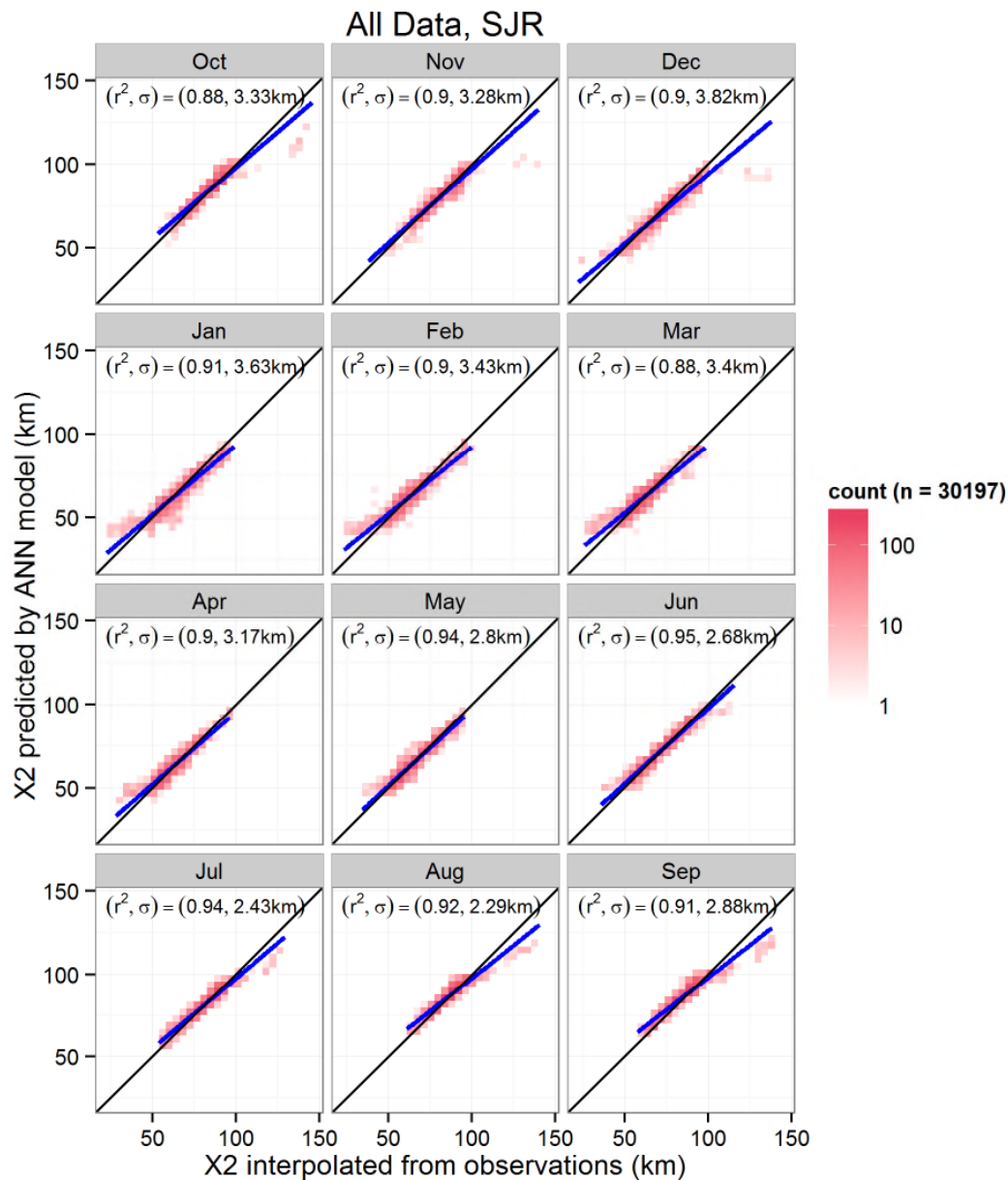


Figure 4-56 San Joaquin River X2 targets interpolated from observed EC data against ANN predictions for all available data, separated by month. The black line is  $y = x$ , and the blue line is a linear regression of the plotted points. Each panel's regression  $r^2$  and standard error,  $\sigma$ , are also shown. Plots are displayed as binned counts of points to prevent overplotting.

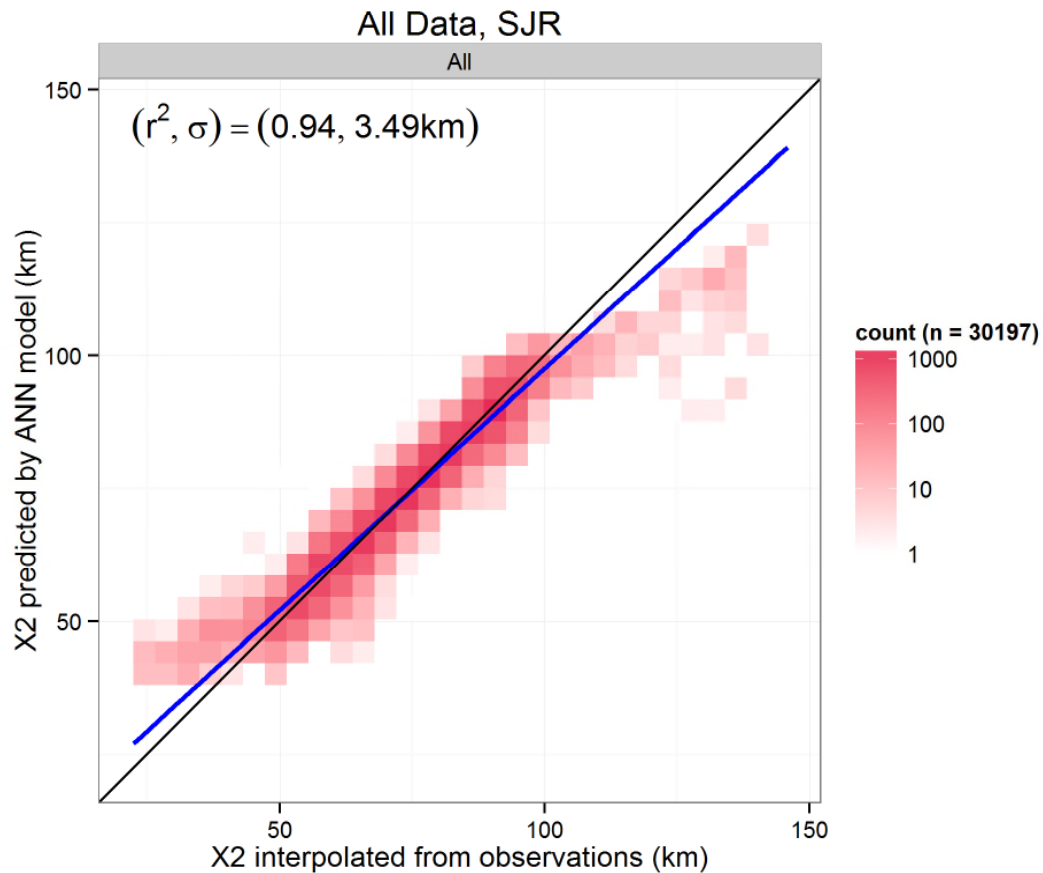


Figure 4-57

San Joaquin River X2 targets interpolated from observed EC data against ANN predictions for all available data, all months combined. The black line is  $y = x$ , and the blue line is a linear regression of the plotted points. Each panel's regression  $r^2$  and standard error,  $\sigma$ , are also shown. The plot is displayed as binned counts of points to prevent overplotting.

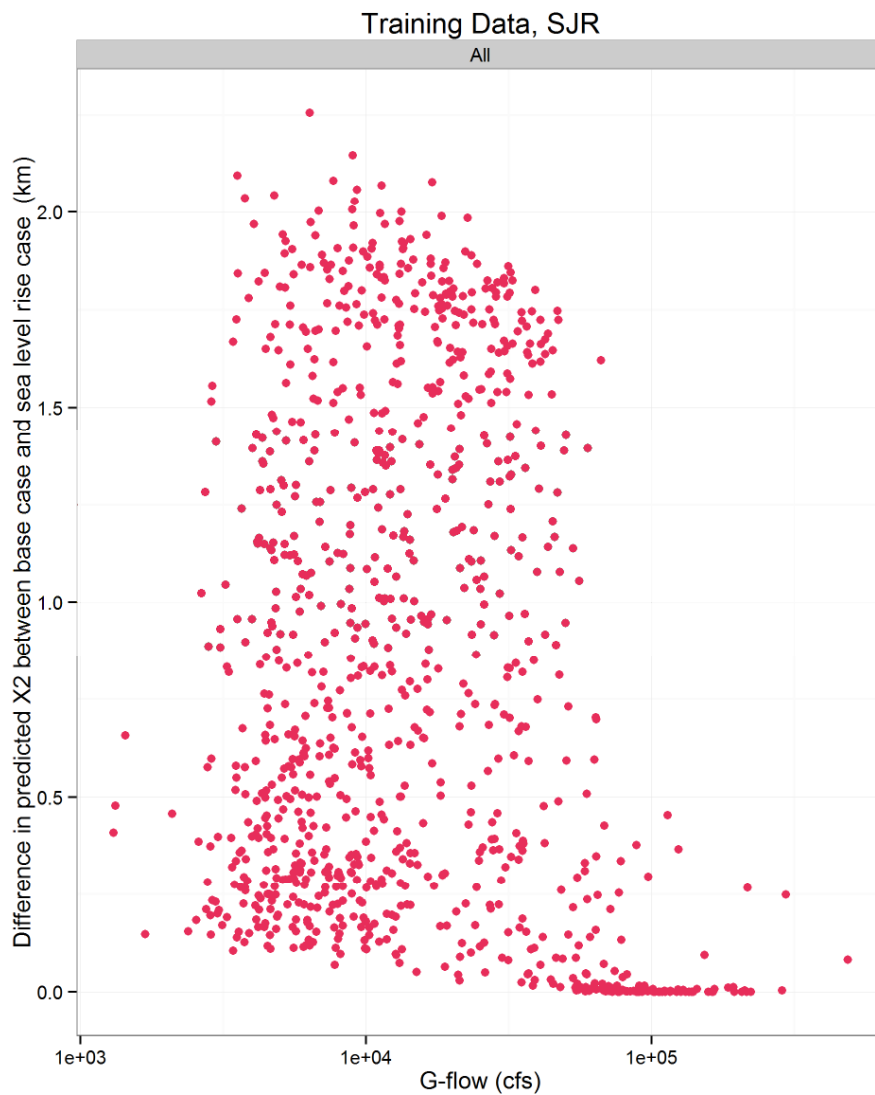


Figure 4-58 Increase in San Joaquin River X2 position due to uniform increase of 0.5 ft to mean sea level input for Approach 3 ANN model, conditioned on G-flow, for the subset of data used to train the model.

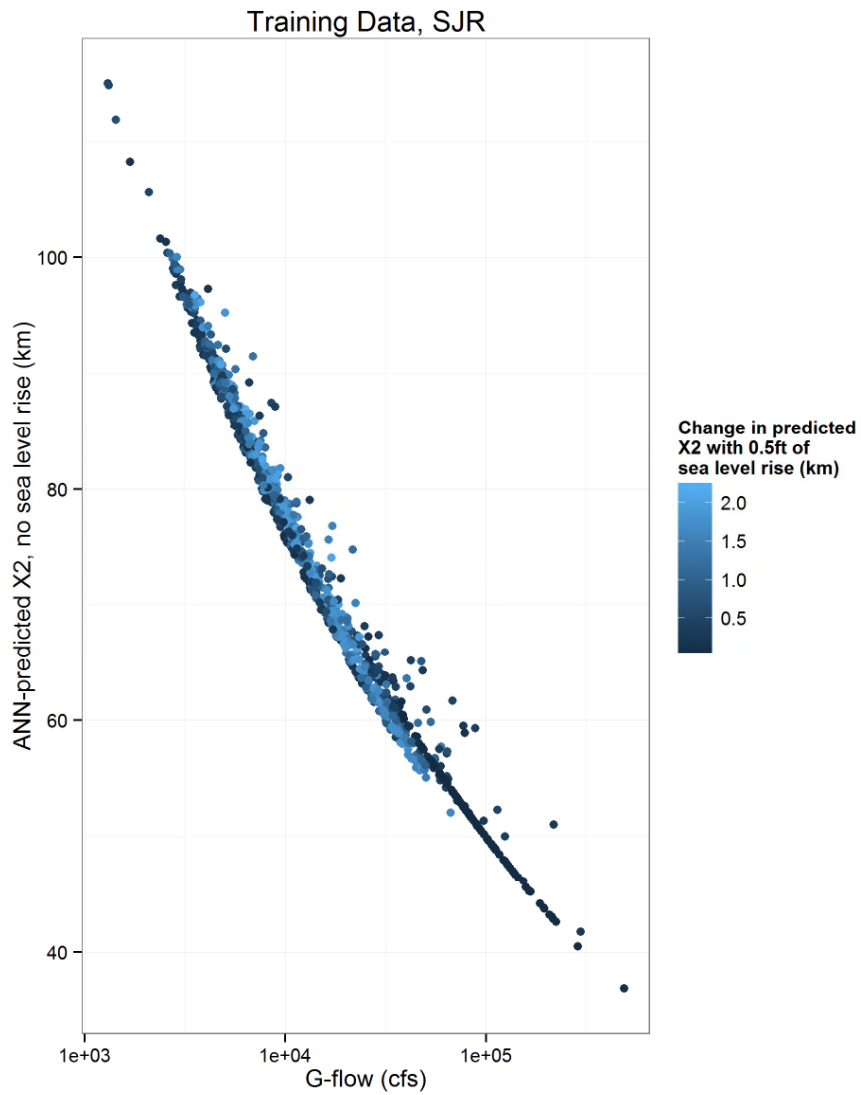


Figure 4-59 Increase in San Joaquin River X2 position due to uniform increase of 0.5 ft to mean sea level input for Approach 3 ANN model, conditioned on G-flow and predicted X2 position, for the subset of data used to train the model.

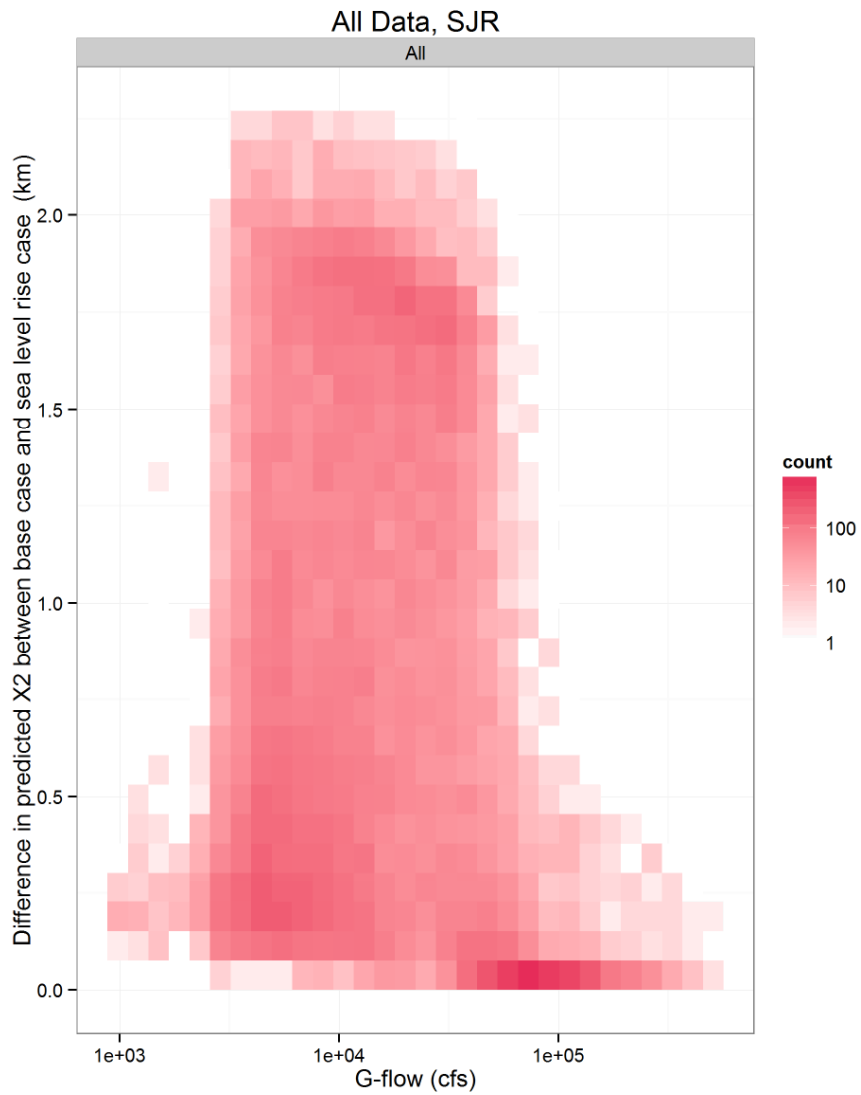


Figure 4-60 Increase in San Joaquin River X2 position due to uniform increase of 0.5 ft to mean sea level input for Approach 3 ANN model, conditioned on G-flow, for all available data. The plot is displayed as binned counts of points to prevent overplotting.

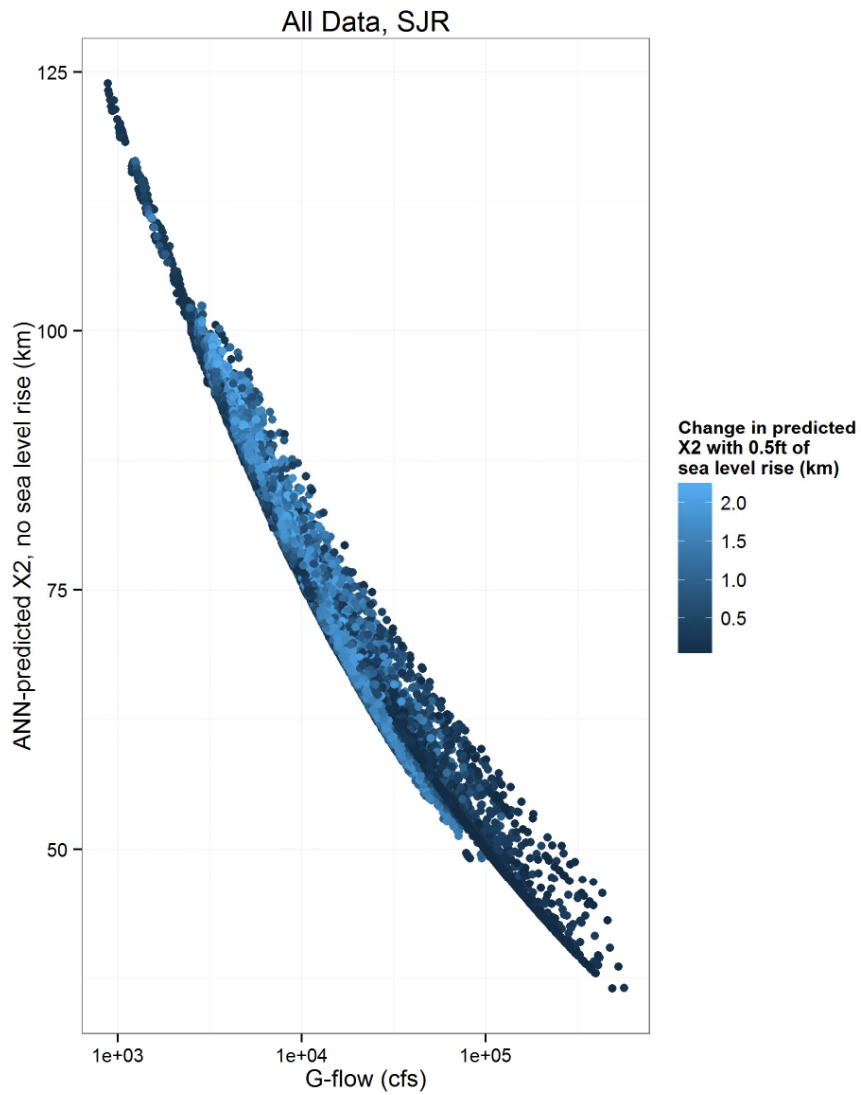


Figure 4-61 Increase in San Joaquin River X2 position due to uniform increase of 0.5 ft to mean sea level input for Approach 3 ANN model, conditioned on G-flow and predicted X2 position, for all available data.

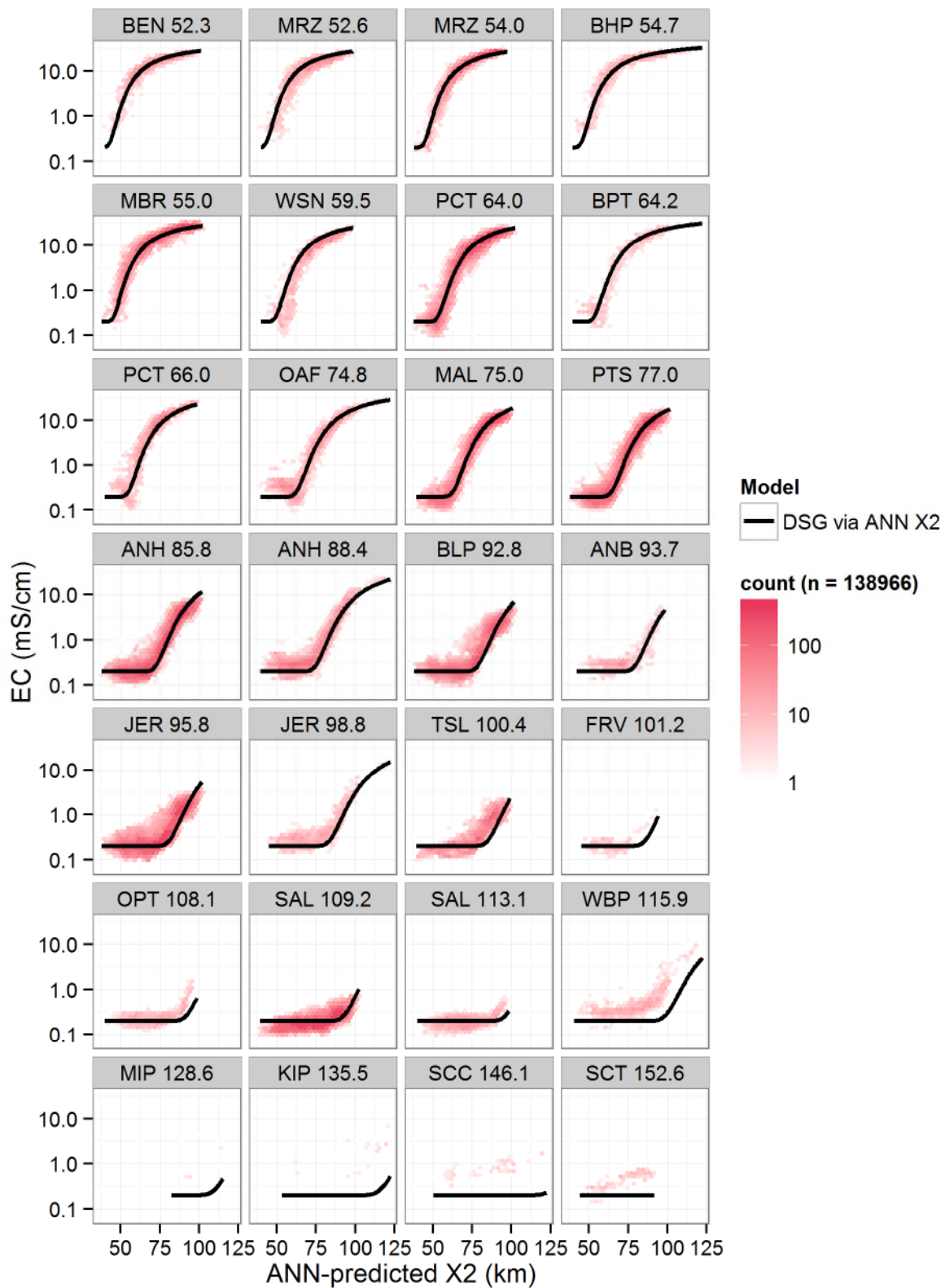


Figure 4-62 DSG component (black) and non-parametric adjustment (blue) model at each station (with channel distance in km) on the San Joaquin River. Observed data are plotted as binned counts to prevent overplotting.

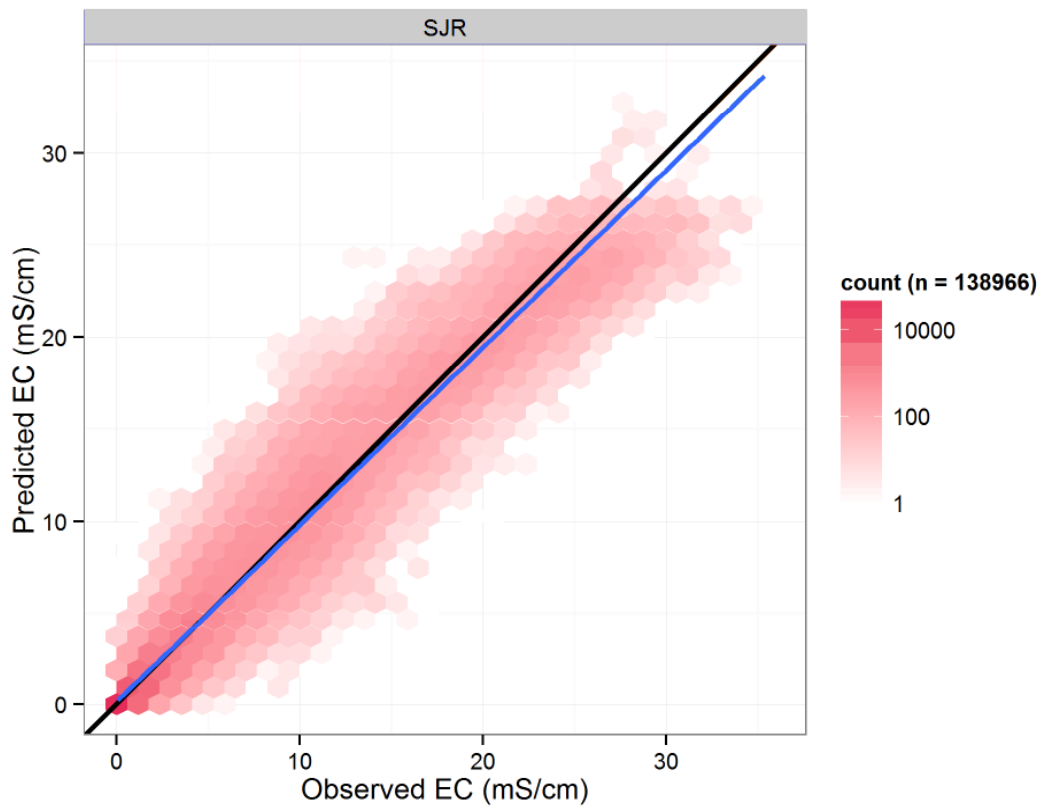


Figure 4-63 San Joaquin River observed EC targets against EC predictions from DSG model using ANN X2. Points are displayed as binned counts to prevent overplotting. The black line is  $y = x$ , and the blue line is a linear regression of the underlying points.

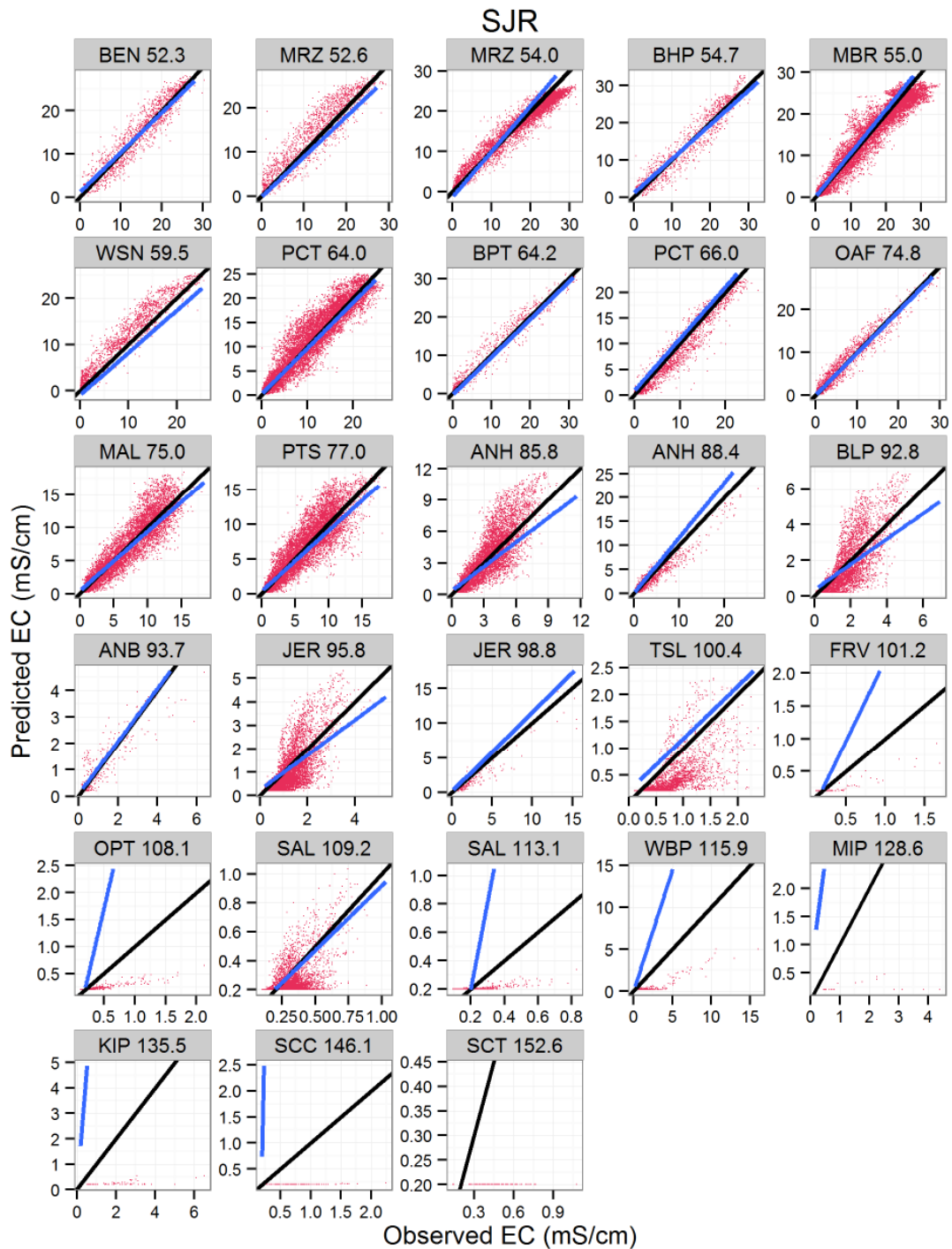


Figure 4-64 Observed EC targets against EC predictions from DSG model using ANN X2, at each station along the San Joaquin River. Each black line is  $y = x$ , and each blue line is a linear regression of the underlying points. Duplicated station names at different distances come from combining Bulletin 23 and CDEC datasets.

#### 4.8 EVALUATION OF ANN MODEL PERFORMANCE WITH RESPECT TO X2

This section provides additional comparison of ANN model predictions of X2 with interpolated values. The quality of fits associated with the DSG-based models (Models 2A-1 and 2B-1) is assessed in Table 4-14. The DSG-ANN approach provides an overall  $r^2$  of 0.96 for the Sacramento River branch and 0.90 for the San Joaquin River branch, ranging from 0.71 to 0.96 depending on the month and river branch. The quality of fits associated with the DSG-residual ANN-based models (Models 3A and 3B) is assessed in Table 4-15. The DSG residual-based approach provides an overall  $r^2$  of 0.95 for the Sacramento River branch and 0.94 for the San Joaquin River branch, ranging from 0.86 to 0.96 depending on the month and river branch. Taken together, both ANN modeling approaches appear to represent the X2 isohaline reasonably well for all but the most extreme conditions over a large period of record. However, the DSG residual-based approach appears to perform consistently better for the San Joaquin River branch.

#### 4.9 COMPARISON TO DAILY DSG MODEL

The daily DSG model is evaluated using an approach that is consistent with the approach used for the ANN model above. This approach assumes constant values of  $\Phi_1$  and  $\Phi_2$ <sup>4</sup>. The quality of these fits is assessed in Table 4-16. There is an overall  $r^2$  of 0.93 for both rivers, ranging from 0.86 to 0.95 depending on the month and river.

#### 4.10 COMPARISON TO DAILY K-M MODEL

The K-M equation can also be expressed in daily form (Kimmerer and Monismith, 1992):

$$\text{Daily X2}(t) = 10.16 + 0.945 * \text{X2}(t-1) - 1.487 * \log_{10}(\text{Q}_{\text{out}}(t)) \quad \text{Eq. 4.1}$$

This equation was used for comparison with the other methods discussed above (ANN and daily DSG model). The X2 value was not calculated for days when the Net Delta Outflow ( $\text{Q}_{\text{out}}$ ) was negative, which occurred at various times in the early part of the record. The exclusion of these days, which are normally hard to fit, may favorably bias the comparison of the K-M model. The fit statistics are shown in Table 4-17. The  $r^2$  of the overall fit is 0.89, somewhat lower than for the ANN and the daily DSG model, and ranges from 0.76 to 0.93.

#### 4.11 COMPARISON TO MACWILLIAMS ET AL. (2015) MODEL

MacWilliams presented a new interpretation of X2 using bottom salinity data derived from a three-dimensional hydrodynamic model (output for 1994-1997), and a modified form of the Monismith et al. (2002) equation. Here we present a comparison of the new model to the data on X2 over the longer time horizon, albeit obtained from surface salinity measurements (Hutton et al., 2015) (Figure 4-65). In applying this model we needed to make a modification to account for the negative flows that occur in our longer record. The calculation is not made for negative flows, the model is reinitialized with steady state X2 values after flows go negative. The inter-model comparison shows the relevance of the data used for any modeling exercise. In this case, the MacWilliams et al. (2015) estimates

---

<sup>4</sup>  $\phi_1 = 456$  (Sacramento River),  $\phi_1 = 502$  (San Joaquin River),  $\phi_2 = -0.193$  (Sacramento River),  $\phi_2 = -0.203$  (San Joaquin River)

fit the interpolated X2 data less well than either the DSG or one of the ANN models developed here (Model 3A used for comparison).

**Table 4-14**  
**Scatterplot Statistics of ANN Model (Models 2A-1 and 2B-1), Grouped by River and Month**  
**ANN X2 (km) = C1 + C2\*Observed X2 (km)**

Branch	Month	C2	C1	r <sup>2</sup>	Standard Error (km)
SAC	Jan	0.91	5.45	0.91	3.69
SAC	Feb	0.87	8.08	0.91	3.46
SAC	Mar	0.87	8.38	0.90	3.16
SAC	Apr	0.91	5.69	0.92	2.92
SAC	May	0.93	4.20	0.95	2.64
SAC	Jun	0.96	3.28	0.96	2.48
SAC	Jul	0.95	4.31	0.96	2.07
SAC	Aug	0.96	3.93	0.95	1.90
SAC	Sep	0.96	4.02	0.96	1.87
SAC	Oct	0.91	7.41	0.93	2.18
SAC	Nov	0.95	4.19	0.93	2.52
SAC	Dec	0.97	2.44	0.95	2.80
SAC	All	0.96	2.89	0.96	2.79
SJR	Jan	0.85	9.08	0.89	4.18
SJR	Feb	0.86	8.63	0.88	4.06
SJR	Mar	0.87	8.72	0.87	3.85
SJR	Apr	0.93	4.85	0.90	3.55
SJR	May	0.99	0.82	0.93	3.30
SJR	Jun	0.99	1.58	0.93	3.43
SJR	Jul	0.92	9.06	0.87	4.01
SJR	Aug	0.79	19.49	0.79	4.05
SJR	Sep	0.69	26.28	0.81	4.04
SJR	Oct	0.66	27.89	0.71	4.48
SJR	Nov	0.76	17.98	0.77	4.50
SJR	Dec	0.78	14.51	0.85	4.48
SJR	All	0.90	7.53	0.90	4.52

**Table 4-15**  
**Scatterplot Statistics of ANN Model (Model 3A and 3B), Grouped by River and Month**  
**ANN Monthly X2 (km) = C1 + C2\*Observed Monthly X2 (km)**

Branch	Month	C2	C1	r <sup>2</sup>	Standard Error (km)
SAC	Jan	0.84	9.41	0.91	3.46
SAC	Feb	0.80	12.14	0.90	3.32
SAC	Mar	0.80	12.41	0.88	3.26
SAC	Apr	0.86	9.24	0.90	3.08
SAC	May	0.89	6.64	0.94	2.71
SAC	Jun	0.89	7.73	0.95	2.50
SAC	Jul	0.88	9.98	0.96	1.96
SAC	Aug	0.93	6.44	0.95	1.92
SAC	Sep	1.03	-0.89	0.95	2.22
SAC	Oct	1.05	-3.33	0.94	2.48
SAC	Nov	0.98	1.31	0.93	2.54
SAC	Dec	0.91	4.99	0.94	2.89
SAC	All	0.95	3.55	0.95	3.13
SJR	Jan	0.83	9.84	0.91	3.63
SJR	Feb	0.80	11.90	0.90	3.43
SJR	Mar	0.81	12.14	0.88	3.40
SJR	Apr	0.87	8.76	0.90	3.17
SJR	May	0.92	5.32	0.94	2.80
SJR	Jun	0.90	7.16	0.95	2.68
SJR	Jul	0.85	12.15	0.94	2.43
SJR	Aug	0.79	18.23	0.92	2.29
SJR	Sep	0.78	19.54	0.91	2.88
SJR	Oct	0.85	12.77	0.88	3.33
SJR	Nov	0.89	8.08	0.90	3.28
SJR	Dec	0.84	10.44	0.90	3.82
SJR	All	0.91	6.65	0.94	3.49

**Table 4-16**  
**Scatterplot Statistics of Daily DSG Model, Grouped by River and Month.**  
**DSG Daily X2 (km) = C1 + C2\*Observed Daily X2 (km)**

Branch	Month	C2	C1	R <sup>2</sup>	Standard Error (km)
SAC	Jan	0.85	8.25	0.89	3.99
SAC	Feb	0.81	10.78	0.88	3.87
SAC	Mar	0.84	10.79	0.87	3.60
SAC	Apr	0.89	7.81	0.90	3.28
SAC	May	0.92	5.61	0.93	2.86
SAC	Jun	0.91	6.70	0.95	2.64
SAC	Jul	0.94	5.43	0.95	2.20
SAC	Aug	1.04	-1.50	0.94	2.21
SAC	Sep	1.14	-8.18	0.95	2.56
SAC	Oct	1.15	-9.59	0.91	3.17
SAC	Nov	1.05	-3.45	0.90	3.31
SAC	Dec	0.95	1.98	0.91	3.66
SAC	All	1.00	0.35	0.93	3.77
SJR	Jan	0.85	7.55	0.89	4.18
SJR	Feb	0.83	9.13	0.88	4.02
SJR	Mar	0.85	9.58	0.86	3.81
SJR	Apr	0.91	5.97	0.90	3.39
SJR	May	0.95	3.27	0.93	2.99
SJR	Jun	0.92	5.75	0.94	2.86
SJR	Jul	0.87	10.34	0.94	2.50
SJR	Aug	0.83	15.47	0.92	2.42
SJR	Sep	0.82	17.06	0.92	2.97
SJR	Oct	0.89	10.56	0.88	3.53
SJR	Nov	0.93	5.11	0.88	3.76
SJR	Dec	0.86	7.39	0.88	4.42
SJR	All	0.94	3.96	0.93	3.94

**Table 4-17**  
**Scatterplot Statistics of Daily K-M Model, Grouped by River and Month.**  
**KM Daily X2 (km) = C1 + C2\*Observed Daily X2 (km)**

Branch	Month	C2	C1	R <sup>2</sup>	Standard Error (km)
SAC	Jan	0.73	18	0.83	4.4
SAC	Feb	0.76	15	0.8	4.9
SAC	Mar	0.83	11	0.79	4.9
SAC	Apr	0.87	8.2	0.84	4.4
SAC	May	0.91	5.6	0.89	3.9
SAC	Jun	0.95	3.4	0.92	3.4
SAC	Jul	1.1	-4.2	0.89	3.6
SAC	Aug	1.1	-9.7	0.8	4.3
SAC	Sep	0.94	6.1	0.89	3.1
SAC	Oct	0.78	17	0.87	2.7
SAC	Nov	0.75	18	0.9	2.4
SAC	Dec	0.75	17	0.9	3.1
SAC	All	0.91	6.3	0.9	4.3
SJR	Jan	0.74	17	0.82	4.9
SJR	Feb	0.8	12	0.79	5.5
SJR	Mar	0.87	8.4	0.78	5.4
SJR	Apr	0.92	4.6	0.83	4.9
SJR	May	0.97	1.2	0.89	4.3
SJR	Jun	1	-1.1	0.93	3.6
SJR	Jul	1.1	-6.7	0.91	3.4
SJR	Aug	1	-2.1	0.84	4.1
SJR	Sep	0.79	18	0.86	3.8
SJR	Oct	0.72	22	0.81	3.8
SJR	Nov	0.7	23	0.84	3.3
SJR	Dec	0.69	21	0.84	4.2
SJR	All	0.91	6.3	0.89	4.9

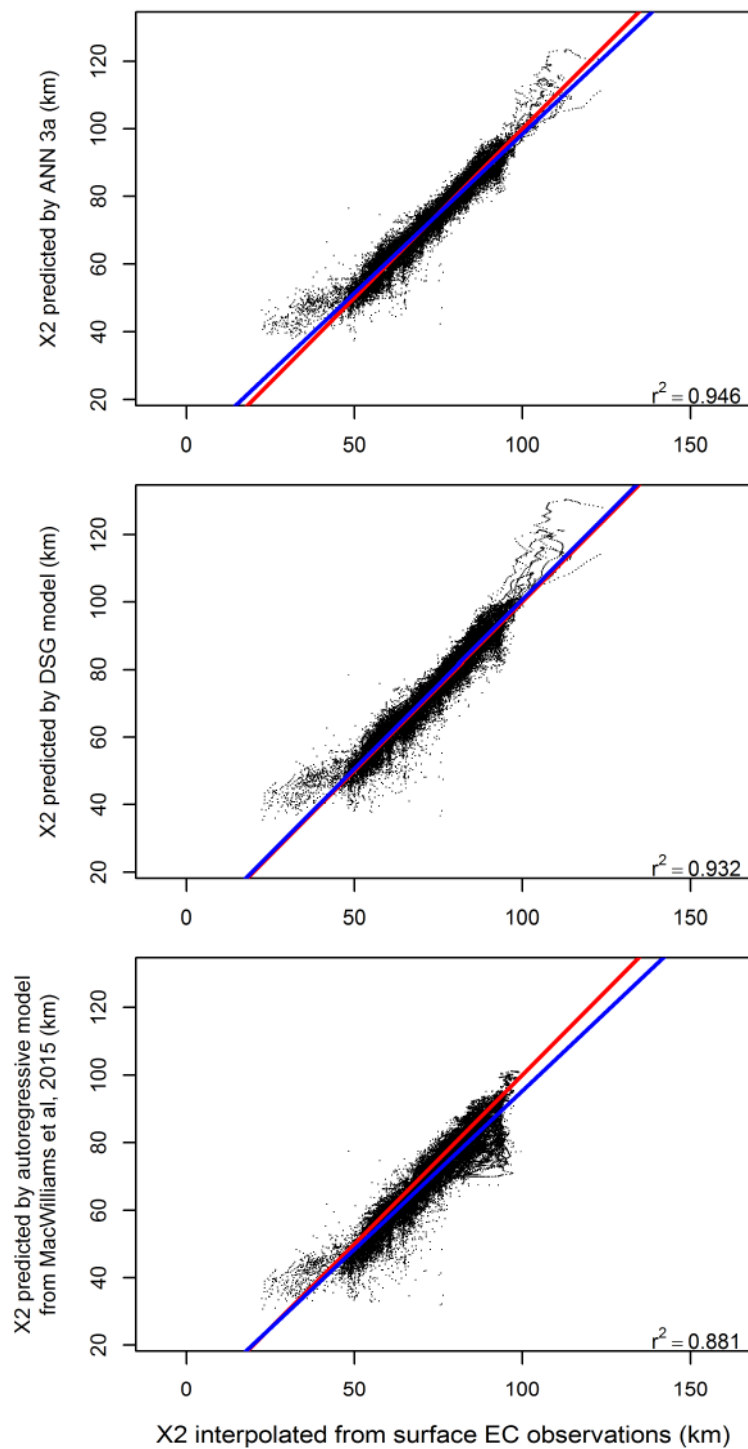


Figure 4-65 Interpolated X2 compared to X2 estimates from ANN model 3A, the daily DSG model and the MacWilliams (2015) model (Red line 1:1; blue line: linear regression). Dates with negative Delta outflows were not used in the MacWilliams et al. computation.



## 5. SUMMARY AND RECOMMENDATIONS

---

This work used the nine-decade-long record of observed daily salinity in Suisun Bay and the western Delta to develop ANNs using various boundary inputs. Although different data-driven modeling approaches have been used to address this problem, most have relied upon freshwater flow (i.e. Delta outflow) as the primary input. Although this variable is indeed the main driver of salinity distribution and of the X2 position, other variables are known to play a role, albeit secondary. This work extends previous work by explicitly incorporating tidal variables (mean sea level and tidal range) and disaggregating Delta outflow into its Sacramento and San Joaquin net flow components (Qrio and Qwest) in the empirical ANN modeling framework.

The ANN modeling exercise identified suitable models based on the quality of the fit to the observed data and on the sensitivity of the models to changes in specific inputs, such as freshwater flow, the Qwest/Qrio flow distribution, and the mean sea level. The goal of the sensitivity analysis was to screen out models that provided a response that was not physically plausible. Thus, for higher mean sea level, we expect higher salinities, all other variables remaining the same. Models that did not indicate this behavior were considered unsuitable for this work. Qwest flows have a more complex relationship with EC, particularly at an upstream station such as Jersey Point. The ANNs showed variable response to Qwest, with smaller changes using the gradient model, and a larger change with using the Jersey Point site-specific model. This is not inconsistent with the observed data, and it is possible that Qwest sensitivity cannot be used a priori as a screening tool in the manner that mean sea level can. In this respect, it is more like the tidal range input, for which we do not have a prior understanding of the response. In general, if we limit our sensitivity to sea level alone, we found that it was possible to obtain ANNs that fit the data well but did not always have a consistent, physically plausible sensitivity response to this input. This behavior of ANNs, which is related to the black-box nature of the underlying equations that constitute the ANN, has been reported in the literature, although it has not been discussed widely (Kingston et al., 2005; Piotrowski and Napiorkowski, 2014). Typically, most published applications of ANNs look only at the quality of the fit (Wu et al., 2014), and not at other validation measures, such as model sensitivity. Sensitivity as a consideration has been reported in a small number of studies (Kingston et al., 2005; Jain et al., 2004; Mount et al., 2013), and is recommended as a tool to enhance model validity (Wu et al., 2014).

An important finding of the sensitivity analysis component of this work was that there was a clear tradeoff between the quality of model fits and of plausible sensitivity response. Models that were larger (more hidden neurons) performed better at fitting the data but were more likely to show unrealistic sensitivity responses. As a consequence of this behavior, in some situations we had to marginally sacrifice the quality of the fit (by reducing the size of the networks) to achieve a reasonable sensitivity. This methodology, which consisted

of screening fit and sensitivity simultaneously, was applied to all of the proposed input combinations considered.

Using the combined evaluation methodology (fit and sensitivity) we developed multiple models for salinity along the gradient and for the X2 isohaline that may be considered for future use. ANN models were developed using EC data and distance from Golden Gate, with no imposed model structure (data-driven approach). ANN models were also developed using the conceptual framework of the DSG model as a constraint, either using the ANNs to fit the DSG parameters (DSG-based approach), or using the ANNs to train to the residual error in the DSG model (DSG residual-based approach). These different approaches have individual strengths; thus, no individual approach can be discarded at this stage. Data driven models are simple, and are not constrained by our prior knowledge of the system. However, they do require continuous data which are limited in the present application. The DSG-based and DSG residual-based approaches are sufficiently flexible to train with data sets that have gaps, and therefore could be applied to the entire period of record. These approaches incorporate the current conceptual model of the system, and the range of results can be constrained to be more realistic than a purely data-driven ANN model.

Specific ANN models (representing combinations of time delays in flows and network size) are discussed in Chapter 4, and for each input set, a specific structure is proposed for future use. The validation results presented here may be used to select a subset of ANN models that can be used in parallel to either represent salinity at a specific location or to calculate the X2 isohaline.

Overall, the ANN models were able to achieve better fits to X2 that obtained through the K-M and DSG models, both of which are currently available statistical tools to understand salinity in the western Delta under different conditions. Because the ANN models were trained on large data sets spanning a variety of conditions, they may be considered a credible alternative to the existing empirical models that also account for variables besides freshwater flow into the western Delta and San Francisco Bay. Future application may thus allow examination of the relative significance of these secondary variables on salinity under specific conditions where improved predictive capability is needed. To a limited extent, the ANN models developed here may also be used to explore scenarios such as those related to future sea level rise. However, such analyses must be cognizant of the limited ability of ANN models to extrapolate beyond their respective training data sets. For scenarios that significantly depart from training conditions, other modeling tools may need to be considered.

## 6. REFERENCES

---

- American Society of Civil Engineers (ASCE). (2000). Artificial Neural Networks in Hydrology, 1. Preliminary Concepts, Vol. 5, No. 2, pp. 115–123.
- BDCP EIR/EIS (2013). Appendix 29A Effects of Sea Level Rise on Delta Tidal Flows and Salinity, on the Internet at:  
[http://baydeltaconservationplan.com/Libraries/Dynamic\\_Document\\_Library/EIR-EIS\\_Appendix\\_29A\\_%E2%80%93\\_Effects\\_of\\_Sea\\_Level\\_Rise\\_on\\_Delta\\_Tidal\\_Flows\\_and\\_Salinity\\_5-10-13.sflb.ashx](http://baydeltaconservationplan.com/Libraries/Dynamic_Document_Library/EIR-EIS_Appendix_29A_%E2%80%93_Effects_of_Sea_Level_Rise_on_Delta_Tidal_Flows_and_Salinity_5-10-13.sflb.ashx).
- Beale, M.H., Hagan, M.T., Demuth, H.B. (2011). Neural Network Toolbox, Mathworks Inc.
- Bishop, C. M. (1995). Neural networks for pattern recognition. Oxford University Press.
- Chen, L. and S. B. Roy (2013). Modeling salinity in Suisun Bay and the western Delta using artificial neural networks, report prepared for Metropolitan Water District of Southern California, April 12.
- Chen, L., Rath, J.S., and S. B. Roy (2014). Modeling salinity in Suisun Bay and the western Delta using artificial neural networks, report prepared for Metropolitan Water District of Southern California, April 18.
- Denton, R.A. (1993). Accounting for antecedent conditions in seawater intrusion modeling – applications for the San Francisco Bay-Delta. Hydraulic Engineering 93 (1): 448–453. Proceedings of ASCE National Conference on Hydraulic Engineering, San Francisco.
- Denton, R.A. (1994) Predicting Surface 14-day EC from NDO, memo to Paul Hutton, April 12.
- Finch, R. and N. Sandhu. (1995). Artificial neural networks with application to the Sacramento – San Joaquin Delta. California Department of Water Resources Delta Modeling Section, Division of Planning.
- Fleenor, W., E. Hanak, J.R. Lund, J.R. Mount. (2008). Delta hydrodynamics and water salinity with future conditions. Technical Appendix C. in Comparing Futures for the Sacramento–San Joaquin Delta, Public Policy Institute of California.
- Gross, E. S., Nidzieko, N. J., MacWilliams, M. L., & Stacey, M. T. (2007). Parameterization of Estuarine Mixing Processes in the San Francisco Estuary based on Analysis of Three-Dimensional Hydrodynamic Simulations. Journal of Estuarine and Coastal Modeling, ASCE, pp. 322–338.

- Gross, E. S., MacWilliams, M. L., & Kimmerer, W. J. (2009). Three-dimensional modeling of tidal hydrodynamics in the San Francisco Estuary. *San Francisco Estuary and Watershed Science*, 7(2).
- Harder, J.A. (1977). Predicting estuarine salinity from river inflows, *Journal of the Hydraulics Division, ASCE*, Vol. 103, pp. 877–888.
- Hoffman, M. D., and A. Gelman. The No-U-Turn Sampler: Adaptively Setting Path Lengths in Hamiltonian Monte Carlo. *Journal of Machine Learning Research* 15 (2014): 1593-1623.
- Hutton, P.H. (2014). Delta Salinity Gradient (DSG) Model. Unpublished technical report, Metropolitan Water District of Southern California, Draft, September 9.
- Hutton, P.H., J. S. Rath, L. Chen, M. J. Unga, and S. B. Roy (2015) Nine Decades of Salinity Observations in the San Francisco Bay and Delta: Modeling and Trend Evaluation. *ASCE Journal of Water Resources Planning and Management*, in review.
- Jain, A., Sudheer, K.P., Srinivasulu, S. (2004). Identification of physical processes inherent in artificial neural network rainfall runoff models. *Hydrol. Process.* 18 (3), 571e581.
- Jassby, A.D., W.J. Kimmerer, S.G. Monismith, C.Armor, J.E. Cloern, T.M. Powell, J.R. Schubel and T.J. Vendlinski. (1995). Isohaline position as a habitat indicator for estuarine populations. *Ecological Applications* 5: 272–289.
- Kimmerer, W. and S. Monismith. (1992). An estimate of the historical position of 2ppt salinity in the San Francisco Bay Estuary. Issue Paper prepared for the fourth technical workshop on salinity, flows and living resources of the San Francisco Bay/Delta estuary. August.
- Kingston, G.B., Maier, H.R., Lambert, M.F. (2005) Calibration and validation of neural networks to ensure physically plausible hydrological modeling. *J. Hydrology*. Vol. 314 (1e4), 158e176.
- List, J. (1994). X2 and the X2/Net Delta Outflow Relationship. Prepared for California Urban Water Agencies, Sacramento, California.
- MacWilliams, M. L., Bever, A. J., Gross, E. S., Ketefian, G. S., Kimmerer, W. J., & Center, R. T. (2015). Three-Dimensional Modeling of Hydrodynamics and Salinity in the San Francisco Estuary: An Evaluation of Model Accuracy, X2, and the Low–Salinity Zone. *San Francisco Estuary and Watershed Science*, 13(1).
- Maier, H.R., A. Jain, G.C. Dandy, K.P. Sudheer. (2010). Methods used for the development of neural networks for the prediction of water resource variables in river systems: current status and future directions. *Environmental Modeling and Software* 25: 891–909.

- Mierzwa, M. (2002). Chapter 4: CALSIM versus DSM2 ANN and G-model Comparisons. Methodology for flow and salinity estimates in the Sacramento–San Joaquin Delta and Suisun Marsh. 23rd Annual Progress Report. June.
- Monismith, S. G., Kimmerer, W., Burau, J. R., & Stacey, M. T. (2002). Structure and flow-induced variability of the subtidal salinity field in northern San Francisco Bay. *Journal of Physical Oceanography*, 32(11), 3003-3019.
- Mount, N.J., Dawson, C.W., Abrahart, R.J. (2013). Legitimising data-driven models: exemplification of a new data-driven mechanistic modelling framework. *Hydrol. Earth Syst. Sci.* 17, 2827e2843.
- Neal, Radford M. Bayesian learning for neural networks. Diss. University of Toronto, 1995.
- Piotrowski, A. P., and Napiorkowski, J. J. (2013). A comparison of methods to avoid overfitting in neural networks training in the case of catchment runoff modelling. *Journal of Hydrology*, 476, 97-111.
- Roy, S.B., J. Rath, L. Chen, M.J. Unga, and M. Guerrero. (2014). Salinity trends in the Suisun Bay and the western Delta (October 1921– September 2012). Final report to San Luis and Delta Mendota Water Authority and Metropolitan Water District of Southern California, January.
- Sandhu, N., D. Wilson, and R. Finch. 1999. Modeling flow-salinity relationships in the Sacramento- San Joaquin Delta using artificial neural networks. Technical Information Record OSP-99-1. California Department of Water Resources. Sacramento, CA.
- Schemel, L. (2001). Simplified conversion between specific conductance and salinity units for use with data from monitoring stations. IEP Newsletter Volume 14, Number 1, Winter.
- Senevirante, S., S.Wu, and Y. Liang. (2008). Chapter 3: Impacts of Sea Level Rise and Amplitude Change on Delta Operations. Methodology for flow and salinity estimates in the Sacramento – San Joaquin Delta and Suisun Marsh. 29th Annual Progress Report. June.
- State Water Resources Control Board (2006). Water Quality Control Plan for the San Francisco Bay/Sacramento-San Joaquin Delta Estuary. Division of Water Rights.
- Wilbur, R. and A. Munevar. (2001). Chapter 7: Integration of CALSIM and Artificial Neural Networks Models for Sacramento–San Joaquin Delta Flow-Salinity Relationships. Methodology for flow and salinity estimates in the Sacramento–San Joaquin Delta and Suisun Marsh. 22nd Annual Progress Report.
- Zhang, J. 2014. SCHISM theory manual. On the Internet at: [http://ccrm.vims.edu/schism/combined\\_theory\\_manual.pdf](http://ccrm.vims.edu/schism/combined_theory_manual.pdf).